

**The importance of bifunctional
enzymes for U(VI) reduction in
*ThermusscotoductusSA-01***

By

Errol Duncan Cason

Submitted in fulfilment of the requirements for the degree

MAGISTER SCIENTIAE

In the

**Department of Microbial, Biochemical and Food
Biotechnology
Faculty of Natural Sciences
University of the Free State
Bloemfontein
Republic of South Africa**

May 2010

Supervisor: Prof. E. van Heerden

Co-supervisor: Dr L Piater

“I may not have gone where I intended to go, but I think I have ended up where I needed to be.”

- Douglas Adams

ACKNOWLEDGEMENTS

Prof. E. van Heerden and Dr. L.A. Piater for pushing me to be a better scientist and always believing in me. Without your guidance and friendship I would not have gotten this far.

Armand and Jacquie for endless patience and friendship.

Mariana and Wilmari, we are the last of our honours group still left in this madness. Now begins the last part of this journey we started together, thanks for hanging in here with me.

Prof. D. Litthauer, Prof J. Albertyn and Dr. D.J. Opperman for their helpful advice during my studies and the preparation of this manuscript

Prof. P. van Wyk (University of the Free State) and Prof. GeatanBorgonie and MyriamClayes (University of Ghent) for their help with the TEM and EDS work.

My better half Ilze, for standing by me through all the mood swings induced by late nights.

Last but certainly not least my parents, Louise and Stephen and brothers, Raymond and Louis for support, friendship and sacrifices all these years.

The NRF and the Ernst & Ethel Eriksen Trust for financial support.

CONTENTS

LIST OF FIGURES	x
LIST OF TABLES	xviii
LIST OF ABBREVIATIONS	xx
1. LITERATURE REVIEW	
1.1 General introduction	1
1.2 The sulfate-reducing bacteria	3
1.2.1 Uranium-reduction under sulfate-reducing conditions	4
1.3 The iron-reducing bacteria	5
1.3.1 Uranium-reduction under Fe(III)-reducing conditions	7
1.3.2 Uranium-reduction by Fe(III)-reducing bacteria under thermophilic conditions	8
1.4 Uranium reductases	9
1.4.1 <i>Desulfovibrioreductase</i> (s)	9
1.4.2 <i>Shewanellareductase</i> (s)	10
1.4.3 <i>Geobacterreductase</i> (s)	12
1.4.3.1 Nanowires in uranium(VI)-reduction	12
1.5 Effect of uranium(VI) on eukaryotes	13
1.6 Reduction by one electron or two	14
1.7 Uranium in the environment	16
1.7.1 Bioremediation of environmental uranium	17
1.7.2 Aerobic interactions with uranium	17
1.7.3 Anaerobic interactions with uranium	18
1.7.4 Reduction-based bioremediation of uranium contaminated aquifers	19
1.8 References	22

2. INTRODUCTION TO PRESENT STUDY

2.1	Introduction	33
2.2	The broad aims of this study	34
2.3	References	34

3. INTERACTIONS OF *THERMUS SCOTODUCTUS* SA-01 WITH URANIUM(VI) UNDER GROWTH AND NON-GROWTH CONDITIONS

3.1	Introduction	38
3.2	Materials and methods	40
3.2.1	Bacterial strain and culture conditions	40
3.2.2	Confirmation of <i>T. scotoductus</i> SA-01	40
3.2.2.1	Genomic DNA extraction and 16S rRNA gene amplification	40
3.2.2.2	Ligation and transformation of the PCR products into a pGEM [®] -T easy vector	42
3.2.2.3	Small scale plasmid isolation	43
3.2.2.4	Restriction Fragment Length Polymorphism (RLFP)	43
3.2.3	Biomass vs optical density	44
3.2.3.1	Dry weight determination	44
3.2.3.2	Dilution range	45
3.2.4	Growth of <i>Thermusscotoductus</i> SA-01	45
3.2.5	Aerobic batch culture studies	45
3.2.5.1	Growth with uranium induced stress with no pre-culturing	45
3.2.5.2	Growth with uranium induced stress with three and six hours pre-culturing	46
3.2.6	Spectrophotometric determination of uranium(VI)	46
3.2.7	Uranium(VI) standard curve	47
3.2.8	Reduction of uranium(VI) by resting cells of <i>T. scotoductus</i> SA-01 under non-growth conditions	48

3.2.8.1	Whole cell uranium(VI) reduction by cells harvested in early and late exponential phase with lactate as electron donor	48
3.2.8.2	Whole cell uranium(VI) reduction with different donors	49
3.2.8.3	Whole cell uranium(VI) reduction at different pH values	49
3.2.8.4	Whole cell uranium(VI) reduction at different temperatures	50
3.2.9	Transmission Electron Microscopy	50
3.2.9.1	Fixation	50
3.2.9.2	Dehydration	51
3.2.9.3	Polymerization	51
3.2.9.4	Lead staining of the material	51
3.3	Results and discussion	53
3.3.1	Confirmation of strain as <i>T. scotoductus</i> SA-01	53
3.3.1.1	Genomic DNA isolation and 16S rRNA gene amplification	53
3.3.1.2	Transformation into <i>E. coli</i> Top 10 competent cells	54
3.3.1.3	Restriction fragment length polymorphism (RFLP) analysis	54
3.3.2	Relating biomass to optical density	56
3.3.3	Growth of <i>T. scotoductus</i> SA-01	58
3.3.3.1	Pre-inoculum	59
3.3.3.2	Inoculum	59
3.3.3.3	Growth curve	60
3.3.4	Effect of uranium on the growth of <i>T. scotoductus</i> SA-01	61
3.3.4.1	Effect of uranium on the growth of <i>T. scotoductus</i> SA-01 with pre-culturing	63
3.3.5	Reduction of uranium(VI) by resting cells	65
3.3.5.1	Uranium(VI) reduction by cells harvested in early as well as late exponential phase with lactate as electron donor	65
3.3.5.2	Uranium(VI) reduction with different electron donors	68
3.3.5.3	Uranium(VI) reduction at different pH and temp values	70
3.3.7	Interactions of uranium with <i>T. scotoductus</i> SA-01	73

3.4	Conclusions	76
3.5	References	78
4. PURIFICATION, IDENTIFICATION, EXPRESSION AND CHARACTERISATION OF THE URANIUM(VI)-REDUCTASE		
4.1	Introduction	81
4.2	Materials and methods	83
4.2.1	Protein expression by <i>Thermusscotoductus</i> SA-01 in response to uranium exposure	83
4.2.1.1	Protein extraction	83
4.2.1.2	Protein concentration determination	83
4.2.1.3	Two dimensional (2D) gel electrophoresis at pH gradients 3 to 10, 5 to 8 and 4 to 7	84
4.2.2	Preparation of subcellular fractions	85
4.2.3	SDS-PAGE	86
4.2.4	Determination of uranium(VI) reduction activity in subcellar fractions	87
4.2.5	Optimization of protocol for isolation of uranium reductase(s) by chromatographic methods	87
4.2.5.1	Extraction of ionically bound membrane proteins	87
4.2.5.2	Screening of optimum chromatographic media	88
4.2.5.3	Isolation of the membrane/periplasmic uranium reductase(s)	88
4.2.6	Sequence determination of unknown protein	89
4.2.6.1	N-terminal sequencing	89
4.2.6.2	MS/MS sequencing	89
4.2.7	Protein expression and purification	90
4.2.7.1	Constructing plasmids containing the uranium(VI)-reductase gene	90

4.2.7.2	Expression and purification of uranium(VI)-reductase	
954.2.8	Modelling	
	96	
4.2.9	Uranium(VI) reduction by purified recombinant protein	97
4.3	Results and discussions	98
4.3.1	Protein expression by <i>Thermusscotoductus</i> SA-01 in response to uranium exposure	98
4.3.2	Determination of uranium(VI) reduction activity in subcellular fractions	100
4.3.3	SDS-PAGE	105
4.3.4	Isolation of uranium reductase(s) by chromatographic methods	105
4.3.4.1	Screening of optimum chromatographic media	105
4.3.4.2	Anion exchange (Super Q-Toyopearl)	106
4.3.4.3	Cation exchange (SP-Toyopearl)	107
4.3.5	Sequence determination of unknown protein	108
4.3.6	Protein expression and purification	115
4.3.6.1	Cloning and sequencing of the ABC gene from <i>Thermus scotoductus</i> SA-01	115
4.3.7	Expression and purification of the recombinant ABC proteins	119
4.3.8	Modelling	121
4.3.9	Characterization of the recombinant ABC proteins	123
4.3.9.1	The effect of pH on uranium(VI) reduction	123
4.3.9.2	The effect of temperature on uranium(VI) reduction	125
4.4	Conclusions	127
4.5	References	129
	SUMMARY	133
	OPSOMMING	135

LIST OF FIGURES

- Figure 1.1:** Transmission electron micrograph of *D. desulfuricans* G20. The location of the cytoplasm, periplasm, inner membrane (IM), and outer membrane (OM) are indicated with arrows (taken from Payne, 2005). 4
- Figure 1.2:** Schematic representation of iron-reduction indicating the colour difference between the two redox states. 6
- Figure 1.3:** Lovley Model of uranium(VI)-reduction for *Desulfovibrio vulgaris*. Each arrow indicates electron flow and implies a single step process (taken from Payne, 2005). 10
- Figure 1.4:** A model for possible electron transport for U(VI)-reduction (taken from Wall and Krumholz (2006), adapted from Beliaev and Saffarini in 1998). MQ, menaquinone; CymA, tetraheme membrane-bound cytochromes; Cct, tetrahemeperiplasmic cytochromes; OmcA, decaheme outer membrane cytochromes; MtrA, decahemeperiplasmic cytochromes; MtrB, outer membrane structural protein, MtrC, decaheme outer membrane cytochrome. 11
- Figure 1.5:** *Geobactersulfurreducens*, with “nanowire” pili seen only on one side of the bacterium (taken from Geobacter Project, 2007). 13
- Figure 1.6:** TEM image of a *Saccharomyces cerevisiae* cell accumulating uranium(VI) outside (arrow A) and inside (arrow B) (taken from Ohnukiet *al.*, 2005). 14
- Figure 1.7:** Organic matter degradation in anaerobic environments (taken from Anderson and Lovley, 2002). 19

Figure 1.8: Conceptualized bioremediation scheme for stimulated uranium(VI)-reduction *in situ* upon bulk addition of a suitable electron donor (taken from Anderson and Lovley, 2002). 20

Figure 3.1: Standard curve indicating the relationship between uranium(VI) and OD ($R^2 = 0.9991$). Standard deviations are smaller than the symbols. 47

Figure 3.2: Genomic DNA extracted from *T. scotoductus*. Lane M, MassRuler™ DNA ladder (Fermentas); Lane 1, isolated gDNA. 53

Figure 3.3: Amplification of 16S rRNA fragment using genomic DNA. Lane M, MassRuler™ DNA ladder (Fermentas); Lane 1, amplified 16S fragment; Lane 2, Negative Control. 54

Figure 3.4: Restriction digest with *Sma*I and *Avr*II. A) *T. scotoductus*SA-01 16S rRNA fragment. Lane M, MassRuler™ DNA ladder (Fermentas); Lane 1, *Avr*II digested fragment; Lane 2, *Sma*I digested fragment. B) Virtual digest of both the 16S rRNA fragments from *T. scotoductus*SA-01 and *T. thermophilus*HB27. Lane 1, *T. scotoductus*SA-01 16S digested with *Avr*II; Lane 2, *T. scotoductus*SA-01 16S digested with *Sma*I; Lane 3, *T. thermophilus*HB27 16S digested with *Avr*II; Lane 4, *T. thermophilus*HB27 16S digested with *Sma*I. 55

Figure 3.5: Standard curve indicating the the relationship between Biomass vs OD standard curve. Standard deviations are smaller than symbols, symbols represent data in triplicate. 58

Figure 3.6:Growth curve of *T scotoductus*SA–01 pre-inoculum in TYG medium. Standard deviations are smaller than symbols, symbols represent data in triplicate. 59

Figure 3.7: Growth curve of *T. scotoeductus* SA-01 in TYG medium, growth started from cells in late exponential phase obtained from pre-inoculum. Standard deviations are smaller than symbols, symbols represent data in triplicate. 60

Figure 3.8: Growth curve of *T. scotoeductus* SA-01 in TYG medium. Standard deviations are shown. 61

Figure 3.9: Growth of *T. scotoeductus* SA-01 in TYG medium (■) amended with 0.25 mM (▲), 0.5 mM (▼), 0.75 mM (◆), 1.0 mM (●), 1.25 mM (□) and 1.5 mM (△) uranium(VI) during inoculation (t = 0). Standard deviations are shown or are smaller than symbols. 62

Figure 3.10: Growth curves for *T. scotoeductus* SA-01 in TYG medium (■), amended with 1.5 mM (▲), 2.0 mM (◆), 3.0 mM (□) and 5.0 mM (△) uranium(VI) after 6 hours of growth and 1.5 mM (▼) and 2.0 mM (●) uranium(VI) added during inoculation. Standard deviations are mostly smaller than symbols. 64

Figure 3.11: (A) Whole cell reduction of uranium(VI) by the thermophile *T. scotoeductus* SA-01 under anaerobic conditions. Cells harvested in late exponential phase with assay solution containing 0.25 mM uranium(VI) and 10 mM lactate as electron donor (■), control assay solution of cells harvested in late exponential phase containing 0.25 mM uranium(VI) and no electron donor (▲), cells harvested in early exponential phase with assay solution containing 0.25 mM uranium(VI) and 10 mM lactate as electron donor (◆), control assay solution of cells harvested in early exponential phase containing 0.25 mM uranium(VI) and no electron donor (●), control assay solution lacking cells with 10 mM lactate (▼). Symbols represent an average of data in triplicate. (B) Whole cell reduction of uranium(VI) by the thermophile *T. scotoeductus* SA-01 under anaerobic conditions after 20 h, note the formed uranium(IV) black precipitate. (C) Cells from (B) after overnight exposure to oxygen,

note the disappearance of the formed precipitate. 66

Figure 3.12: Whole cell reduction of uranium(VI) by the thermophile *T. scotoductus* SA-01 under anaerobic conditions. Autoclaved cells harvested in late exponential phase with assay solution containing 0.25 mM uranium(VI) and 10 mM lactate as electron donor (■), control assay solution of cells harvested in late exponential phase containing 0.25 mM uranium(VI) and 10 mM lactate as electron donor (▲), control assay solution lacking cells with 10 mM lactate (◆). Standard deviations are smaller than symbols. Symbols represent an average of data in triplicate. 67

Figure 3.13: (A) Percentage uranium(VI) reduced by the thermophile *T. scotoductus* SA-01 under anaerobic conditions with different electron donors after 2 hours. Symbols represent an average of data in triplicate. **(B)** Whole cell uranium(VI) reduction by the thermophile *T. scotoductus* SA-01 under anaerobic conditions with different electron donors, Acetate (■), Glucose (▲), Pyruvate (▼), Lactate (◆), and H₂ (●). A control with no electron donor (□) can also be observed. 69

Figure 3.14: (A) Whole cell reduction of uranium(VI) by the thermophile *T. scotoductus* SA-01 under anaerobic conditions at different pH 5.5 (■), pH 6.0 (▲), pH 6.5 (▼), pH 7.0 (◆), pH 7.5 (●), pH 8.0 (◇), pH 8.5 (□), pH 9.0 (△), pH 5.5 Blank (▽) and pH 9.0 Blank (○). Standard deviations are shown. **(B)** Optimum pH of whole cell uranium(VI) reduction. 71

Figure 3.15: (A) Whole cell reduction of uranium(VI) by the thermophile *T. scotoductus* SA-01 under anaerobic conditions at temperature 35 °C (■), 45 °C (▲), 55 °C (▼), 65 °C (◆) and 75 °C (●) with the appropriate cell free controls at 35 °C (□), 45 °C (△), 55 °C (▽) 65 °C (○) and 75 °C (◇). Standard deviations are shown. Standard deviations are shown **(B)** Percentage uranium(VI) reduced after 8 hours. 72

- Figure 3.16:** TEM electron micrographs of *T. scotoductus* SA-01 cells in the absence of uranium (A) and in the presence of 1.25 mM of uranium (B, C). 74
- Figure 3.17:** Elemental analysis with SEM-coupled EDS. (A) Heavy metal cluster. (B) Results from mapping showing uranium scattering. (C) Pin-point analysis performed by EDS. 75
- Figure 4.1:** BCA protein assay kit standard curve ($R^2 = 0.9960$). 84
- Figure 4.2:** Vector map of pET28b(+). 93
- Figure 4.3:** 2-D SDS-PAGE gels, stained with Coomassie® Brilliant Blue of IPG strips pH 3 to 10. (A) From cells grown in 1.25 mM uranium. (B) From cells grown in TYG medium with no uranium. 99
- Figure 4.4:** 2-D SDS-PAGE gels, stained with Bio-Rad Flamingo® Fluorescent Stain of IPG strips pH 4 to 7. A) From cells grown in 1.25 mM uranium. B) From cells grown in TYG medium with no uranium. 99
- Figure 4.5:** 2-D SDS-PAGE gels, stained with Bio-Rad Flamingo® Fluorescent Stain of IPG strips pH 5 to 8. A) From cells grown in 1.25 mM uranium. B) From cells grown in TYG medium with no uranium. 100
- Figure 4.6:** Uranium(VI) reduction activity of the periplasmic fractions of SA-01, after dialysis. 101
- Figure 4.7.** Uranium(VI) reduction activity of the different protein fractions from *T. scotoductus* SA-01, after dialysis. (■) Periplasm; (▼) Cytoplasm; (◆) Membrane; (●) Combination of periplasmic and membrane fractions; (▲) Combination of the periplasmic, cytoplasmic and membrane fractions. 102

Figure 4.8: Uranium(VI) reduction activity of the different protein fractions from *T. scotoductus* SA-01, after dialysis and being purged with 10% H₂ mix gas. (■) Periplasm; (▼) Cytoplasm; (◆) Membrane; (▲) Combination of the periplasmic, cytoplasmic and membrane fractions; (●) Combination of the periplasmic and membrane fraction; (△) Combination of the periplasmic and cytoplasmic fractions; (▽) Combination of the membrane and cytoplasmic fractions. 103

Figure 4.9: Uranium(VI) reduction activity of the combination of the membrane and periplasmic fractions from *T. scotoductus* SA-01, after dialysis and being purged with 10% H₂ gas, hydroquinone and a combination of both as electron donors. (■) H₂ and hydroquinone as electron donor; (▲) Hydroquinone as electron donor; (▼) H₂ as electron donor. 104

Figure 4.10: Formed precipitate from the reduction of uranium(VI) by the combination of the membrane and periplasmic fractions from *T. scotoductus* SA-01, after dialysis with 10% H₂ gas and hydroquinone as electron donors. Photo taken inside the anaerobic cabinet. 104

Figure 4.11: SDS-PAGE gel electrophoresis of subcellular fractions. Lane M, Precision Plus Protein™ Standards (Bio-Rad); Lane 1, Periplasmic fraction; Lane 2, Membrane fraction; Lane 3, Cytoplasmic fraction. 105

Figure 4.12: Elution profile obtained for the purification step on Super Q-Toyopearl anion exchange resin. The regions between the arrows (A-B), (C-D) and (E-F) were monitored for uranium(VI) reduction activity. 106

Figure 4.13: Elution profile for the SP Toyopearl, peaks D, E and F produced uranium(VI) reduction activity. 107

Figure 4.14: SDS-PAGE gel electrophoresis of selected fractions from chromatographic separation on the SP Toyopearl resin. Lane M, Precision Plus Protein™ Standards (Bio-Rad); Lane 1, Peak B; Lane 2, Peak C 16; Lane 3, Peak D; Lane 4, Peak E; Lane 5, Peak A-A. 108

Figure 4.15: A-D show the annotated fragmentation spectra for the different sized spectra. All sizes are a value of mass divided by charge (m/z). (A) 1464.744; (B) 1753.86; (C) 1541; (D) 1892. 114

Figure 4.16: PCR product from amplification of the ABC transporter gene. Lane M, Molecular mass marker ; Lane 1, the amplified ABC transporter, peptide-binding protein. 115

Figure 4.17: pGEM®-T Easy plasmid containing the ABC gene digested with *EcoRI* and *NdeI*. Lane M, Molecular mass marker; Lanes 1 to 10, the clones screened for inserts. 116

Figure 4.18: pET28b(+) plasmid containing the ABC gene digested with *EcoRI* and *NdeI*. Lane M, Molecular mass marker; Lanes 1 to 10 the clones screened for inserts. 117

Figure 4.19: Elution profile for purification of the pET28b(+) expressed protein. 120

Figure 4.20: (A) SDS-PAGE analysis of the recombinant ABC protein when using the pET28b(+). Lane M, Precision Plus Protein™ Standards(Bio-Rad); Lane 1, Protein at 4h after induction. (B) SDS-PAGE analysis of all proteins after IPTG induction. Lane M, Precision Plus Protein™ Standards (Bio-Rad); Lane 1, 0h after induction; Lane 2, 2h after induction. 121

Figure 4.21:(A) and (B) Homology model of ABC peptide binding protein from *T. scotoductus* SA-01. The surface exposed disulphide bond which is hypothesized to be involved in the reduction of uranium is shown in yellow. (C) Detail of the environment of the disulphide bond . 122

Figure 4.22: Reduction of uranium(VI) at different pH values. (A) pH values (■) 5.5, (▲) 6.0, (▼) 6.5, (△) pH 7.0, (◆) 5.5 protein free control, (●) pH 6.0 protein free control, (□) pH 6.5 protein free control, (▽) pH 7.0 protein free control. (B) pH values (▲) 7.5, (■) 8.0, (▼) 8.5, (◆) 9.0, (□) pH 7.5 protein free control, (●) pH 8.0 protein free control, (△) pH 8.5 protein free control, (▽) pH 9.0 protein free control 124

Figure 4.23: Reduction of uranium(VI) at different temperature values. (A) 35°C. (B) 45 °C. (C) 55 °C. (D) 65°C. (E) 75 °C.(■) The indicated temperature, (□) protein free control. 125

Figure 4.24: Reduction of uranium(VI) at 55 °C (■) and 65°C (▲) with the blank rate subtracted. 126

LIST OF TABLES

Table 1.1: Bacteria shown to reduce U(VI) to U(IV) (taken from Wall and Krumholz, 2006).	2
Table 3.1. Master mix for the hot start PCR reactions.	41
Table 3.2. Composition of materials of a hot start PCR program.	41
Table 3.3. Ligation mixture composition for the pGEM [®] -T Easy vector system.	42
Table 3.4. Restriction digests reaction composition.	44
Table 3.5. Values obtain from dry weight determination.	56
Table 3.6. Dilution range used as well as optical density reading.	46
Table 3.7. Values used for construction of the Biomass to OD standard curve.	57
Table 3.8. Specific growth rate and doubling time values for growth curves of <i>T. scotoductus</i> SA-01 in different concentrations of uranium.	63
Table 3.9. Biomass before and after uranium(VI) addition.	64
Table 4.1. Master mix for the hot start PCR reactions using Excel [®] Taq polymerase (CoreBioSystem).	91
Table 4.2. Ligation mixture composition for the pGEM [®] -T Easy vector system.	91
Table 4.3. Restriction digests reaction composition.	92

Table 4.4. Restriction digest reaction composition.	94
Table 4.5. Ligation mixture composition for the pET28b(+) vector system.	94
Table 4.6. Primer sequences utilized during sequencing.	95
Table 4.7. Relevant proteins with a 100% sequence identity to the protein query DNSLVIG.	109
Table 4.8. ClustalW alignment of the proteins with 100% sequence identity to the protein query DNSLVIG.	110
Table 4.9. ClustalW alignment of peptide peptide ABC transporter, peptide-binding proteins from <i>T. scotoductus</i> SA-01, <i>T. thermophilus</i> HB8 and HB27.	111
Table 4.10. Sequences obtained from fragmentation spectra,	112
Table 4.11. Sequence alignments of the reference ABC gene form the <i>T. scotoductus</i> SA-01 genome database and the cloned ABC gene form <i>T. scotoductus</i> SA-01.	117

LIST OF ABBREVIATIONS

%	Percentage
°C	Degrees Celsius
A	Absorbance
ABC	ATP-binding cassette
ATP	Adenosine triphosphate
BCA	Bicinchoninic acid
BLAST	Basic Local Alignment Search Tool
BSA	Bovine serum albumin
DEAE	Diethylaminoethyl
DNA	Deoxyribonucleic acid
EDS	Electron dispersive spectrum
EDTA	Ethylenediaminetetraacetic acid
EM	Electron microscopy
g	Gram
g/l	Gram per liter
gDNA	Genomic DNA
h	Hour
IPTG	Isopropyl β -D-1-thiogalactopyranoside
kb	kilobasepair
kDa	kilo Dalton
kV	kilo Volt
LB	Luria-Bertani
μ g	Microgram
μ g/ml	Microgram per milliliter
μ l	Microliter
μ m	Micrometer
μ M	Micromolar
μ mol	Micromole

M	Molar
Mg/ml	Milligram per milliliter
min	Minute
ml	Milliliter
ml/min	Milliliter per minute
mm	Millimeter
mM	Millimolar
MOPS	3-(N-Morpholino)propanesulfonic acid hemisodium salt
Mr	Relative molecular mass
MWCO	Molecular weight cut-off
NADH	Reduced nicotinamide adenine dinucleotide
NADP ⁺	Nicotinamide adenine dinucleotide phosphate
NADPH	Reduced nicotinamide adenine dinucleotide phosphate
ng/μl	Nanogram per microliter
nm	Nanometer
OD	Optical density
ORF	Open reading frame
PAGE	Polyacrylamide gel electrophoresis
PCR	Polymerase chain reaction
RFLP	Restriction fragment length polymorphisms
RNA	Ribonucleic acid
rpm	Revolutions per minute
SDS	Sodium Dodecyl Sulphate
TE-buffer	Tris-EDTA buffer
TEM	Transmission Electron Microscopy
Tris	2-Amino-2-(hydroxymethyl)-1,3-propanediol
TYG	Tryptone, yeast extract, glucose
U	Units
UV	Ultraviolet
UV-Vis	Ultraviolet –visible

V/cm	Volts per centimetre
v/v	Volume per volume
W	Watt
w/v	Weight per volume
x g	Times gravity
x	Times
X-Gal	5-bromo-4-chloro-3-indolyl-beta-D-galactopyranosidehosphate

Chapter 1

Literature review

1.1 General introduction

Uranium is the forty-ninth most abundant metal in the earth's crust and thus natural uranium is quite ubiquitous in nature, primarily as 3 of its 17 known isotopes, namely ^{238}U (99.27%), ^{235}U (0.72%) and ^{234}U (0.005%) (Wall and Krumholz, 2006). Uranium can be readily oxidized and reduced, with the most important oxidation states of uranium being uranium(IV) and uranium(VI), as found in uranium dioxide (UO_2) and uranium trioxide (UO_3). Uranium is readily oxidized under oxic conditions to the soluble salt of uranyl ion (UO_2^{2+}), and is thus in the uranium(VI) oxidation state, when reduced to uranium (IV) the solubility decreases and precipitation occurs (Lovley and Coates, 1997). The process of uranium-reduction was generally thought to be dominated by abiotic reactions until the recent discovery of anaerobic microorganisms capable of coupling growth to uranium-reduction (Lovley *et al.*, 1991). This discovery indicated that microorganisms can catalyse the oxidation and reduction of uranium and proved them to play a significant, and perhaps dominant, role in the biogeochemical cycling of uranium (Ehrlich, 1990). Microbial interactions with the uranyl ion have been extensively studied over the last two decades, with a growing list of organisms capable of uranium(VI)-reduction (Table 1.1) being discovered. However, it has been established that predominantly dissimilatory Fe(III)-reducing (Lovley *et al.*, 1991) and sulfate-reducing microorganisms (Lovley and Phillips, 1992a, Lovley *et al.*, 1993a) are able to reduce uranium(VI) to uranium(IV). Sulfate-reducing bacteria (SRB) and iron-reducing bacteria (IRB) constitute a phylogenetically diverse group of organisms from hyperthermophilic Archaea to anaerobic Proteobacteria. Included in this diverse range of organisms, species of the *Geobacter*, *Shewanella* and *Desulfovibrio* genera are the most intensively studied due to their remarkable respiratory versatility, which includes the ability to utilize uranium(VI) as a terminal electron

acceptor (Lovley and Phillips, 1992b; Nealson and Saffarini, 1994; Lovley *et al.*, 2004). Additionally, the dissimilatory iron- and sulphate-reducing bacteria are environmentally ubiquitous, are found over an extensive range of pH and salt concentrations, and can tolerate a variety of heavy metals and dissolved sulfides (Jones *et al.*, 1976; Liu *et al.*, 2002). Utilization of such a wide spectrum of terminal electron acceptors is largely due to the diversified respiratory network found in these organisms (Marshall *et al.*, 2008). Literature (Shelobolina *et al.*, 2004) indicated that *c*-type cytochromes form an integral part of the terminal reductase complexes, and these observations indicate that cytochromes are either involved in the transfer of electrons to the terminal electron acceptors or are the terminal reductases. Localization of these various cytochromes was observed in the periplasm and with either the cytoplasmic or outer membrane (Myers and Myers, 1992).

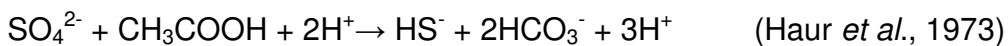
Table 1.1: Bacteria shown to reduce U(VI) to U(IV) (taken from Wall and Krumholz, 2006).

<i>Anaeromyxobacter dehalogenans</i> strain 2CP-C
<i>Cellulomonas flavigena</i> ATCC TCC 482 482 ^a
<i>Cellulomonas</i> sp. ES5
<i>Cellulomonas</i> sp. WS18
<i>Cellulomonas</i> sp. WS01 82
<i>Clostridium</i> sp.
<i>Clostridium sphenoides</i> ATCC TCC 19403
<i>Deinococcus radiodurans</i> R1
<i>Desulfomicrobium norvegicum</i> (formerly <i>Desulfovibrio baculatus</i>) DSM 1741
<i>Desulfotomaculum reducens</i>
<i>Desulfosporosinus orientis</i> DSM 765
<i>Desulfosporosinus</i> sp. P3
<i>Desulfovibrio baarsii</i> DSM 2075
<i>Desulfovibrio desulfuricans</i> ATCC TCC 29577
<i>Desulfovibrio desulfuricans</i> strain G20 (to be renamed <i>Desulfovibrio alaskensis</i>)
<i>Desulfovibrio</i> sp. UFZ B 490 72, 73
<i>Desulfovibrio sulfodismutans</i> DSM 3696
<i>Desulfovibrio vulgaris</i> Hildenborough ATCC TCC 29579
<i>Geobacter metallireducens</i> GS-15
<i>Geobacter sulfurreducens</i>
<i>Pseudomonas putida</i>
<i>Pseudomonas</i> sp.
<i>Pseudomonas</i> sp. CRB5

Pyrobaculum islandicum
Salmonella subterranean sp. nov. strain FRC1
Shewanella alga BrY
Shewanella oneidensis MR-1 (formerly *Alteromonas putrefaciens*, then
Shewanella putrefaciens MR-1)
Shewanella putrefaciens strain 200
Thermoanaerobacter moanaerobacter sp.
Thermoterrabacterium moterrabacterium ferrireducens
Thermus scotoductus SA-01
Veillonella alcalescens (formerly *Micrococcus lactilyticus lactilyticus*)

1.2 The sulfate-reducing bacteria

Sulfate-reducing bacteria (SRB) are microorganisms characterized by their ability to utilize sulfate as a sole electron acceptor during growth, reducing it to sulfide. Most sulfate-reducing bacteria can also use other oxidized sulfur compounds such as sulfite and thiosulfate, or elemental sulfur (Postgate, 1976). A typical overall conversion equation is given below (neglecting the small amount of organic material required to produce biomass):



Eight electrons are transferred from the energy source acetic acid to the electron acceptor sulfate in order to produce sulfide. Microbially produced reduced sulfide serves as a source of sulphur for both higher plants and animals. The main genus for SRB is *Desulfovibrio* which are Gram-negative, slightly curved rods, typically about 1µm in length (Figure 1.1). Depending on their oxidative capability, SRB can be divided into two subgroups: firstly, the group which can completely oxidize the organic substrate to CO₂, and, secondly, the group that produces acetate as an end product from incomplete oxidation of the organic substrate (Ibrahim *et al.*, 1981). The term 'dissimilatory sulphate-reduction' applies to the metabolic process of terminal electron transfer to sulphate and its subsequent reduction, where sulfate is not assimilated into any organic compound. In contrast, assimilatory sulphate-reduction is coined as the process

whereby sulfate is enzymatically reduced to sulphide, incorporated into cysteine, and then utilized in protein production (Kredich, 1996). Hydrogen gas can be utilized as an electron acceptor by most, but not all, during growth by sulphate-reduction (Postgate, 1976). Most SRB are considered to be strict anaerobes with exposure to oxygen being lethal in most cases, but some do however display varying levels of oxygen tolerance (Fournier *et al.*, 2003). Several species of SRB have been described for their ability to reduce inorganic aqueous ions in solution, while others have been shown to metabolize not only sulfate, but Fe(III), Cr(VI), U(VI), Mn(IV) and Tc(VII), among others (Lovley and Phillips, 1992b; Lovley *et al.*, 1993a; Tebo and Obratsova, 1998).

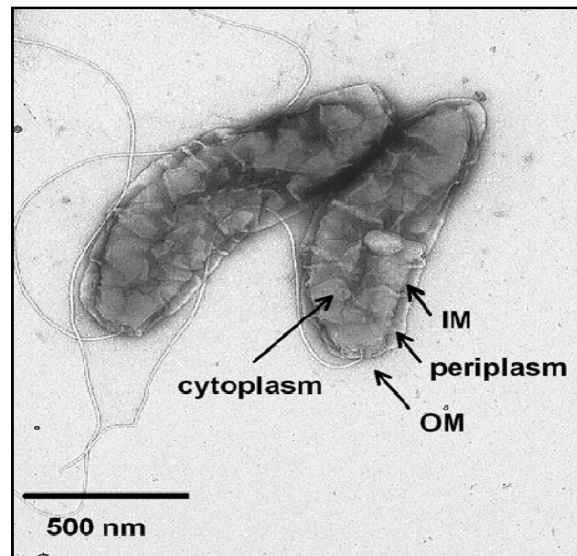


Figure 1.1: Transmission electron micrograph of *D. desulfuricans* G20. The location of the cytoplasm, periplasm, inner membrane (IM), and outer membrane (OM) are indicated with arrows (taken from Payne, 2005).

1.2.1 Uranium-reduction under sulfate-reducing conditions

Until the 1980's, uranium(VI)-reduction in anoxic environments was believed to be due to abiotic reduction by sulfide, hydrogen or organic matter since sulfate-reduction is a dominant microbial process in these environments (Langmuir, 1978; Maynard 1983). This close association between sulfide and uranium

minerals in anoxic environments posed a potential mechanism for uranium(VI)-reduction by sulfide (Adler, 1974). At relatively high concentrations of uranium(VI), larger than 3 mg/l (13 μ M) at pH 7 and 35°C (Mohaghegi *et al.*, 1985), abiotic reduction of uranium(VI) by sulfide has been demonstrated. This, however, does not explain the persistence of environmentally relevant concentrations, less than 0.8 mg/l (3.36 μ M) in environments where sulfide is present. This indicates that there is little potential for abiotic reduction of uranium(VI) in natural environments (Anderson *et al.*, 1989; Lovley *et al.*, 1991). In natural environments, the redox potential (E_h) of the U(IV)/U(VI) couple should be between -0.042 to 0.086 V depending on the Ca^{2+} and CO_3^{2-} concentrations. On the basis of thermodynamic principles, it could be predicted that uranium(VI) would be a preferred electron acceptor to SO_4^{2-} , S^0 or CO_2 (Wall and Krumholz, 2006). These predications are indicative that under natural conditions, sulfate-reducing organism would have the ability to reduce uranium quite effectively.

1.3 The iron-reducing bacteria

Dissimilatory metal-reducing bacteria (DMRB) possess the ability to reduce a wide array of different metals and radionuclides which include Fe(III), Mn(IV), U(VI), Cr(VI), Co(III) and Tc(VIII), among others (Gorby and Lovley, 1992; Lovley *et al.*, 1991; Wildung *et al.*, 2000). It is well established that DMRB-facilitated reduction accounts for the majority of valence transitions of the oxidized ferric form, Fe(III), to the reduced ferrous form, Fe(II) (Figure 1.2), in anoxic, non-sulfidogenic and low-temperature environments. In order for a microorganism to be able to donate electrons to an electron acceptor, thereby reducing the said electron acceptor, it has to have a redox potential in a range where it is low enough to not be toxic but also high enough to be energetically favorable. Here, Fe(III) meets these criteria. The microbial reduction of Fe(III) to Fe(II) has been proven to be of great biological significance since iron plays an essential metabolic role in cellular processes where it can be either a component of metalloproteins or a co-factor for enzymatic reactions. Iron can also serve as an

energy source in catabolic iron metabolism for some microorganisms (Nealson and Saffarini, 1994). Similarly to the sulfate-reducing bacteria described previously, microbial iron-reduction can also occur in an assimilatory or dissimilatory fashion. Dissimilatory iron-reducers can be grouped into two major groups: those that support growth by conserving energy from electron transfer to Fe(III) (Lovley *et al.*, 1991; Nealson and Saffarini, 1994), and those that do not (Lovley, 1987).

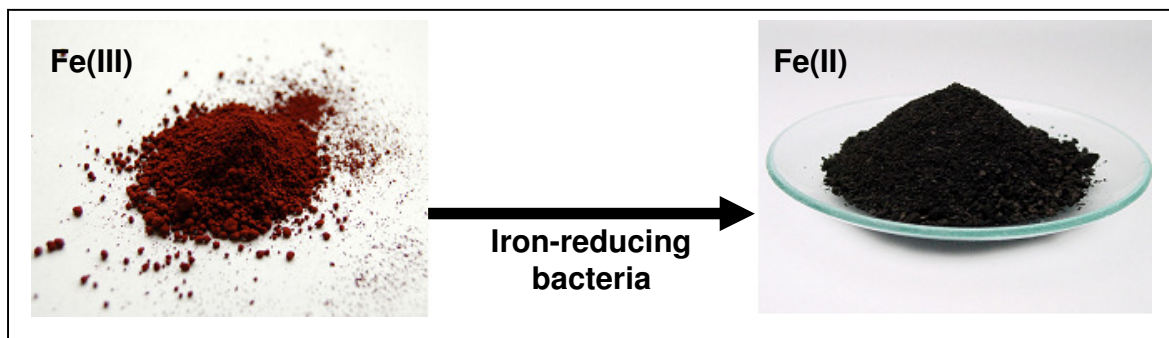


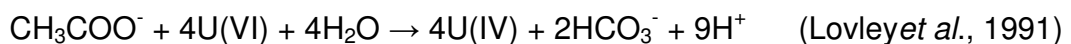
Figure 1.2: Schematic representation of iron-reduction indicating the colour difference between the two redox states.

DMRB are ubiquitous in nature and have been isolated from a variety of anoxic environments. 16S rRNA gene sequence evidence has determined that dissimilatory iron-reducing bacteria (DIRB) are widely distributed among bacteria and include genera from *Geobacter* (Lovley *et al.*, 1993c), *Shewanella* (Myers and Nealson, 1988), *Pelobacter* (Lovley *et al.*, 1995), *Ferrimonas* (Rossello-Mora *et al.*, 1993), among others. Although most DIRB described are obligately anaerobic, there are some exceptions which include *Shewanella* spp. (Myers and Nealson, 1998) and *Ferrimonas balearica* (Rossello-Mora *et al.*, 1993).

1.3.1 Uranium-reduction under Fe(III)-reducing conditions

In mining environments where uranium contamination is present, high concentrations of NO_3^- and SO_4^{2-} will occur resulting from past acidic extractions and ongoing bioleach processes within uranium mill tailing piles (Abdelouas *et al.*, 1999). In the presence of high concentrations of NO_3^- , the stimulated

anaerobic processes will more than likely be dominated by NO_3^- -reduction since this is more energetically favourable. In contrast, if NO_3^- is absent in the system, the next most favorable process, Mn(IV)-reduction, will become dominant. However, since Mn(IV) abundance is generally low in the environment, it is not likely to be a major electron acceptor in comparison to Fe(III) (Lovley, 1995). Since Fe(III) is abundant in the environment, metabolic processes coupled to Fe(III)-reduction are likely to dominate upon NO_3^- depletion and the possibility exists that the Fe(III)-reducing bacteria could be dominant under these circumstances. Fe(III)-reducing bacteria are known to reduce uranium(VI) and are predicted to be the dominant uranium(VI)-reducers during *in situ* uranium(VI)-reduction (Lovley *et al.*, 1991; Gorby and Lovley, 1992). Here, the concept of microbial respiratory uranium-reduction is still in its infancy. In 1991, Lovley and co-workers proved that Fe(III)-reducing bacteria have the ability to couple growth to the reduction of uranium(VI). This is not surprising since, when compared to Fe(III)-reduction, thermodynamic calculations indicate that, per electron transferred, acetate oxidation coupled to uranium(VI)-reduction has the potential to yield more than twice the energy available from Fe(III)-reduction (Cochran *et al.*, 1987; Lovley *et al.*, 1991). These results indicate that a Fe(III)-reducing microorganism can obtain energy for growth by oxidizing acetate with the reduction of uranium(VI) to uranium(IV) according to:



Fe(III) reducers from the genera *Geobacter* and *Shewanella* have been the focus point for investigations regarding microbial uranium(VI)-reduction (Wall and Krumholz, 2006). These organisms have shown the ability to utilize uranium(VI) as an electron acceptor by coupling the oxidation of acetate (*Geobacter*) or hydrogen (*Shewanella*) and obtaining, in the process, enough energy for growth (Lovley *et al.*, 1991). Members of the *Geobacter* family have been found to be present in a wide array of anaerobic environments and molecular studies have

indicated them as the dominant members of the Fe(III)-reducing microbial community in these environments (Rooney-Varga *et al.*, 1999).

1.3.2 Uranium-reduction by Fe(III)-reducing bacteria under thermophilic conditions

Thermophilic conditions have been defined as conditions of elevated temperatures between 45 and 80°C, and above. A thermophile is an organism, a type of extremophile, adapted to growth in these extreme conditions. Recently, several thermophilic dissimilatory iron-reducing bacteria (DIRB) have been identified, including *Bacillus infernus* (Boone *et al.*, 1995), *Thermoterrabacterium* (Slobodkin *et al.*, 1997), *Deferribacter thermophilus* (Green *et al.*, 1997) and *Thermoanaerobacter* spp. (Liu *et al.*, 1997). Some thermophilic Fe(III)-reducing microorganisms are even capable of uranium(VI)-reduction which might explain high temperature uranium deposits (Kieft *et al.*, 1999; Kashefi and Lovley, 2000). *Thermus scotoductus* SA-01, a deep subsurface *Thermus* species, isolated 3.2 kmbls from a South African gold mine, grows optimally at 65°C and is able to utilize various terminal electron acceptors such as Fe(III), Cr(VI), both aerobically and anaerobically (Möller and van Heerden, 2006; Opperman and Van Heerden, 2007), Mn(IV) and Co(III). It has also shown the ability to reduce uranium(VI) in cell suspension with lactate as an electron donor (Kieft *et al.*, 1999). The hyperthermophilic organism, *Pyrobaculum islandicum*, has an optimal growth temperature of 100°C and is able to reduce uranium(VI) by using hydrogen as an electron donor (Kashefi and Lovley, 2000). Thus far, none of these organisms has shown the ability to couple growth to uranium(VI)-reduction.

1.4 Uranium reductases

The list of bacteria able to reduce uranium(VI) to uranium(IV) is growing (Table 1.1), but still a complete understanding of the biochemistry involved in this process in any one of the bacteria is lacking. To this end, the

identity of the uranium(VI) reductase and the pathway of electron flow from substrates to enzyme have been sought to: “better understand the enzymatic process, to make an evaluation of the ecological distribution of the potential of uranium reduction, to identify any amendments that might stimulate the reduction, and to determine the possibility of genetic manipulation to increase the amount or activity of the reductase” (Wall and Krumholz, 2006). Since uranium has no known biological function, and is not known to be an essential component of any enzyme or biological structure, a dedicated “uranium-reductase” has not been identified.

1.4.1 *Desulfovibrio* reductase(s)

Although sulfate-reducers couple the oxidation of hydrogen or lactate to the reduction of uranium(VI), they are unable to obtain enough energy for growth from this mechanism (Lovley and Phillips, 1992b). As stated previously, most of the work done on sulfate-reducers regarding enzymatic uranium-reduction has been performed on organisms of the *Desulfovibrio* genera, since they have the ability to tolerate high levels of uranium, up to 24 mM, and it has been found that strains containing hydrogenase and a tetraheme cytochromes c_3 were capable of uranium(VI)-reduction. Thus, the suggested hypothesis is a pathway of electron flow with hydrogen as an electron donor to hydrogenase to cytochromes c_3 to uranium(VI) (Figure 1.3) (Lovley *et al.*, 1993b).

Involvement of the tetraheme cytochromes c_3 was confirmed during whole cell experimentation where the oxidation the reduced cytochromes c_3 was observed during uranium(VI)-reduction, but not during sulfate-reduction with hydrogen as the electron donor (Elias *et al.*, 2004).

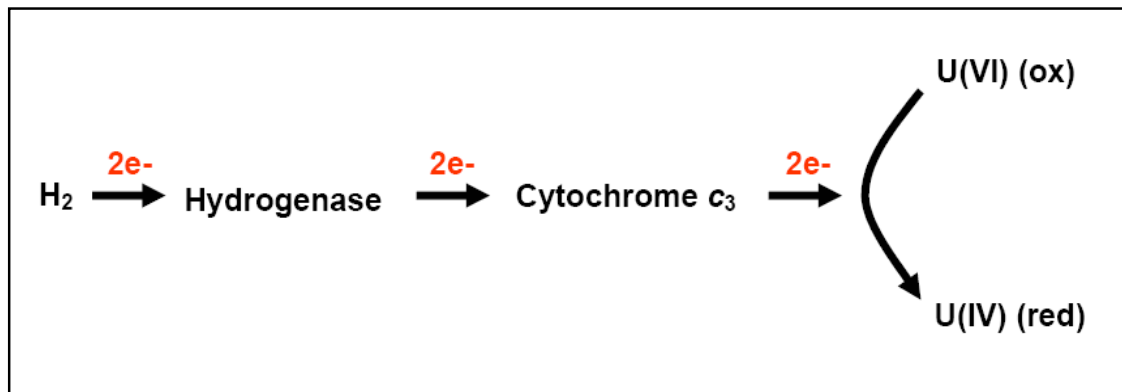


Figure 1.3: Lovley Model of uranium(VI)-reduction for *Desulfovibrio vulgaris*. Each arrow indicates electron flow and implies a single step process (taken from Payne, 2005).

1.4.2 *Shewanella reductase(s)*

Although a large number of microorganisms have been identified to be able to reduce uranium(VI), only four strains are known to be able to obtain enough energy from uranium(VI) respiration to support growth: *Geobacter metallireducens* (Lovley and Phillips, 1992b), *Desulfotomaculum reducens* (Shelobolina *et al.*, 2004), *Carboxydotherrmus ferrireducens* (previously *Thermoterrabacterium ferrireducens*) (Kennedy *et al.*, 2004; Slobodkin *et al.*, 2006) and the facultative anaerobe *Shewanella putrefaciens* (Lovley and Phillips, 1992b). The assumption was thus made that the reductases utilized by those microorganisms capable of growth by metal reduction coupling, might also be the reductases functioning in uranium(VI)-reduction. Early work with *Shewanella putrefaciens* indicated that cells limited for Fe were unable to use Fe(III) as a terminal electron acceptor and also displayed a major decrease in c-type cytochromes content (Obuekwe and Westlake, 1987). This discovery gave a clear indication that cytochromes were involved in the transfer of electrons to the terminal electron acceptors or that they were the terminal reductases. Subsequently, various cytochromes from *Shewanella* have been shown to be localized in the periplasm with either the cytoplasmic or outer membrane (Myers and Myers, 1992). Further mutant analysis has started to implicate other proteins and cytochromes to be involved in metal reduction and a model (Figure 1.4) for electron transfer was proposed by

Beliaev and Saffarini in 1998. This model emphasized the possibility of reduction at multiple sites in the periplasm and outer membrane. Mutant analysis also showed that several proteins were needed for optimal uranium(VI)-reduction which include a protein involved in menaquinone biosyntheses (MenC), an outer membrane protein (MtrB), a periplasmic decaheme cytochrome (MtrA), an outer membrane decaheme cytochrome (MtrC, also named OmcB) and a tetraheme cytochrome (CymA). It was also found that multiple pathways for uranium(VI)-reduction was possible since mutants lacking one or more of the electron transfer components were still able to reduce uranium(VI) although not as efficiently (Bencheikh-Latmani *et al.*, 2005). This result supports the hypothesis that: “Uranium reductases are likely non-specific, low potential electron donors present in both the periplasm and the outer membrane” (Wall and Krumholtz, 2006).

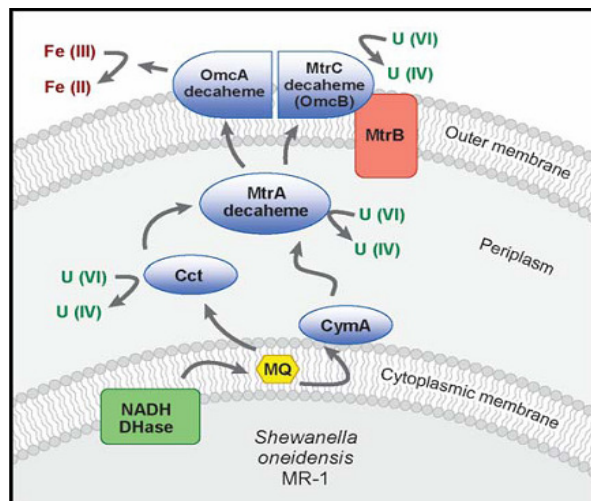


Figure 1.4: A model for possible electron transport for U(VI)-reduction (taken from Wall and Krumholz (2006), adapted from Beliaev and Saffarini in 1998). MQ, menaquinone; CymA, tetraheme membrane-bound cytochromes; Cct, tetraheme periplasmic cytochromes; OmcA, decaheme outer membrane cytochromes; MtrA, decaheme periplasmic cytochromes; MtrB, outer membrane structural protein; MtrC, decaheme outer membrane cytochrome.

1.4.3 *Geobacter* reductase(s)

As stated previously, very little is known about the mechanism of microbial uranium(VI)-reduction and a complete understanding of this process in any of the

bacteria capable of uranium(VI)-reduction is thus still lacking. It is thought that subcellular location of microbially reduced uranium(IV) might suggest the localization of the uranium reductases as well. In early studies on *Geobacter metallireducens* (Gorby and Lovley, 1992), large amounts of extracellular uranium(IV) precipitate were detected at the cell surface indicating that this might be the site of uranium(VI)-reduction. However, due to the fact that the initial products of enzymatic uranium(VI)-reduction are between 1-5 to 200 nm, and thus being very small might be able to diffuse out of the periplasm prior to forming extracellular precipitates. In fact, subsequent studies performed on *G. sulfurreducens* have implicated periplasmic proteins being involved in uranium(VI)-reduction and also found uranium(IV) precipitate within the periplasm of cells actively reducing uranium(VI) (Shelobolina *et al.*, 2007). These studies have indicated that both periplasmic and outer membrane cytochrome's can play a role in microbial uranium(VI)-reduction. In a study by Shelobolina and co-workers in 2007 on *G. sulfurreducens*, they found that among the periplasmic cytochromes, only MacA, appeared to play a significant role in uranium(VI)-reduction and found evidence for extracellular uranium-reduction due to the significant impact on uranium(VI)-reduction obtained by elimination of outer membrane cytochromes. Once again though, elimination of possible reductases by mutation did decrease uranium(VI)-reduction, but it did not completely eliminate the capacity of the bacteria to do so.

1.4.3.1 Nanowires in uranium(VI)-reduction

G. sulfurreducens has shown the ability to interact with insoluble terminal electron acceptors, like the oxides of Fe(III) and Mn(IV), by means of pili. These pili have been observed to only be produced on one side of the bacterium (Figure 1.5). Through mutant analysis it was observed that these "nanowire" pili were necessary for reduction of insoluble Fe(III) oxides but not for attachment to the substrate. Conducting probe atomic force microscopy showed that the pili were highly conductive. It has been inferred that these nanowires conduct the

electrons from the electron donor to the acceptor to allow growth (Reguera *et al.*, 2005).

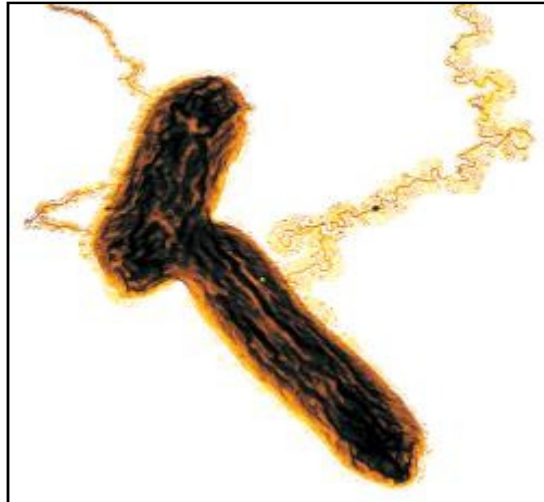


Figure 1.5: *Geobacter sulfurreducens*, with “nanowire” pili seen only on one side of the bacterium (taken from Geobacter Project, 2007).

One can thus assume that these “nanowires” can also be involved in uranium(VI)-reduction due to localization of the precipitated reduced uranium(IV). These “nanowires” have also been observed in *S. oneidensis* and *D. desulfuricans* G20 (Wall and Krumholz, 2006).

1.5 Effect of uranium(VI) on eukaryotes

Yeast is known to accumulate uranium(VI) and, in the case of *Saccharomyces cerevisiae*, this accumulation has been observed as needle-like fibrils on the cell surface (Figure 1.6) (Volesky and May-Phillips, 1995; Ohnuki *et al.*, 2005).

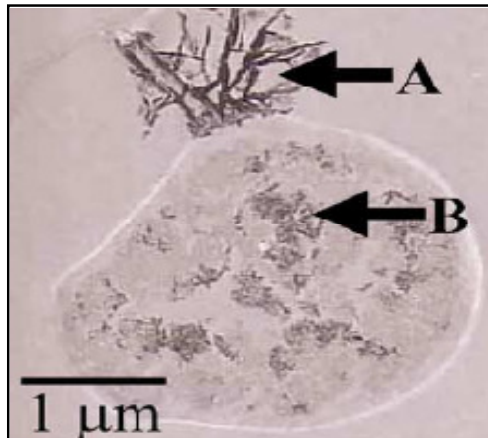


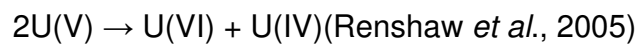
Figure 1.6: TEM image of a *Saccharomyces cerevisiae* cell accumulating uranium(VI) outside (arrow A) and inside (arrow B) (taken from Ohnuki *et al.*, 2005).

Living and dead biomass of *S. cerevisiae* has been found to differ in their ability to accumulate uranium(VI). Dead cells of *S. cerevisiae* have been found to be able to accumulate 40% more uranium(VI) than their living counterparts (Volesky and May-Phillips, 1995). Ohnuki and co-workers (2005) found that sorbed uranium(VI) on the cell's surfaces reacts with phosphates released by the cells to form the mineral H-autunite, HUO_2PO_4 , hence the cell's surface offers the specific conditions for this geochemical reaction. In a study conducted by Sakamoto and co-workers in 2007, protein expression was studied by 2D gel electrophoresis and the expression pattern of proteins was compared between uranium(VI) exposed and non-exposed cells of *S. cerevisiae*. They found that there were yeast proteins at pH 6.8 and 35 kDa, and pH 6.9 and 35 kDa being expressed in cells exposed to ^{238}U , but not to ^{233}U and also proteins at pH 7.2 and 20 kDa being expressed in cells exposed to ^{233}U but not to ^{238}U . To date, however, these proteins havenot been characterized (Sakamoto *et al.*, 2007).

1.6 Reduction by one electron or two?

For the reduction of uranium(VI) to uranium(IV), two electrons are required, however the mechanism by which a microorganism delivers the said two electrons has not been conclusively elucidated for any bacteria capable of

uranium-reduction (Wall and Krumholtz, 2006). During uranium(VI)-reduction, uncharged species of uranium(IV) will precipitate out of solution as the mineral uraninite. It has, however, been observed that this formation of uraninite precipitate will not occur directly upon its formation, but this delay of precipitation has yet to be explained (Gorby and Lovley, 1992). These results have led to two schools of thought. It is possible that uranium(VI) is reduced directly to uranium(IV) by a two electron transfer system, as described previously, where the two electrons are passed from an electron donor such as lactate or hydrogen to the cytochrome-type proteins by an unknown electron transfer chain, which in turn will then reduce the uranium(VI). Alternatively, the mechanism proposed by Renshaw and co-workers (2005) seems to indicate the formation of an uranium(V) intermediate, by one electron transfer, followed by disproportionation to uranium(VI) and uranium(IV). In this regard, uranium(V) disproportionates readily:



This particularly happens at pH values below neutral. Through X-ray absorption studies they found the substantial formation of uranium(V) before the appearance of uranium(IV), which indicated that the biological transformation may proceed *via* one-electron reduction of uranium(VI). Furthermore, when *G. sulfurreducens* was challenged with Neptunium(V), this compound was used as a proxy for uranium(V) since it does not disproportionate. *G. sulfurreducens* did not reduce the pentavalent actinide and thus, by extrapolation, it was concluded that uranium(V) was an unlikely substrate for reduction as well. Consequently, single-electron reduction of uranium(VI) to uranium(V) followed by disproportionation was suggested as a likely mechanism for reduction (Renshaw *et al.*, 2005).

1.7 Uranium in the environment

The possible migration of uranium from uranium-mining and –processing operations, as well as from the deep subsurface repositories of nuclear fuel and other radioactive wastes, is of serious environmental concern. Although uranium is radioactive, it is the chemical toxicity that is of greatest ecological risk (Markich, 2002). Uranium has no biological function and is 20 to 40 times more toxic to cells at low concentrations than either copper or nickel (LeDuc *et al.*, 1997). On a microbial scale, uranium will bind to the cell leading to metabolic inhibition (Bencheikh-Latmani and Leckie, 2003) and in humans and animals uranium ingestion could lead to kidney failure and cancer (Kurttioet *al.*, 2006). Since uranium is the forty-ninth most abundant element in the earth's crust, it is not rare, but the anthropogenic use of uranium for nuclear research, fuel production and weapons manufacturing only furthers the spread of uranium contamination in the environment (Markich, 2002). Where uranium was utilized in the production of weapons and fuel, much higher levels of radiation exist than from mining effluents. Contamination of groundwater with uranium has mainly been due to uranium mining and processing activities. Most of these mining sites have very low levels of uranium contamination and, most of the time, the sources of the uranium contamination have been contained (Wall and Krumholtz, 2006). The mobility of uranium in the environment is largely determined by its oxidation state. Oxidized uranium, uranium(VI), is relatively soluble and thus mobile in the environment. Reduced uranium, uranium(IV), is highly insoluble and will thus precipitate out of solution. This oxidation state is most often associated with uranium-containing ores. Presumably, these uranium-containing ores occur as the soluble uranium(VI), mobilized in oxidized groundwater where it comes in contact with an organic-rich region localized in the permeable sedimentary rock. This organic material then has the ability to act as an electron source for uranium(VI)-reduction which results in the localization of uranium(IV) ore deposits (Langmuir, 1978).

1.7.1 Bioremediation of environmental uranium

Reduced uranium(IV) is highly insoluble in water and oxidized uranium(VI) is highly soluble and thus making it mobile thus giving microbially catalyzed processes the potential to affect the fate of uranium in an environmental setting. Microorganisms have the ability to catalyze the oxidation and reduction of uranium and therefore influence the mobility and localization of uranium in the environment (Wall and Krumholz, 2006). Stimulation of uranium-reduction in contaminated aquifers has proven to be a usable method for removal of uranium from contaminated ground water *in situ*. This approach could prove applicable at many uranium-contaminated sites across the world (Lovley *et al.*, 1991). The reduction of uranium by microorganisms also has the potential to remove uranium from waste streams generated by industry (Lovley and Phillips, 1992a). The understanding of these microbially-catalyzed redox reactions for the interaction with uranium is pivotal to the process of uranium recovery from ore-containing materials as well as uranium accumulation in anaerobic sediments. By utilizing *Acidithiobacillus ferrooxidans* Choi and co-workers (2004) were able to extract 80% of uranium from the schists containing only 0.01% U_3O_8 by weight, within 60 h at a pulp density of 100 g-ore/L. Only 18% of the uranium was extracted without microbial activity.

1.7.2 Aerobic interactions with uranium: bioleaching processes

Extracting of uranium from higher grades of uranium ore's (2.5-12.2%) are usually done by chemical extraction, however these deposits are being globally depleted, it has resulted in the increased exploitation of lower grade deposits (0.04-0.4%) (Brierley, 1978). Ore deposits containing uranium usually consist of a high proportion of uranium(IV) (Plant *et al.*, 1999) and, since efficient recovery of uranium depends on the oxidation of uranium(IV) to uranium(VI), thereby creating a soluble and easily recovered form of uranium, this process has widely

been used in the recovery of uranium from low grade ores (Agate 1996; Bosecker 1997; Munoz et al. 1995). Lower grade uranium ores are usually extracted in an aerobic, acid leaching process enhanced by the presence of acid-tolerant, Fe(II)- and S⁰-oxidizing bacteria. Under acidic conditions, Fe(III) is added to the uranium-containing ore since it is an effective oxidant for uranium(IV). When added, it will solubilize the uranium as uranium(VI) while the Fe(III) is being reduced to Fe(II) which, in turn, can then be regenerated by Fe(II)-oxidizing bacteria such as *Acidithiobacillus ferrooxidans*. *T. ferrooxidans* has the ability to couple growth to aerobic oxidation of Fe(II) and can thereby enhance uranium recovery (Brierley, 1978; Bosecker, 1997). It has also been found that bacteria capable of metal-oxidation can also directly oxidize uranium(IV) to uranium(VI). Strains of *A. ferrooxidans* that were cultured in the presence of uranium(VI) have displayed the ability to oxidize uranium(IV) directly and it was shown that it can couple metabolic processes, but not growth, to uranium(IV) oxidation (DiSpirito and Tuovinen, 1982). This observation indicates that there is a possibility that uranium solubilization during acidic bioleaching processes results from both direct and indirect microbial oxidation (Bosecker, 1997). This mechanism of uranium mobilization is a potential mechanism for uranium contamination of groundwater.

1.7.3 Anaerobic interactions with uranium

Generally, groundwater found at uranium-contaminated sites is of an aerobic nature and thus most of the uranium is mobilized as uranium(VI). Anaerobic conditions can be created by the addition of organics since aerobic bacteria couple the oxidation of organic matter to the reduction of dissolved oxygen as the terminal electron acceptor. Oxygen is therefore most rapidly depleted in sediments containing large amounts of organic matter (Chapelle, 1993). This depletion of oxygen will, in turn, create an environment suitable for uranium(VI)-reduction and therefore precipitation of uranium *in situ*. Also, the degradation of organic matter under anaerobic conditions initially results in the generation of

hydrogen and low molecular weight organic acids such as acetate *via* the successive activities of hydrolytic and fermentative organisms (Figure 1.7) (Lovley and Chapelle, 1995) which can be utilized as electron donors during redox coupled reactions. Thus, anaerobic microbial redox reactions have the potential to remove uranium(VI) effectively from the contaminated groundwater. Studies have shown that the easiest way to promote uranium(VI)-reduction in a contaminated aquifer is the addition of acetate as an electron donor to simulate the activity of dissimilatory metal-reducing microorganisms (Lovley *et al.*, 1991). A strategy for long term uranium-reduction still needs to be optimized but the immobilization of uranium will depend on the anaerobic process(es) stimulated *in situ* and the way in which microorganisms interact with uranium.

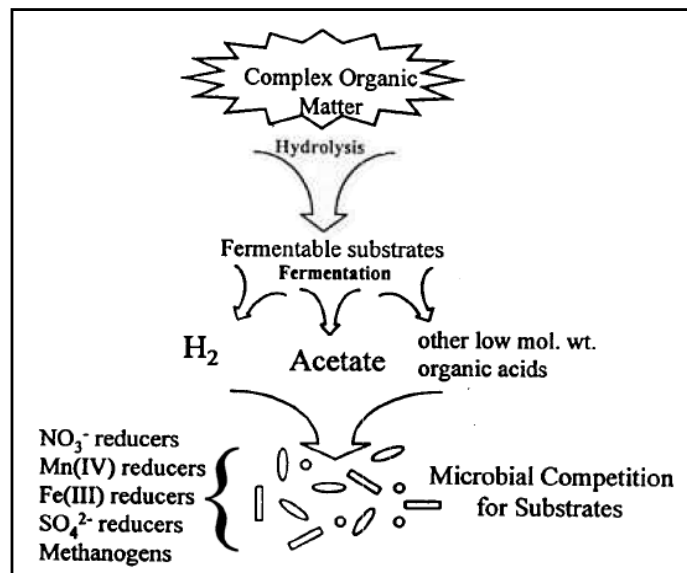


Figure 1.7: Organic matter degradation in anaerobic environments (taken from Anderson and Lovley, 2002).

1.7.4 Reduction-based bioremediation of uranium contaminated aquifers

As mentioned above, microbial reduction of uranium(VI) is a viable biotechnique for the removal of uranium from industrial waste streams and thus prevention of further spreading of uranium contamination into the environment. Development of uranium bioremediation techniques has focused on stimulation of uranium(VI)-

reduction by addition of a suitable source of organic carbon forming a zone of stimulated anaerobic activity that is positioned perpendicular to groundwater flow paths that serves as a zone for uranium immobilization. This zone of anaerobic activity then prevents the further migration of uranium within the subsurface (Figure 1.8) (Lovley and Phillips, 1992a; Anderson and Lovley, 2002). If one is to consider such a system on a per cell basis, the potential for enzymatic reduction of uranium(VI) is much higher than say biosorption techniques due to the limited availability of sorption sites at the cell surface (Lovley and Phillips, 1992a). In *Desulfovibrio*, the amounts of precipitated uranium reported (11 g uranium(VI) g⁻¹ dry cells) (Lovley and Phillips, 1992a) are comparable to that of phosphatase-mediated uranium precipitation (9 g uranium(VI)/g dry cells) (Macaskie, 1991) and will probably be even higher in a flow-through system (Lovley and Phillips, 1992a).

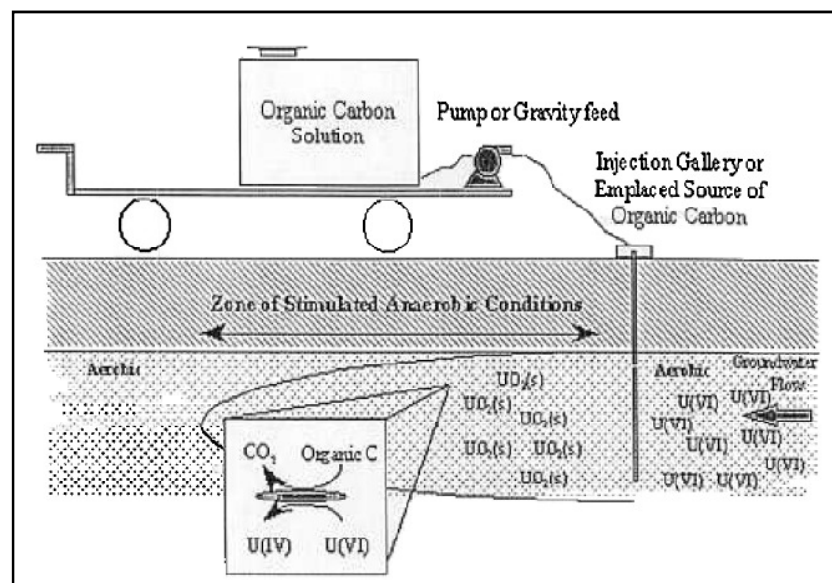


Figure 1.8: Conceptualized bioremediation scheme for stimulated uranium(VI)-reduction *in situ* upon bulk addition of a suitable electron donor (taken from Anderson and Lovley, 2002).

For the design of a such a bioreduction system, it is imperative that one considers the kinetics of uranium(VI)-reduction in the presence of the uranium-reducing species as well as the various organic ligands that can affect the rates of

bioreduction and potentially inhibit uraninite precipitation. Half saturation constants (K_s) for uranium(VI)-reduction average about 0.5 mM for *Desulfovibrio* species (Spear *et al.*, 1999) and 0.13 mM for *Shewanella* species (Truex *et al.*, 1997) with maximum specific reduction rates (k) of 1.38 mmol uranium(VI)mg/ h and 0.24 mmol uranium(VI) mg/ h respectively. These specific results suggest that the *Desulfovibrio*-mediated reduction might be kinetically more favourable than *Shewanella*-mediated reduction but studies done by Ganesh and co-workers (1997) showed that the latter bioreduction will occur faster when uranium is complexed with polydentate ligands than in the case of *Desulfovibrio*-based bioreduction which, in turn, will occur faster when uranium is complexed with monodentate ligands. These studies indicate that the process design for the flow-through uranium bioreduction process will depend on the choice of uranium(VI)-reducing bacteria employed for a given environment.

1.8References

Abdelouas, A., Lutze, W. and Nuttall, H.E. (1999) Uranium contamination in the subsurface: characterization and remediation. In: P. C. Burns & R. Finch (eds), *Uranium: Mineralogy, Geochemistry and the Environment*. Washington, DC: Mineralogical Society of America. pp433-473.

Adler, H.H. (1974) Concepts of uranium-ore formation in reducing environments in sandstone and other sediments. *Formation of UraniumOre Deposits: Proceedings of a Symposium*. Athens. pp141-168.

Agate, A.D.(1996) Recent advances in microbial mining. *World Journal of Microbiology and Biotechnology*.**12**:487–495.

Anderson, R.T., Fleisher, M.Q. and LeHuray, A.P. (1989) Concentration, oxidation state, and particulate flux of uranium in the Black sea. *Geochimica et Cosmochimica Acta*. **53**: 2215-2224.

Anderson, R.T. and Lovley, D.R. (2002) Microbial redox interactions with uranium: an environmental perspective. InM. Keith-Roach, and F. Livens (eds), *Interactions of Microorganisms with Radionuclides*. Elsevier Science Limited, Amsterdam. pp205-223.

Beliaev, A.S. and Saffarini, D.A. (1998) *Shewanella putrefaciens mtrB* encodes an outer membrane protein required for Fe(III) and Mn(IV) reduction. *The Journal of Bacteriology*. **180**:6292-6297.

Bencheikh-Latmani R. and Leckie J.O. (2003) Association of uranyl with the cell wall of *Pseudomonas fluorescens* inhibits metabolism. *Geochimica Et Cosmochimica Acta*.**67**:4057–4066.

Bencheikh-Latmani, R., Williams, S.M., Haucke, L., Criddle, C.S. and Wu, L. (2005) Global transcriptional profiling of *Shewanella oneidensis* MR-1 during Cr(VI) and U(VI) reduction. *Applied and Environmental Microbiology*. **71**:7453-7460.

BioMineWiki. (2007)

http://wiki.biomine.skelleftea.se/wiki/index.php/Sulfate_reducing_bacteria

Boone, D.R., Liu, Y., Zhao, Z., Balkwill, D.L., Drake, G.R., Stevens, T.O. and Aldrich, H.C. (1995) *Bacillus infernus* sp. nov. Fe(III)- and Mn(IV)-reducing anaerobe from the deep terrestrial subsurface. *International Journal of Systematic and Evolutionary Microbiology*. **45**:441–448.

Bosecker, K. (1997) Bioleaching: metal solubilization by micro-organisms. *FEMS Microbiology Reviews*. **20**:591-604.

Brierley, C.L. (1978) Bacterial leaching. *Critical Reviews in Microbiology*. **6**: 207-262.

Chapelle, F.H. (1993) Ground-water Microbiology and Geochemistry. New York: John Wiley & Sons. pp424-431.

Chapelle, F.H. and Lovley, D.R. (1992) Competitive exclusion of sulfate reduction by Fe(III)-reducing bacteria: a mechanism for producing discrete zones of high-iron ground water. *Ground Water*. **30**:29-36.

Choi, M., Cho, K., Kim, D. and Hee-Wook, R. (2004) Bioleaching of uranium from low grade black schists by *Acidithiobacillus ferrooxidans*. *World Journal of Microbiology & Biotechnology*. **21**:377-380

Cochran, J.K., Carey, A.E., Sholkovitz, E.R. and Suprenant, L.D. (1986) The geochemistry of uranium and thorium in coastal marine sediments and sediment pore waters. *Geochimica et Cosmochimica Acta*. **50**:663–680.

DiSpirito, A.A. and Tuovinen, O.H. (1982) Kinetics of uranous ion and ferrous iron oxidation by *Thiobacillus ferrooxidans*. *Archives of Microbiology*. **133**:33-37.

Ehrlich, H.L. (1990) *Geomicrobiology*. Marcel Dekker, Inc. New York, pp. 441–448.

Elias, D.A., Suflita, J.M., McInerney, M.J. and Krumholz, L.R. (2004) Periplasmic cytochrome *c*₃ of *Desulfovibrio vulgaris* is directly involved in H₂-mediated metal but not sulfate reduction. *Applied Environmental Microbiology*. **70**:413-416.

Fournier, M., Zhang, Y., Wildschut, J.D., Dolla, A., Voordouw, J.K., Schriemer, D.C., and Voordouw, G. (2003) Function of oxygen resistance proteins in the anaerobic, sulfate-reducing bacterium *Desulfovibrio vulgaris* Hildenborough. *Journal of Bacteriology*. **185**:71-79.

Ganesh, R., Robinson, K.G., Reed, G.D. and Sayler, G.S. (1997) Reduction of hexavalent uranium from organic complexes by sulfate and iron-reducing bacteria. *Applied and Environmental Microbiology*. **63**:4385-4391.

Green, A.C., Patel, B.K.C. and Sheehy, A.J. (1997) *Deferribacter thermophilus* gen. nov., sp. nov., a novel thermophilic manganese- and iron-reducing bacterium isolated from a petroleum reservoir. *International Journal of Systematic and Evolutionary Microbiology*. **47**:505–509.

Geobacter Project. (2007) <http://geobacter.org>

Gorby, Y.A. and Lovley, D.R. (1992) Enzymatic uranium precipitation. *Environmental Science and Technology*. **26**:205–207.

Haur, A., Hladiková, J. and Šmejkal, V. (1973) Procedure of direct conversion of sulphates into SO₂ for mass spectrometric analysis of sulphur. *Isotopes in Environmental and Health Studies*. **9**:329 – 331.

Ibrahim M.B., Lindström, E.B., Nedwell, D.B. and Balba, M.T. (1981) Evidence for coexistence of two distinct functional groups of sulfate-reducing bacteria in salt marsh sediment. *Applied and Environmental Microbiology*. **42**:985–992.

Jones, H.E., Trudinger, P.A., Chambers, L.A. and Pylotis, N.A. (1976) Metal accumulation by bacteria with particular reference to dissimilatory sulphate-reducing bacteria. *Zeitschrift Fur Allgemeine Mikrobiologie*. **16**:425-435.

Kashefi, K. and Lovley, D. R. (2000) Reduction of Fe(III), Mn(IV), and toxic metals at 100°C by *Pyrobaculum islandicum*. *Applied and Environmental Microbiology*, **66**, 1050-1056.

Kennedy, D.W., Marshall, M.J., Dohnalkova, A.C., Saffarini, D.A., and Culley, D.E. (2004) Role of *Shewanella oneidensis* c-type cytochromes in uranium reduction and localization. *American Society of Microbiology 105th General Meeting*. Q-389 (abstr.).

Kieft, T.L., Fredrickson, J.K., Onstott, T.C., Gorby, Y.A., Kostandarithes, H.M., Bailey, T.J., Kennedy, D.W., Li, S.W., Plymale, A.E., Spadoni, C.M. and Gray, M.S. (1999) Dissimilatory reduction of Fe(III) and other electron acceptors by a *Thermus* isolate. *Applied Environmental Microbiology*. **65**:1214-1221.

Kredich, N.M. (1996) Biosynthesis of cysteine *In Escherichia coli* and *Salmonella*. *Cellular and Molecular Biology*, Ed. in Chief, Neidhardt, F.C. pp514-527.

Kurttio, P., Harmoinen, A., Saha, H., Salonen, L., Karpas, Z., Komulainen, H. and Auvinen, A. (2006) Kidney toxicity of ingested uranium from drinking water. *American Journal of Kidney Diseases*. **47**: 972-982.

Langmuir, D. (1978) Uranium solution-mineral equilibria at low temperatures with applications to sedimentary ore deposits. *Geochimica et Cosmochimica Acta*. **42**:547-569.

LeDuc, L.G., Feroni, G.D. and Trevors, J.T. (1997) Resistance to heavy metals in different strains of *Thiobacillus ferrooxidans*. *World Journal of Microbiology and Biotechnology*. **13**:453-455.

Lovley, D.R. (1987) Organic matter mineralization with reduction of ferric iron. *Geomicrobiology Journal*. **5**:375-399.

Lovley, D.R. and Chapelle, F.H. (1995) Deep subsurface microbial processes. *Reviews of Geophysics*. **33**:365-381.

Lovley, D.R. and Coates, J.D. (1997) Bioremediation of metal contamination. *Current Opinion in Biotechnology*. **8**:285-289.

Lovley, D.R., Holmes, D.E. and Nevin, K.P. (2004) Dissimilatory Fe(III) and Mn(IV) reduction. *Advances in Microbial Physiology*. **49**:219-286.

Lovley, D.R., Phillips, E.J.P., Gorby, Y.A. and Landa, E.R. (1991) Microbial reduction of uranium. *Nature*. **350**:413-416.

Lovley, D.R. and Phillips, E.J.P. (1992a) Bioremediation of uranium contamination with enzymatic uranium reduction. *Environmental Science*. **26**:2228-2234.

Lovley, D.R. and Phillips, E.J.P. (1992b) Reduction of uranium by *Desulfovibrio desulfuricans*. *Applied Environmental Microbiology*. **58**:413-416.

Lovley, D.R., Phillips, E.J.P., Lonergan, D.J., and Widman, P.K. (1995) Fe(III) and S⁰ reduction by *Pelobacter carbinolicus*. *Applied and Environmental Microbiology*. **61**:2132–2138.

Lovley, D.R., Roden, E.E., Phillips, E.J.P. and Woodward, J.C. (1993a) Enzymatic iron and uranium reduction by sulfate-reducing bacteria. *Marine Geology*. **113**:41-53.

Lovley, D.R., Widman, P.K., Woodward, J.C. and Phillips, E.J.P. (1993b) Reduction of uranium by cytochrome *c*₃ of *Desulfovibrio vulgaris*. *Applied and Environmental Microbiology*. **59**: 3572-3576.

Lovley, D. R., Giavannoni, S.J., White, D.C., Champine, J.E., Phillips, E.J.P., Gorby, Y.A. and Goodwin, S. (1993c) *Geobacter metallireducens* gen. nov. sp. nov., a microorganism capable of coupling the complete oxidation of organic matter to the reduction of iron and other metals. *Archives of Microbiology*. **159**:336–344.

Liu, S., Zhou, J., Zhang, C., Cole, D.R., Gajdarziska-Josifovska, M. and Phelps, T.J. (1997) Novel thermophilic Fe(III)-reducing bacteria from the deep subsurface: the evolutionary implications. *Science*. **277**:1106–1108.

Liu, C., Gorby, Y.A., Zachara, J.M., Fredrickson, J.K. and Brown, C.F. (2002) Reduction kinetics of Fe(III), Co(III), U(VI), Cr(VI) and Tc(VII) in cultures of dissimilatory metal-reducing bacteria. *Biotechnology and Bioengineering*. **80**: 637-649.

Macaskie, L.E. (1991) The application of biotechnology to the treatment of wastes produced from the nuclear fuel cycle: biodegradation and bioaccumulation as a means of treating radionuclide-containing streams. *Critical Reviews in Biotechnology*. **11**:41-112.

Markich, S.J. (2002) Uranium speciation and bioavailability in aquatic systems: an overview. *Science World Journal*. **2**:707-729.

Marshall, M.J., Beliaev, A.S., Dohnalkova, A.C., Kennedy, D.W., Shi, L., Wang, Z., Boyanov, M.I., Lai, B., Kemner, K.M., McLean, J.S., Reed, S.B., Culley, D.E., Bailey, V.L., Simonson, C.J., Saffarini, D.A., Romine, M.F., Zachara, J.M. and Fredrickson, J.K. (2006) c-Type cytochrome-dependant formation of U(IV) nanoparticles by *Shewanella oneidensis*. *PLoS Biology*. **4**:e268.

Maynard, J.B. (1983) *Geochemistry of Sedimentary Ore Deposits*. NewYork: Springer-Verlag.p305.

Mohagheghi, A., Updegraff, D. M. and Goldhaber, M.B. (1985). The role of sulfate-reducing bacteria in the deposition of sedimentary uranium ores. *Geomicrobiology Journal*. **4**:153-173.

Möller, C. and van Heerden, E. (2006) Isolation of a soluble and membrane-associated Fe(III) reductase from the thermophile, *Thermus scotoductus* (SA-01). *FEMS Microbial Letters*. **265**(2):237-243.

Munoz, J.A., Gonzalez, F., Blazquez, M.L. and Ballester, A. (1995) A study of the bioleaching of a Spanish uranium ore. Part I: a review of the bacterial leaching in the treatment of uranium ores. *Hydrometallurgy*. **38**:39–57.

Myers, C.R. and Myers, J.M. (1992) Localization of cytochromes to the outer membrane of anaerobically grown *Shewanella putrefaciens* MR-1. *The Journal of Bacteriology*. **174**:3429-38.

Myers, C.R., and Nealson, K.H. (1988) Bacterial manganese reduction and growth with manganese oxide as the sole electron acceptor. *Science*. **240**:1319–1321.

Nealson, K.H. and Saffarini, D. (1994) Iron and Manganese in anaerobic respiration: Environmental significance, physiology, and regulation. *Annual Review of Microbiology*. **48**:311-343.

Obuekwe, C. and Westlake, D.W. (1982) Effects of medium composition on cell pigmentation, cytochromes content and ferric reduction in *Pseudomonas* sp. isolated from crude oil. *Canadian Journal of Microbiology*. **28**: 989-992.

Ohnuki, T., Ozaki, T., Yoshida, T., Sakamoto, F., Kozai, N., Wakai, E., Francis, A.J., and Iefuji, H. (2005) Mechanisms of uranium mineralization by the yeast *Saccharomyces cerevisiae*. *Geochimica et Cosmochimica Acta*. **22**:5307-5316.

Opperman, D.J. and Van Heerden, E. (2007) Aerobic Cr(VI) reduction by *Thermus scotoductus* strain SA-01. *Journal of Applied Microbiology*. **103**:1907-1913.

Payne, R.B. (2005) Energy metabolism and U(VI) reduction by *Desulfovibrio*. Ph.D thesis. University of Missouri-Columbia.

Plant, J.A., Simpson, P.R., Smith, B. and Windley, B.F. (1999) Uranium ore deposits-products of the radioactive Earth. In P. C. Burns & R. Finch (Eds). *Uranium: Mineralogy, Geochemistry and the Environment*. Washington, DC: Mineralogical Society of America. pp255-319.

Postgate, J.R. (1956) Iron and the synthesis of cytochrome *c*₃. *Journal of General Microbiology* **15**: 186-193.

Renshaw, J.C., Butchins, L.J.C., Livens, F.R., May, I., Charnock, J.M. and Lloyd, J.R. (2005) Bioreduction of uranium: environmental implications of a penavalent intermediate. *Environmental Science and Technology*. **39**:5657-60.

Reguera, G., McCarthy, K.D., Metha, T., Nicoll, J.S., Tuominen, M.T. and Lovley, D.R. (2005) Extracellular electron transfer via microbial nanowires. *Nature*. **435**:1098-101.

Rooney-Varga, J., Anderson, R.T., Fraga, J.L., Ringleberg, D. and Lovley, D.R. (1999) Microbial communities associated with anaerobic benzene degradation in a petroleum- contaminated aquifer. *Applied and Environmental Microbiology*. **65**:3056-3063.

Rossello-Mora, R.A., Ludwig, W., Kempfer, P., Amann, R. and Schleifer, K.H. (1995) *Ferrimonas balearica* gen. nov., sp. nov., a new marine facultative Fe(III)-reducing bacterium. *Systematic and Applied Microbiology*. **61**:196–202.

Sakamoto, F., Nankawa, T., Kozai, N., Fujii, T., Iefuji, H., Francis, A.J. and Ohnuki, T. (2007) Protein expression of *Saccharomyces cerevisiae* in response to uranium exposure. *Journal of Nuclear and Radiochemical Sciences*. **8**:133-138.

Shelobolina, E.S., Sullivan, S.A., O'Neill, K.R., Nevin, K.P. and Lovley, D.R. (2004) Isolation, characterization, and U(VI)-reducing potential of a facultatively anaerobic, acid-resistant bacterium from low-pH, nitrate- and U(VI)-contaminated subsurface sediment and description of *Salmonella subterranean* sp. nov. *Applied Environmental Microbiology*. **70**:2959-2965.

Shelobolina, E.S., Coppi, M.V., Korenevsky, A.A., DiDonato, L.N., Sullivan, S.A., Konishi, H., Xu, H., Leang, C., Butler, J.E., Kim, B., and Lovley, D.R. (2007) Importance of *c*-Type cytochromes for U(VI) reduction by *Geobacter sulfurreducens*. *BMC Microbiology*. **7**:16-25.

Slobodkin, A., Reysenbach, A.-L. Strutz, N., Dreier, M. and Wiegel, J. (1997) *Thermoterrabacterium ferrireducens* gen. nov., a thermophilic anaerobic dissimilatory Fe(III)-reducing bacterium from a continental hot spring. *International Journal of Systematic and Evolutionary Microbiology*. **47**:541–547.

Slobodkin, I., Sokolova, G., Lysenko, A.M. and Wiegel, J.(2006) Reclassification of *Thermoterrabacterium ferrireducens* as *Carboxydothemus ferrireducens* comb. nov., and emended description of the genus *Carboxydothemus*. *International Journal of Systematic and Evolutionary Microbiology*. **56**:2349-2351.

Spear, J.R., Figueroa, L.A. and Honeyman, B.D. (1999) Modeling the removal of uranium U(VI) from aqueous solutions in the presence of sulfate reducing bacteria. *Environmental Science and Technology*. **33**:2667-2675.

Tebo, B.M. and Obratzsova, A.Y. (1998) Sulfate-reducing bacterium grows with Cr(VI), U(VI), Mn(IV) and Fe(III) as electron acceptors. *FEMS Microbial Letters*. **162**:193-198.

Truex, M.J., Peyton, B.M., Valentine, N.B. and Gorby, Y.A. (1997) Kinetics of U(VI) reduction by a dissimilatory Fe(III)-reducing bacterium under non-growth conditions. *Biotechnology and Bioengineering*. **55**:490-496.

Volesky, B. and May-Phillips, H.A. (1995) Biosorption of heavy metals by *Saccharomyces cerevisiae*. *Applied Microbiology and Biotechnology*. **42**:797–806.

Wall, J.D. and Krumholz, L.R., (2006) Uranium reduction. *Annual Review of Microbiology*. **60**:149-66.

Wildung, R.E., Gorby, Y.A., Krupka, K.M., Hess, N.J., Li, S.W., Plymale, A.E., McKinley J.P. and Fredrickson, J.K. (2000) Effect of electron donor and solution chemistry on products of dissimilatory reduction of technetium by *Shewanella putrefaciens*. *Applied and Environmental Microbiology*. **66**:2451–2460.

Chapter 2

Introduction to present study

2.1 Introduction

In the past, literature has indicated that soluble uranium(VI) can be reduced to less soluble uranium(IV) by pure cultures of bacteria (Lovley and Phillips, 1992; Lovley *et al.*, 1993; Payne *et al.*, 2002). In this regard, microorganisms reduce metals to fulfil various functions in cell metabolism such as energy metabolism (dissimilatory reduction), biosynthesis (assimilatory reduction), detoxification or for no function at all (non-specific reduction). A large variety of metal-reducing microorganisms reduce uranium(VI), including members of the genera *Desulfovibrio* (Payne, 2002), *Geobacter* (Lovley *et al.*, 1991), *Anaeromyxobacter* (Rademacher *et al.*, 2006), *Deinococcus* (Fredrickson *et al.*, 2000), *Clostridium* (Francis *et al.*, 1994), *Desulfosporosinus* (Suzuki *et al.*, 2003) and *Shewanella* (Ganesh *et al.*, 1997). Some thermophilic bacteria capable of uranium(VI) reduction have also been identified, and include members of the genera *Thermoanaerobacter* (Roh *et al.*, 2002), *Pyrobaculum* (Kashefi and Lovley, 2000), and most importantly for this study, *Thermus* (Kieft *et al.*, 1999). A member of the *Thermus* genera, namely *Thermus scotoductus* SA-01, was very attractive for a study on microbial uranium(VI) reduction since it is readily cultured in anaerobic as well as aerobic conditions and, although Kieft and coworkers (1999) showed that it has the ability to reduce uranium(VI), no further work in this regard has been done to date on this bacteria. Additionally, a recent draft of the genome sequence of *T. scotoductus* SA-01 has also become available (Gounder, 2009).

To date only very limited and incomplete studies have been undertaken to address the mechanism of uranium(VI) reduction. For example, a purified hydrogenase and periplasmic cytochrome *c3* purified from *Desulfovibrio vulgaris*, a organism unable to utilize uranium(VI) as a terminal electron acceptor (Lovley

and Phillips, 1992), was the first enzyme displaying uranium(VI)-reductase activity. Also, in *Geobactersulfurreducens* a cytochrome *c*-type protein was identified as an uranium(VI)-reductase (Lloyd *et al.*, 2003). In both *D. vulgaris* and *G. sulfurreducens*, cytochrome mutants were still able to reduce uranium(VI) although at decreased levels (Lloyd *et al.*, 2003), indicating that *D. vulgaris* and *G. sulfurreducens* contain multiple uranium(VI) reductases.

Although *T. scotoductus* SA-01 has no cytochrome *c*3 proteins (Gounder, 2009), it still has the ability to reduce uranium(VI). No data is currently available pertaining to which proteins might be involved in the reduction in this bacteria.

2.2 The broad aims of this study

Firstly, to determine the effect of uranium on actively growing cells as well as well as the capabilities to reduce U(VI). Secondly, identification of the sequences of the protein-encoding genes in question and their metabolic functionality so as to finally access the possible versatility of such proteins in this extremophile.

2.3 References

Francis, A.J., Dodge, C.J., Lu, F.L., Halada, G.P. and Clayton, C.R.(1994) XPS and XANES studies of uranium reduction by *Clostridium* sp. *Environmental Science and Technology*. **28**:636-639.

Fredrickson, J.K., Kostandarithes, H.M., Li, S.W., Plymale, A.E. and Daly, M.J.(2000) Reduction of Fe(III), Cr(VI), U(VI), and Tc(VII) by *Deinococcus radiodurans* R1. *Applied and Environmental Microbiology*. **66**:2006-11.

Ganesh, R., Robinson, K.G., Reed, G.D. and Sayler, G.S.(1997) Reduction of hexavalent uranium from organic complexes by sulfate- and iron-reducing bacteria. *Applied and Environmental Microbiology*. **63**:4385-4391.

Gounder, K. (2009) PhD thesis: Genome sequencing of the extremophile *Thermus scotoductus* SA-01 and expression of selected genes. University of the Free State, South Africa.

Kashefi, K. and Lovley, D.R.(2000) Reduction of Fe(III), Mn(IV), and toxic metals at 100 degrees C by *Pyrobaculum islandicum*. *Applied and Environmental Microbiology*. **66**:1050-1056.

Kieft, T.L., Fredrickson, J.K., Onstott, T.C., Gorby, Y.A., Kostandarithes, H.M., Bailey, T.J., Kennedy, D.W., Li, S.W., Plymale, A.E., Spadoni, C.M. and Gray, M.S. (1999) Dissimilatory reduction of Fe(III) and other electron acceptors by a *Thermus* isolate. *Applied Environmental Microbiology*. **65**:1214-1221.

Lloyd, J. R., Leang, C., Myerson, A.L.H., Coppi, M.V., Cuifo, S., Methe, B., Sandler, S.J. and Lovley, D.R.(2003) Biochemical and genetic characterization of PpcA, a periplasmic c-type cytochrome in *Geobacter sulfurreducens*. *Biochem. J.* **369**:153-161.

Lovley, D.R., Phillips, E.J.P., Gorby, Y.A. and Landa, E.R. (1991) Microbial reduction of uranium. *Nature*. **350**:413-416.

Lovley, D.R. and Phillips, E.J.P. (1992) Bioremediation of uranium contamination with enzymatic uranium reduction. *Environmental Science*. **26**:2228-2234.

Lovley, D.R., Widman, P.K., Woodward, J.C. and Phillips, E.J.P. (1993) Reduction of uranium by cytochrome *c₃* of *Desulfovibrio vulgaris*. *Applied and Environmental Microbiology*. **59**: 3572-3576.

Payne, R.B., Gentry, D.M., Rapp-Giles, B.J., Casalot, L. and Wall, J.D. (2002) Uranium Reduction by *Desulfovibrio desulfuricans* Strain G20 and a Cytochrome *c₃* Mutant. *Applied and Environmental Microbiology*. **68**:3129-3132.

Rademacher, L.K., Lundstrom, C.C., Johnson, T.M., Sanford, R.A., Zhao, J. and Zhang, Z. (2006) Experimentally determined uranium isotope fractionation during reduction of hexavalent U by bacteria and zero valent iron. *Environmental Science and Technology*. **40**:6943-6948.

Roh, Y., Liu, S.V., Li, G., Huang, H., Phelps, T.J., and Zhou, J. (2002) Isolation and characterization of metal-reducing *Thermoanaerobacter* strains from deep subsurface environments of the piceance basin, Colorado. *Applied and Environmental Microbiology*. **68**:6013–6020.

Slobodkin, A.I., Zavarzina, D.G., Sokolova, T.G., and Bonch-Osmolovskaya, E.A. (1999) Dissimilatory reduction of inorganic electron acceptors by thermophilic anaerobic Prokaryotes. *Mikrobiologiya*. **68**:600–623.

Suzuki, Y., Kelly, S.D., Kemner, K.M. and Banfield, J.F.(2003) Microbial populations stimulated for hexavalent uranium reduction in uranium mine sediment. *Applied and Environmental Microbiology*. **69**:1337-1346.

Chapter 3

Interactions of *Thermus scotoductus* SA-01 with uranium(VI) under growth and non-growth conditions

3.1 Introduction

A thermophilic bacterium was isolated in 1999 by Kieft and co-workers from groundwater sampled at a depth of 3.2 kmbls in Mponeng, WitwatersrandBasin, Republic of South Africa. The ambient rock temperature where the sample was taken was about 60°C. From enrichments it was found that this strain obtained had >98% homology to *Thermus* strain NMX2 A.1 and phylogenetic analysis of the 16S rRNA gene sequences showed that the isolated organism was indeed a member of the genus *Thermus*, closely related to the strains NMX2 A.1 and V17(Balkwill *et al.*, 2004). The strain also had a filamentous morphology consistent with the placement within the genus *Thermus* and as such the isolate was designated *Thermus* strain SA-01. Further 16S rRNA gene sequence analysis and genomic DNA-DNA hybridizations placed strain SA-01 in the type species *scotoductus* which led to the current taxonomic status of strain SA-01: *Thermus scotoductus* SA-01 (Balkwill *et al.*, 2004). It was shown that strain SA-01 has the ability to couple growth to the reduction of Fe(III) as a sole electron donor and it was also able to couple the oxidation of organic substrates to the reduction of a wide array of electron acceptors such as nitrate, Fe(III), Mn(IV) and S⁰. *T. scotoductus* SA-01 has shown the ability to reduce certain metals under non-growth conditions, including Co(III)-EDTA, Tc(VII), Cr(VI) (Opperman and Van Heerden, 2007), and uranium(VI) (Kieft *et al.*, 1999) under anaerobic conditions.

Previous studies have indicated that some of the dissimilatory Fe(III)-reducing microorganisms also have the ability to reduce uranium(VI) to uranium(IV). *Geobacter metallireducens* and *Shewanella putrefaciens* can both conserve

energy to support growth from uranium(VI) reduction (Lovley *et al.*, 1991). *Desulfovibrio desulfuricans* can also reduce uranium(VI), but does not have the ability to conserve enough energy to support growth from this reaction. Very little is known about the exact mechanisms involved in the reduction of uranium(VI) in any of these organisms.

The aims of this chapter were:

- To determine the uranium(VI) toxicity threshold of growing culture of *T. scoto ductus* SA-01
- Characterizing the ability of *T. scoto ductus* SA-01 to reduce uranium(VI)
- Evaluating the effect of various physico-chemical parameters on uranium(VI) reduction

3.2 Materials and methods

3.2.1 Bacterial strain and culture conditions

T. scotoductus SA-01 (ATCC 700910; American Type Culture Collection) was routinely cultured aerobically in a complex organic medium, TYG (5 g tryptone, 3 g yeast extract and 1 g glucose in 1 L ddH₂O, pH 7.0) at 65°C with shaking (160 rev/min). The culture utilized in this study was obtained directly from Dr. Thomas Kieft, New Mexico Institute of Mining and Technology, from the original stored culture before submission to the culture collection.

3.2.2 Confirmation of *T. scotoductus* SA-01

3.2.2.1 Genomic DNA extraction and 16S rRNA gene amplification

Genomic DNA was extracted according to the method described by Labuschagne and Albertyn (2007). *T. scotoductus* SA-01 was cultured in TYG medium until an optical density of 0.9. A sample of the culture (5 ml) was centrifuged (14 000 × *g*, 2 min), the supernatant was removed by means of aspiration. DNA isolation buffer (500 µl) (100 mM Tris-HCl, pH 8.0; 50 mM EDTA; 1% SDS) and 200 µl glass beads were added to the pellet. The suspension was then vortexed vigorously (4 min) followed by immediate cooling on ice (5 min). Ammonium acetate (275 µl), 7 M, pH 7.0, was added and the suspension mixed by vortexing, incubated at 65°C (5 min) and on ice (5 min). Chloroform (500 µl) was added, mixed by vortexing and centrifuged (14 000 × *g*, 5 min, 4°C). The supernatant was precipitated with an equal volume of isopropanol at room temperature (5 min) followed by centrifugation (14 000 × *g*, 5 min, 4°C). The pellet was washed with 70% ethanol, air dried and dissolved in 50 µl sterile water. gDNA concentrations were determined on the NanoDrop Spectrophotometer ND-1000 (Thermo Scientific).

The PCR reaction was assembled as described in Table 3.1 and 3.2, cycling started with a 5 min at 95°C hot start step of the gDNA-containing master mix. After this, the cycling was paused, 0.3 µl Kapa (Kapa Biotechnology) *Taq* polymerase (3units/µl) enzyme added and cycling resumed. Amplifications were run for 30 cycles in a thermal cycler PXE 0.2 (Thermo electron corporation) after an initial denaturation at 95°C for 5 min. Each cycle was run at 95 °C for 30 sec, 52 °C for 45 sec and 72 °C for 90 sec and final extension at 72 °C for 10 min.

Table 3.1. Master mix for the hot start PCR reactions.

Component	Amount for 1 reaction (µl)
Primer 27F (10 µM)	1
Primer 1492R (10 µM)	1
dNTPs (10 mM)	1
Buffer10 X *	5
BSA (10µg/µl)	2
Sterile water	34.70

Primer 27F 5' - AGA GTT TGA TCM TGG CTC AG - 3' (Lane, 1991)

Primer 1492R 5' - GGT TAC CTT GTT ACG ACT T-3' (Lane, 1991)

The buffer contained adequate [MgCl₂]

Table 3.2. Composition of materials of a hot start PCR program.

	Reaction	Negative control
Master Mix (µl) *	44.70	44.70
DNA (80-95 ng) (µl)	5	5 [#]

(*)Refer to Table 3.1, (#) sterile water

An agarose gel 1% (w/v) was prepared supplemented with 0.6 µl ethidium bromide (EtBr) (3 µl of a 10 mg/ml of stock in 50 ml gel) added for visualization. PCR product (10 µl) was added to 2 µl loading dye (Fermentas) before loading onto the gel. The MassRuler™ DNA ladder (Fermentas) was used to determine

the size of bands visualized on the gel using the ChemiDoc XRS (Bio-Rad Laboratories) gel documentation system.

The 16S rRNA gene PCR product (20µl) was loaded onto the 1% (w/v) agarose gel for fractionation by electrophoresis. The bands corresponding to the expected amplicon size of 1500 bp were excised under a low frequency UV-light and transferred into eppendorf tubes, followed by purification of the 16S rRNA gene fragments using the Biospin Gel Extraction kit (Bioflux) according to the manufacturer's specifications.

3.2.2.2 Ligation and transformation of the PCR products into a pGEM[®]-T easy vector

The procedure was followed according to the manufacturer's instruction (Promega) and assembled as described in Table 3.3. For high efficiency, the ligation reaction was performed overnight at 4°C.

Table 3.3. Ligation mixture composition for the pGEM[®]-T Easy vector system.

Component	Sample Volume (µl)	Control Volume (µl)
2X Rapid ligation buffer	5	5
pGEM [®] -T Easy vector (50 ng)	0.8	1
PCR product (75 ng)*	0.8	-
pUC DNA	-	1
T4 DNA ligase (3 Weiss units/µl)	1	1
Sterilised Milli Q H ₂ O	1.2	1
Total	10	10

* Depending on the fragment length and using the molar ratio 1:3 of insert DNA: vector. A positive control test was performed in order to test the efficiency of the *E. coli* Top10 competent cells (host cell) and was ligated in the same manner as the PCR products of interest.

The ligation mixture (2 μ l) was added to *E.coli* Top10 competent cells (50 μ l), incubated on ice for 30 min followed by a heat shock step at 42°C for 40 sec and immediate cooling on ice for 2 min, after which 700 μ l of SOC (LB medium supplemented with 50 μ l 2 M magnesium and 100 μ l 1 M glucose solution) medium was added. The culture was then incubated at 37°C for 1 h in a shaker rotating with 175 rpm. The transformation mix (50 μ l) was then plated out on AIX plates (LB medium [tryptone 10 g/l; yeast extract 5 g/l; NaCl 10 g/l] supplemented with ampicillin [10 mg/ml], IPTG [isopropylthio- β -D-galactoside, 24 mg/500 ml], X-gal [5-bromo-4-chloro-3-indolyl- β -D-galactoside, 20 mg/500 ml] and 15 g/l agar). The plates were incubated at 37°C for 16 h followed by selection of white colonies. Representative colonies (10 per plate) were inoculated into 5 ml LB medium supplemented with 10 mg/ml ampicillin and incubated at 37°C for 16 h.

3.2.2.3 Small scale plasmid isolation

The plasmids from transformed cells were isolated according to the Biospin Plasmid DNA Extraction Kit (Bioflux) manufacturer's specifications. The bacterial culture (1.5 ml) was centrifuged for 1 min and the supernatant decanted, followed by addition of 400 μ l ice-cold complete lysis solution and vigorous mixing. This was incubated for 5 min at room temperature and the bacterial lysate transferred into an assembled spin column. Cell debris was removed by centrifugation for 1 min at room temperature. The resultant DNA was washed with 400 μ l and the DNA eluted using 50 μ l elution buffer.

3.2.2.4 Restriction Fragment Length Polymorphism (RLFP)

The purified plasmid, obtained from section 3.2.2.3, was subjected to a restriction digest (Table 3.4) using *Nde*I and *Not*I to cut the 16S rRNA gene fragment out of the plasmid. The restriction digest (10 μ l) was loaded onto the 1% (w/v) agarose gel. The band corresponding to the 16S rRNA gene fragment (1500 bp)

was excised under a low frequency UV-light and transferred into eppendorf tubes, followed by purification of the 16S rRNA gene fragments using the Biospin Gel Extraction kit (Bioflux) according to the manufacturer's specifications.

The restriction digest (Table 3.4) was performed on the purified 16S rRNA gene PCR product using *Sma*I and *Avr*II endonuclease in order to assess the inserts sizes of the bands obtained.

Table 3.4. Restriction digests reaction composition.

Component	Volume (µl)
PCR Product	5
Buffer (10 X)	1
Sterile Milli Q	
H ₂ O	3
Restriction enzyme (5 000 U/ml)	1
Total volume	10

The restriction digest reactions were incubated at 37°C for 3 h. The results were evaluated on a 1% (w/v) agarose gel as described in section 3.2.2.1.

3.2.3 Biomass vs optical density

3.2.3.1 Dry weight determination

Glass tubes were baked overnight at a temperature of 105°C and placed in a dessicator. Following this, the tubes were weighed on an analytical scale (tubes were always handled with a pincet). *T. scotoductus* SA-01 was grown to an optical density of 1.2 and 10 ml/tube of culture was dispensed into three tubes,

centrifuged (3000 *xg*, 10 min), the cells were washed twice with distilled water and the tubes were baked at a temperature of 105 °C for 12 h and weighed.

3.2.3.2 Dilution range

A dilution range was made by adding the appropriate volume of culture to a determined volume of medium. The optical density of each sample in the dilution range was measured on a Spectronic® Genesys™ 5 at 600 nm (Madrid and Felice, 2005).

3.2.4 Growth of *Thermus scotoductus*SA-01

*T. scotoductus*SA-01 was plated out, from a glycerol stock, on a TYG plate and allowed to grow for 24 hours at 65 °C, this was then replated on solid TYG plates and allowed to grow for 24 hours at 65 °C. A pre-inoculum was then prepared by inoculating a loop full of growth from the plate in 50 ml of liquid TYG medium. This was grown for 8 hours at 65 °C and a 10% (v/v) inoculation of growth was made into liquid TYG medium. This was then grown for 8 hours at 65 °C after which a 5% (v/v) inoculation of growth was made into liquid TYG medium. *T. scotoductus* was grown in liquid TYG medium at 65 °C, samples were extracted every 2 hours and optical density measured on a Spectronic® Genesys™ 5 at 600nm.

3.2.5 Aerobic batch culture studies

3.2.5.1 Growth with uranium induced stress with no pre-culturing

The growth of *T. scotoductus* SA-01 was evaluated under aerobic conditions in TYG medium supplemented with uranium(VI) concentrations ranging from 0.25 mM to 1.5 mM. uranium(VI) was prepared by dissolving $\text{UO}_2(\text{CH}_3\text{COO})_2 \cdot 2\text{H}_2\text{O}$ (SPI-Chem)(Kieft *et al.*, 1999) in deionized water and the concentration

adjusted to 100 mM. Growth was initiated in 500 ml Erlenmeyer flasks containing 100 ml of medium using standardized inocula (5% v/v) to approximately 0.06g of cells (dry weight) per litre. For investigation, *T. scotoeductus* SA-01 was cultured in media containing a final concentration of 0 (control), to 1.5 mM uranium(VI) for 24h at 65°C with shaking (160 rev min⁻¹) and the optical density (600 nm) was recorded at 2 hour intervals on a Spectronic® Genesys™ 5.

3.2.5.2 Growth with uranium induced stress with three and six hours pre-culturing

Growth was initiated in 500 ml Erlenmeyer flasks containing 100 ml of medium using standardized inocula (5% v/v) to approximately 0.06g of cells (dry weight) per litre. *T. scotoeductus* SA-01 was first cultured for 3 and 6 hours in media containing no uranium(VI), after 3 and 6 hours of growth a final concentration of 1.5 mM to 5 mM of uranium(VI) for 24h at 65°C with shaking (160 rev/min) and the optical density (600 nm) was recorded at 2 hour intervals on a Spectronic® Genesys™ 5.

3.2.6 Spectrophotometric determination of uranium(VI)

All reagents were of analytical reagent grade. Deionized distilled water was used for the preparation of standard solutions. A 100 mM uranium(VI) stock solution was prepared by dissolving UO₂(CH₃COO)₂·2H₂O (SPI-Chem) in water. The prepared solution was stored in the dark and used for sequential dilution. 2-(5-bromo-2-pyridylazo)-5-diethylaminophenol (5-Br-PADAP) (Sigma-Aldrich) was used to prepare a 0.05% solution by dissolving the reagent in ethanol. The complexing ligand solution (pH 7.8) was prepared by dissolving 1 g of NaF and 13 g of sulphosalicylic acid in 40 ml water, the pH was adjusted with NaOH and the solution diluted to 100 ml. The buffer solution (pH 7.8) was prepared by diluting 14 g of TEA in 80 ml of water, the pH was then adjusted with perchloric acid, and solution left to stand overnight. Before use, the pH of the buffer solution

was checked and adjusted to 7.8 if necessary. All optical density measurements were made on a Spectronic® Genesys™ 5 at 600 nm (Johnson and Florence, 1971).

3.2.7 Uranium(VI) standard curve

Uranium(VI) dilutions were made by diluting the stock solution with water. 100 μl of the uranium(VI) was taken in a 1.5 ml eppendorf tube containing 25 μl of complexing solution. To the above, the 100 μl of the buffer solution and 80 μl of Br-PADAP solution was added and made up with 620 μl ethanol and 75 μl water. This coloured solution was allowed to stand for about 2 h and absorbance measured at 578 nm against a reagent blank (Johnson and Florence, 1971). A uranium(VI) standard curve was constructed by plotting the absorbance reading against the known uranium(VI) concentration (Figure 3.1).

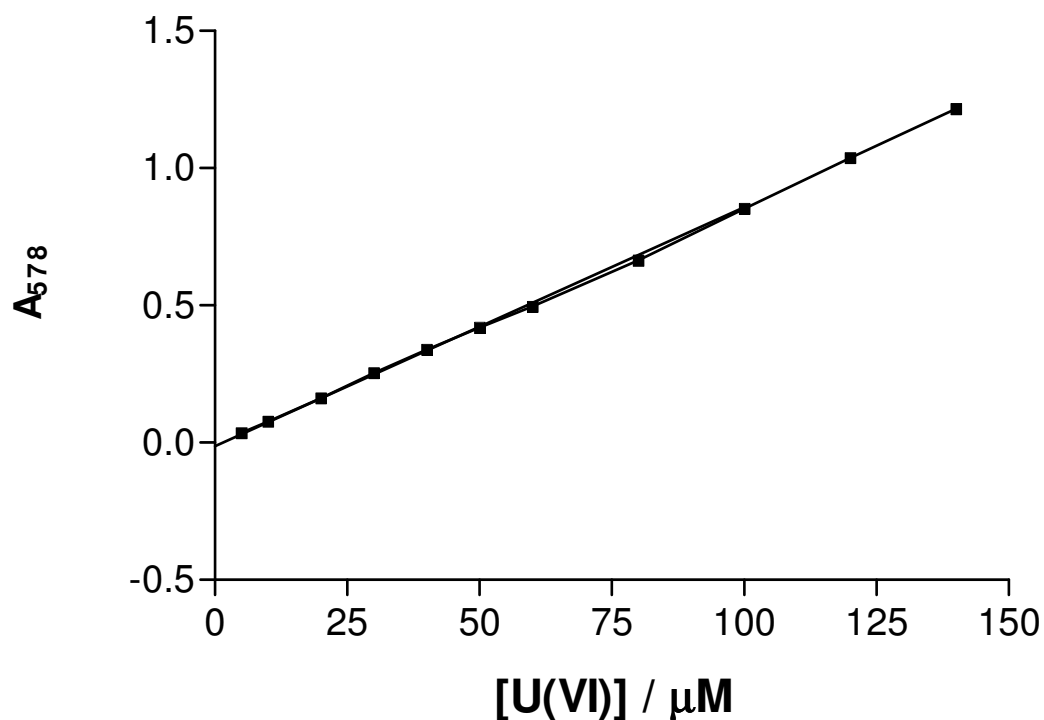


Figure 3.1: Standard curve indicating the relationship between uranium(VI) and OD ($R^2 = 0.9991$). Standard deviations are smaller than the symbols.

3.2.8 Reduction of uranium(VI) by resting cells of *T. scotoductus* SA-01 under non-growth conditions

The ability to reduce uranium by whole cells under non-growth conditions was determined by measuring the decrease in hexavalent uranium. Uranium(VI) was analyzed spectrophotometrically according to the 5-Br-PADAP method described in 3.2.7. All experiments were performed in an anaerobic chamber to prevent reduced uranium(IV) from being oxidized to uranium(VI) (Lovley *et al.*, 1991), cells were incubated under non-growth conditions to prevent any unwanted chemical reduction. Along with a cell-free control, an electron donor free control was also prepared. The whole cell reduction was set up as described by Kieft and co-workers (1999), with the exceptions that a wider range of parameters would be evaluated. *T. scotoductus* SA-01 cells were harvested from growth standardized inoculum and unless otherwise specified, cells were grown until late exponential phase (8 h), as previously determined. The cells in the uranium(VI) reduction experiments were washed three times with 20 mM MOPS buffer, pH 7.0, and the suspension purged with O₂-free N₂. Preceding the assay, the suspension and all reagents were transferred to an anaerobic chamber with a 10% CO₂ / 10% H₂ / 80% N₂ headspace.

In an attempt to determine optimal conditions for whole cell uranium(VI) reduction, numerous variables were assayed which included various electron donors as well as growth phase

3.2.8.1 Whole cell uranium(VI) reduction by cells harvested in early and late exponential phase with lactate as electron donor

T. scotoductus SA-01 cells were harvested in early (4 h) as well as late exponential (8 h) phase. To initiate the assay, a sample of the cells was added to a tube containing the assay solution (0.25 mM uranyl acetate in anaerobic 20 mM MOPS buffer, pH 7.0, with 2 mM sodium lactate as electron donor) and

subjected to the spectrophotometric assay described in 3.2.7. A reagent blank was also prepared as well as a heat inactivated cell control.

3.2.8.2 Whole cell uranium(VI) reduction with different electron donors

T. scotoductus SA-01 cells were harvested and washed as described above. 10 mM sodium acetate, glucose and sodium pyruvate were prepared as stock solutions and purged with O₂-free N₂. To initiate the assay, a sample of the culture was added to a tube containing the assay solution (uranyl acetate plus one of the aforementioned electron donors) to a final concentration of 0.25 mM uranium(VI) and 2 mM electron donor, and subjected to analysis as described in 3.2.7. To determine if hydrogen will had any effect on reduction, *T. scotoductus* SA-01 cells were harvested and washed as described above but the suspension was purged with H₂-gas to introduce H₂ as electron donor (Payne *et al.*, 2002). Uranium(VI) reduction was assayed as described in 3.2.7. Reagent blanks as well as electron donor free blanks were also prepared.

3.2.8.3 Whole cell uranium(VI) reduction at different pH values

MOPS (20 mM), MES (20 mM) and Tris-HCl (20 mM) buffers were prepared and heated to 65°C. At 65°C, the pH of the 20 mM MES was adjusted to 5.5 and 6.0, the pH of the 20 mM MOPS was adjusted to 6.5 and 7.5 and the pH of the 20 mM Tris-HCl was adjusted to 8.0, 8.5 and 9.0. *T. scotoductus* SA-01 cells were harvested, washed and resuspended in one of the pH calibrated buffers. The suspension was then purged with O₂-free N₂. Uranyl acetate was added to a final concentration of 0.25 mM uranium(VI), and subjected to analysis as described in 3.2.7.

3.2.8.4 Whole cell uranium(VI) reduction at different temperatures

MOPS (20 mM) was prepared and heated to 35, 45, 55, 65 and 75 °C. At each of these temperature values, the pH was adjusted to 7.0. *T. scotoductus* SA-01 cells were harvested, washed and resuspended in one of the pH calibrated buffers. The suspension was then purged with O₂-free N₂. Uranyl acetate was added to a final concentration of 0.25 mM uranium(VI), and subjected to analysis as described in 3.2.7.

3.2.9 Transmission Electron Microscopy

To study the interactions of higher concentrations of the metal with the microorganism, cells were grown in TYG medium containing a final concentration of 1.25 mM of uranium(VI). These cells were then subsequently subjected to fixation, dehydration and polymerization for further TEM and SEM studies.

3.2.9.1 Fixation

Cells were centrifuged (10 000 $\times g$ at room temperature) for one minute and washed twice with phosphate buffer (0.1 M, pH 7). Cells were then suspended in a phosphate buffer (0.1 M, pH 7) and glutaraldehyde (3% final concentration) solution overnight. The mixture was then centrifuged (10 000 $\times g$ at room temperature) for 5 min and the supernatant removed. Cells were immediately washed with phosphate buffer (0.1 M, pH 7) and centrifuged again. This wash step was repeated once. In a fume cupboard, 4% osmium tetroxide was added to a final concentration of 0.5% and left for 2 h after which the mixture was centrifuged (10 000 $\times g$ at room temperature) for 5 minutes and the supernatant removed. Cells were washed once with phosphate buffer (0.1 M, pH 7). A 1% agar solution was prepared by dissolving 0.1 g agar powder in 10 ml of distilled water and the solution was kept in a 65°C water bath to prevent the agar from solidifying. A few drops of molten agar were added to the cells, mixed well and

this agar-cells mixture withdrawn and left to solidify on a microscope slide. The agar-cell droplet was then cut into small pieces using a scalpel blade and transferred to a 50% acetone solution for 30 min for the first step of dehydration.

3.2.9.2 Dehydration

After 30 minutes, the excess acetone solution was withdrawn and 70% acetone added. This was left for 30 minutes, repeated with a 95% solution and three times with a 100% acetone solution of which the first submersion into 100% acetone was performed for 1 h and not just 30 min.

3.2.9.3 Polymerization

Epoxy was prepared by weighing (not volumetric measuring, due to the high viscosity of the liquids) of the following components, 23 g VCD (vinylcyclohexene dioxide), 62 g NSA (nonenyl succinic anhydride), 14 g DER736 (diglycidyl ether of polypropylene glycol) and 1 g DMAE [(S1) dimethylaminoethanil] added together by constant stirring. Approximately 1 ml of 100% acetone solution and 1 ml of prepared epoxy was added to the cells and left for 8 h. The acetone-epoxy mixture was then withdrawn and replaced with 1 ml of pure epoxy and this was then left for 8 h. The epoxy blocks were then filled up with the epoxy and the agar-cells squares, and this was placed in the oven at 70°C for 8 h. Blocks were trimmed using an ultramicrotome and then cut into thin sections of approximately 0.2 µm. These sections were collected on a copper grid.

9.2.9.4 Lead staining of the material

1 L of distilled water was boiled for 15 min and left to cool. An amount of 0.665 g lead (Pb) was quantitatively transferred to a 25 ml volumetric flask and dissolved in some of the boiled distilled water. 0.88 g of nitrate was also added and dissolved in the flask containing the dissolved Pb. The Lead-nitrate mixture was

then shaken for 30 min after which 4 ml 1 N sodium hydroxide (NaOH) was added. The 25 ml volumetric flask was then filled to the mark with the boiled distilled water and left to stand for 5 min. NaOH pellets were then placed around the rim of a Petri-dish containing wax. A drop of the Pb-nitrate mixture was placed in the middle of the wax Petri-dish and the grid placed with the material face down into the drop. This was then left to stain for 8 min after which the grid was rinsed three times with the boiled distilled water. The first rinse was performed in a mixture of 1 N NaOH and boiled distilled water. Electron micrographs were taken with a Philips CM 100 (The Netherlands) TEM.

3.3 Results and discussion

3.3.1 Confirmation of strain as *T. scotoeductus* SA-01

3.3.1.1 Genomic DNA isolation and 16S rRNA gene amplification

gDNA was successfully extracted from *T. scotoeductus* SA-01, as described in section 3.2.2.1,. The extracted gDNA (2013 ng/μl) was visualized on a 1% agarose gel as indicated in Figure 3.2.

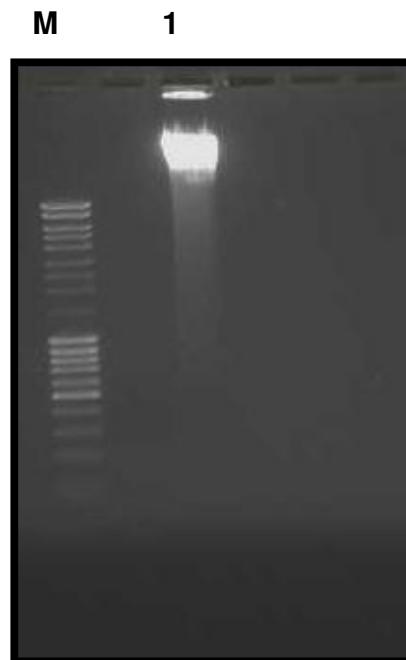


Figure 3.2: Genomic DNA extracted from *T. scotoeductus*. Lane M, MassRuler™ DNA ladder (Fermentas); Lane 1, isolated gDNA

The extracted genomic DNA was amplified as described in Section 3.2.2.1 and the expected amplicon of ~1500 bp was obtained (Figure 3.3). The 16S rRNA gene amplicon was excised from the gel and ligated into the pGEM®-T easy vector.

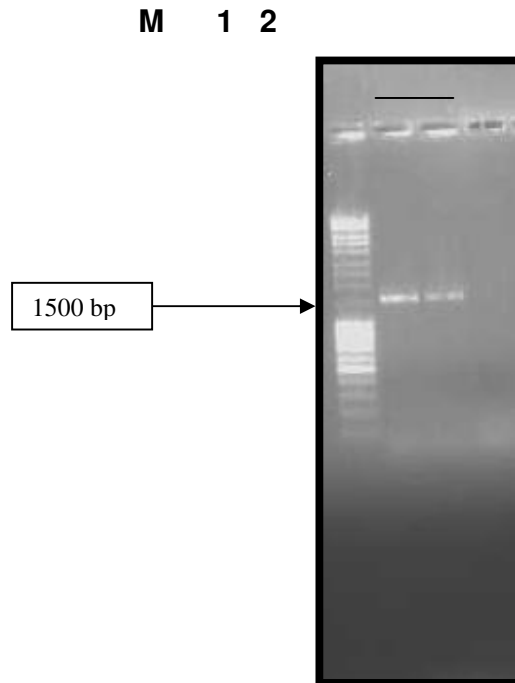


Figure 3.3: Amplification of 16S rRNA gene fragment using genomic DNA. Lane M, MassRuler™ DNA ladder (Fermentas); Lane 1, amplified 16S fragment; Lane 2, Negative Control

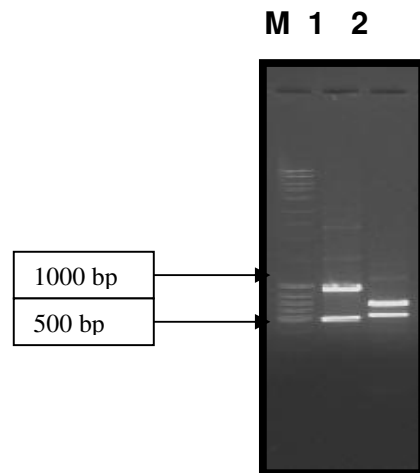
3.3.1.2 Transformation into *E.coli* Top 10 competent cells

The PCR products ligated into the pGEM®-T easy vector were transformed into *E.coli* Top10 competent cells and eventually plated on AIX plates for blue/white selection. Ten white colonies were then selected and grown in LB-media as described in section 3.2.2.2.

3.3.1.3 Restriction fragment length polymorphism (RFLP) analysis

Restriction digest was done on the purified 16S rRNA gene fragment as described in 3.2.2.4 with *Sma*I and *Avr*II endonuclease and the result obtained is shown in Figure 3.4 (A).

(A)



(B)

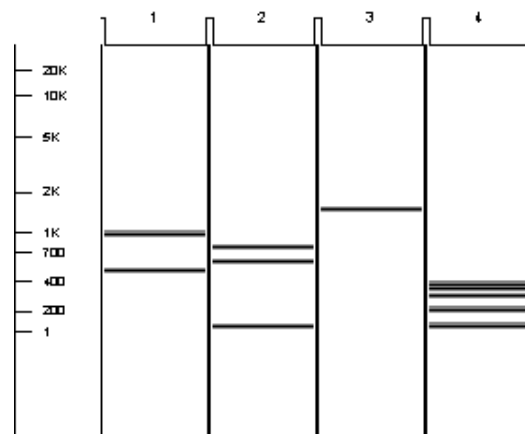


Figure 3.4: Restriction digest with *Sma*I and *Avr*II. A) *T. scoto*ductus SA-01 16S rRNA gene fragment. Lane M, MassRuler™ DNA ladder (Fermentas); Lane 1, *Avr*II digested fragment; Lane 2, *Sma*I digested fragment. B) Virtual digest of both the 16S rRNA gene fragments from *T. scoto*ductus SA-01 and *T. thermophilus* HB27. Lane 1, *T. scoto*ductus SA-01 16S digested with *Avr*II; Lane 2, *T. scoto*ductus SA-01 16S digested with *Sma*I; Lane 3, *T. thermophilus* HB27 16S digested with *Avr*II; Lane 4, *T. thermophilus* HB27 16S digested with *Sma*I.

The combination of these two restriction maps gave a clear indication that the strain was indeed *T. scoto*ductus SA-01. The selected bacterial isolate was confirmed due to a distinctive RFLP pattern (obtained from a virtual digest of the 16S rRNA gene performed on Vector NTI Suite 9, Informax) of the 16S rRNA gene fragments when compared to possible other *Thermus* contamination (Figure 3.4 B).

3.3.2 Relating biomass to optical density

Table 3.5 shows the values obtained from section 3.2.3 in order to determine the weight of cells in 1 liter of medium, from the dry weight obtained from 10 ml.

Table 3.5. Values obtain from dry weight determination.

Tube no	Tube Weight (g)	Weight Tube + Cells	Weight Cells (g/10 ml)	Cell Weight (g/L)
1	12.93	12.93	0.0041	0.41
2	12.71	12.71	0.0042	0.42
3	12.80	12.80	0.0035	0.35
Ave Weight:			0.0039	0.3933

Table 3.6, illustrates the dilution range employed in this study as well as the optical density reading obtained for each the specific dilutions.

Table 3.6. Dilution range used as well as optical density reading.

Dilution Factor	Dilution	OD
2	0.5	0.552
		0.556
		0.556
5	0.2	0.191
		0.191
		0.190
8	0.125	0.109
		0.113
		0.108
10	0.1	0.088
		0.087
		0.091
20	0.05	0.045
		0.043
		0.041
50	0.02	0.017
		0.016
		0.017
80	0.0125	0.011
		0.010
		0.012
100	0.01	0.002
		0.003
		0.003

The standard curve was constructed by plotting the optical density reading of the specific diluted sample vs the cell mass value (Figure 3.5) for the specific diluted sample. The cell mass value was obtained by dividing the value, a, which is equal to the average cell weight in 1 liter of medium by the dilution factor. This is given in Table 3.7.

Table 3.7. Values used for construction of the Biomass to OD standard curve.

Dilution Factor	OD	a / Dilution Factor
2	0.552	0.197
	0.556	
	0.556	
5	0.191	0.079
	0.191	
	0.190	
8	0.109	0.049
	0.113	
	0.108	
10	0.088	0.039
	0.087	
	0.091	
20	0.045	0.02
	0.043	
	0.041	
50	0.017	0.008
	0.016	
	0.017	
80	0.011	0.0049
	0.010	
	0.012	
100	0.002	0.0039
	0.003	
	0.003	
a =		0.3933

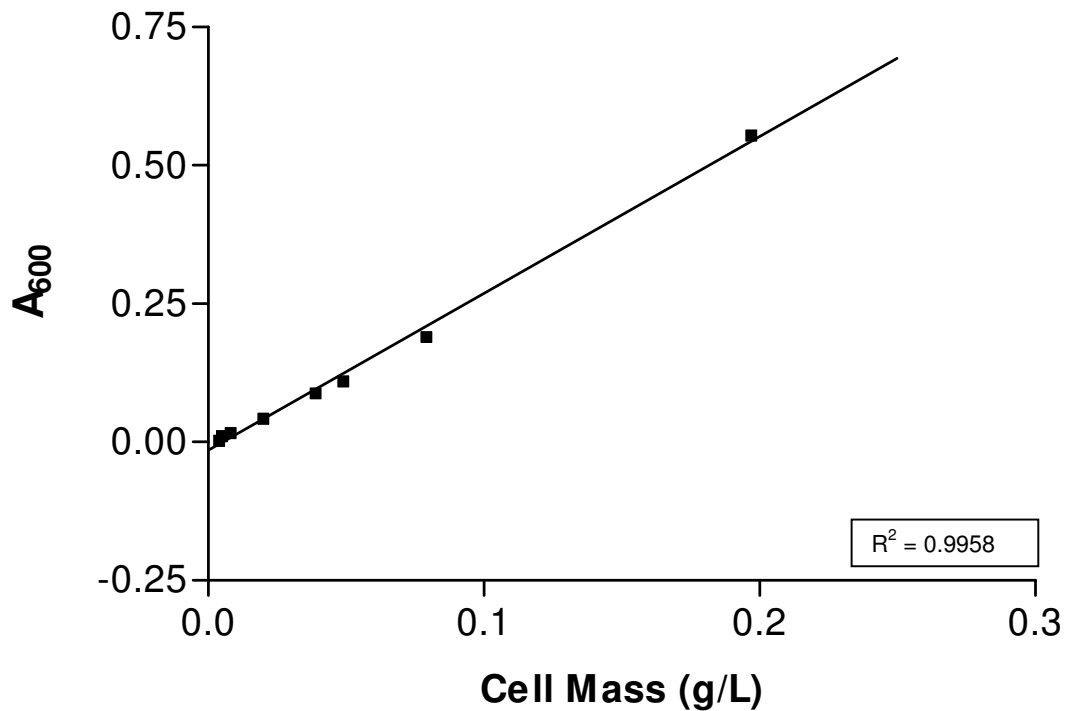


Figure 3.5:Standard curve indicating the the relationship between Biomass vs OD standard curve. Standard deviations are smaller than symbols, symbols represent data in triplicate.

From the standard curve, a biomass amount can be determined at any optical density reading by using the formula:

$$X = (Y - C) / M$$

Where C is the Y-intercept value, X is the biomass, Y is the optical density reading and M is the slope value.

3.3.3 Growth of *T. scotoductus* SA-01

To standardize growth, cells were grown in 50 ml (pre-inoculum) and then in 90 ml (inoculum) of liquid TYG media before the actual growth studies were conducted as described in section 3.2.4. Pre-inocula and inocula were prepared according to guidelines prescribed by Meyrath and Suchanek (1972).

3.3.3.1 Pre-inoculum

The growth curve obtained from *T. scotoeductus* SA-01 inoculated from solid TYG media into 50 ml of liquid TYG media can be seen in Figure 3.6. Subsequently 8 hours was deemed as the time period sufficient for the cells to grow to late exponential phase. It is very important to determine the amount of time needed for the cells to reach late exponential phase, since cells harvested prior to or beyond this stage of development might produce a lag phase of undefined length (Meyrath and Suchanek 1972).

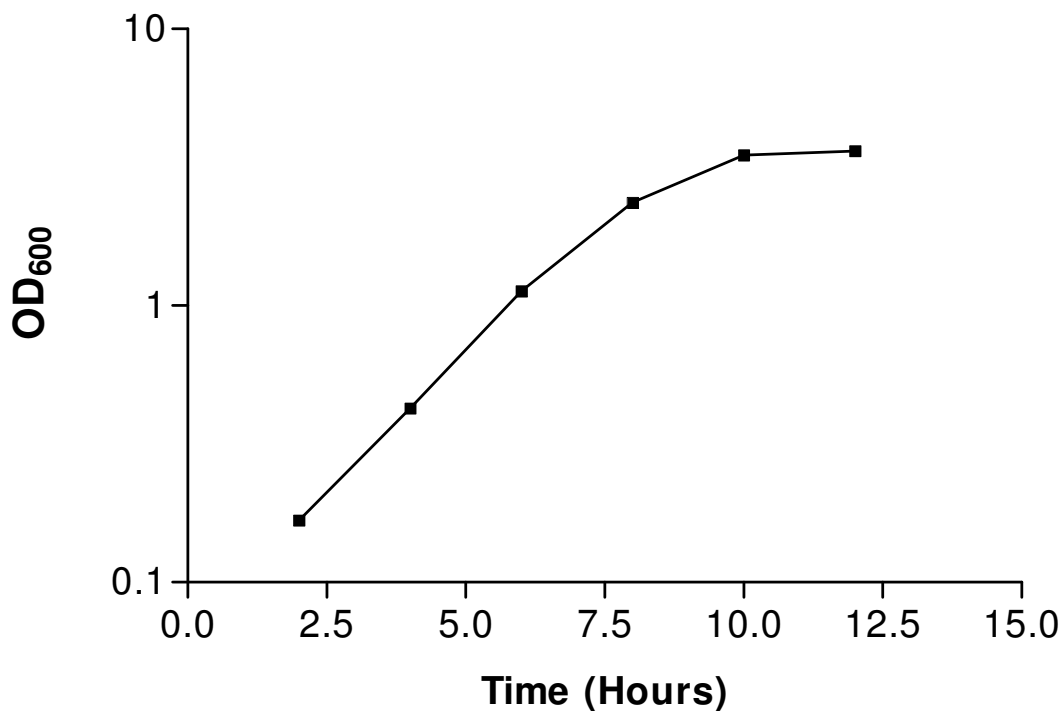


Figure 3.6: Growth curve of *T. scotoeductus* SA-01 pre-inoculum in TYG medium. Standard deviations are smaller than symbols, symbols represent data in triplicate.

3.3.3.2 Inoculum

The growth curve obtained from *T. scotoeductus* SA-01 with a 10% inoculum from the liquid TYG media (pre-inoculum) containing cells grown for 8 hours at 65°C, can be seen below in Figure 3.7. Results indicated that 8 hours was deemed as

the time period sufficient enough for the cells to grow to late exponential phase. Ideally cells should start growing exponentially right after inoculation. To achieve this, cells should be harvested in late exponential phase and a large (3-10%) inoculum should be utilized (Meyrath and Suchanek 1972).

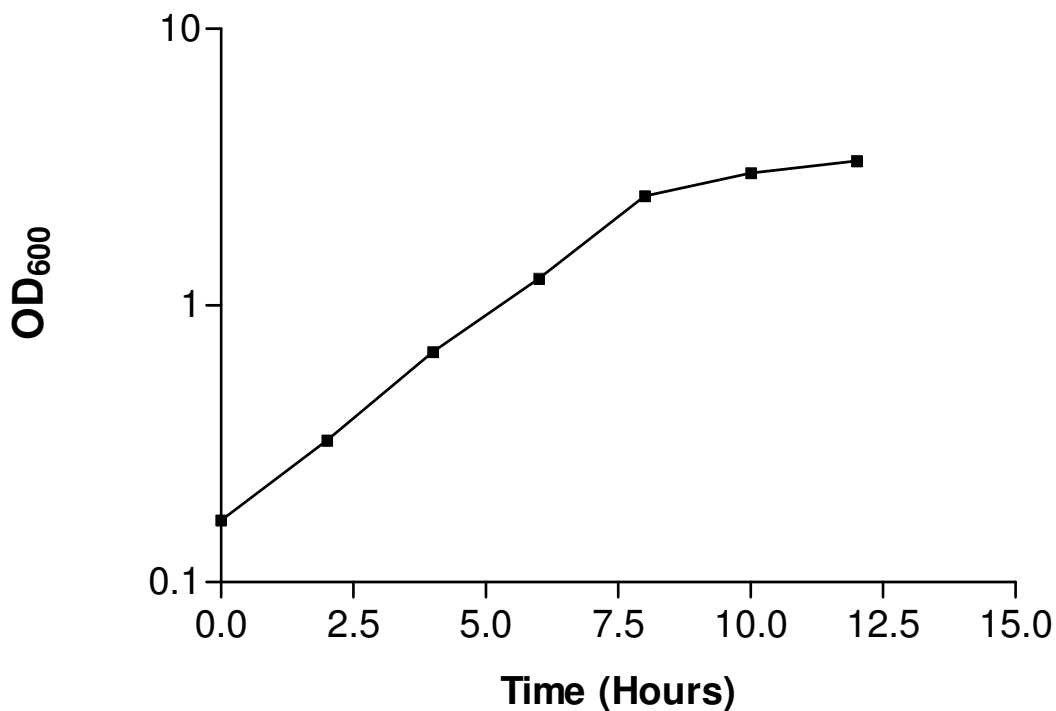


Figure 3.7: Growth curve of *T. scotoductus* SA-01 in TYG medium, growth started from cells in late exponential phase obtained from pre-inoculum. Standard deviations are smaller than symbols, symbols represent data in triplicate.

3.3.3.3 Growth curve

The growth curve obtained from *T. scotoductus* SA-01 when a 5% inoculum from the liquid TYG media (inoculum) containing cell grown for 8 hours at 65°C, can be seen in Figure 3.8. The culture has a specific growth rate of 0.26 h⁻¹ and a doubling time of 2.7 hours. This method of cultivation, pre-inoculum to inoculum to growth study, is designed to deliver maintainable and reproducible population density in a particular stage of development in a set amount of time (Meyrath and Suchanek 1972).

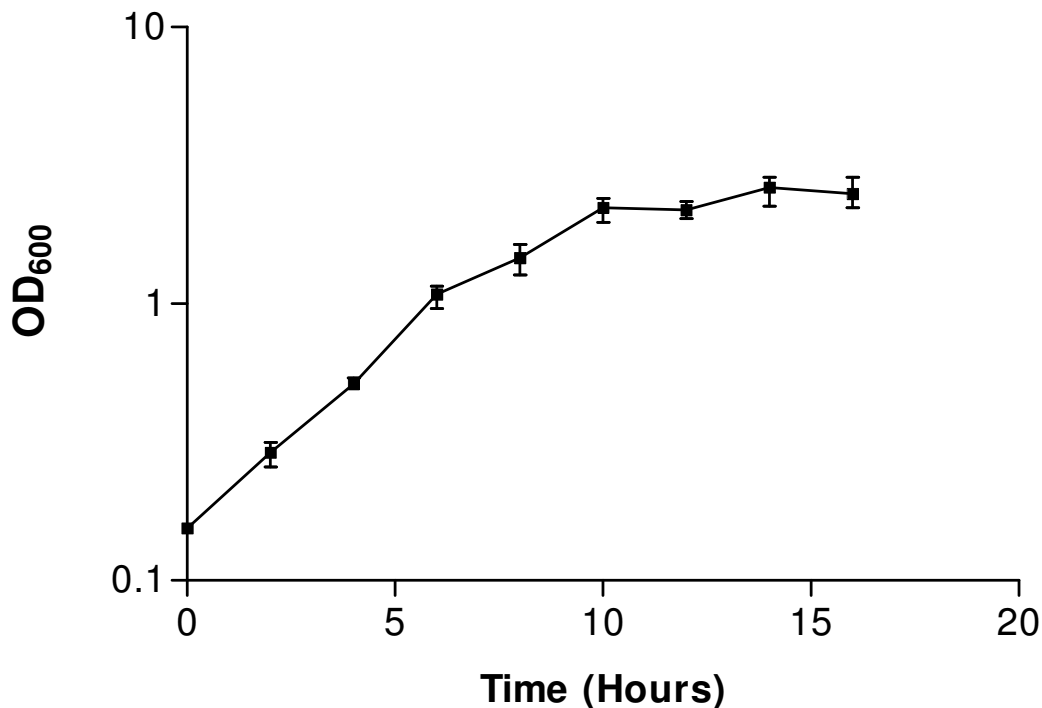


Figure 3.8: Growth curve of *T. scotoductus* SA-01 in TYG medium. Standard deviations are shown.

3.3.4 Effect of uranium on the growth of *T. scotoductus* SA-01

Normally microbial growth is characterized by four distinct growth phases; lag, exponential, stationary and death phase. One question in the relationship between a bacteria and a toxic metal is how that metal will influence the growth behavior. To this end the uranium(VI) tolerance capacity of *T. scotoductus* SA-01 during aerobic growth was evaluated by monitoring growth over time with varying concentrations of uranium as described in section 3.2.5.1. In literature it has been shown that *T. scotoductus* SA-01 has the ability to reduce uranium(VI) under non-growth conditions (Kieft *et al.*, 1999) but to date no studies have been conducted on the effect of uranium on the growth of this organism. Figure 3.9 displays the growth curves of SA-01 cultured in TYG medium in the presence and in the absence of uranium(VI).

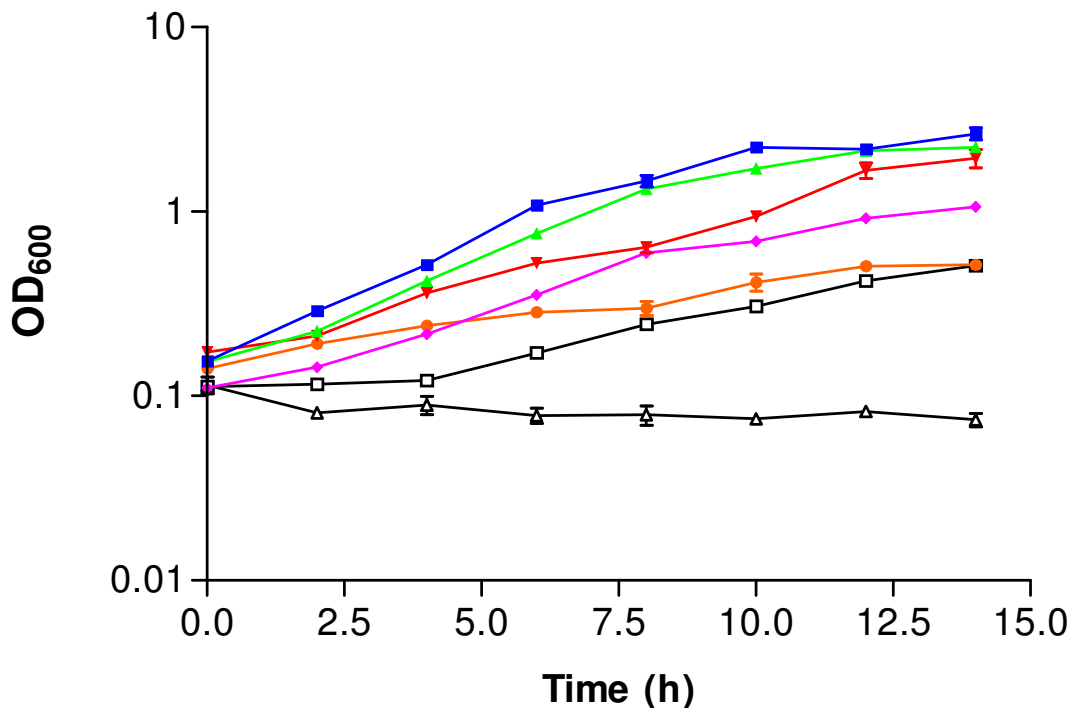


Figure 3.9: Growth of *T. scotoductus* SA-01 in TYG medium (■) amended with 0.25 mM (▲), 0.5 mM (▼), 0.75 mM (◆), 1.0 mM (●), 1.25 mM (□) and 1.5 mM (△) uranium(VI) during inoculation (t = 0). Standard deviations are shown or are smaller than symbols.

For the normal medium cell growth maximizes at 10 hours and then starts to decrease. For cells grown in medium amended with uranium(VI) the growth rate steadily declines (Table 3.8), with a rapid decline observed at concentrations of 0.5 mM and higher. Cells were still able to grow at concentrations up to 1.25 mM of uranium(VI) but no cell growth was observed at concentrations of 1.5 mM and above. These results indicate that the chemical properties of the uranium cause a toxic effect that inhibits the growth of *T. scotoductus* SA-01 since only depleted uranium with extremely low levels of radiation was used in this study. Compared to literature, SA-01 tolerates uranium levels comparable to those that *Acidithiobacillus ferrooxidans* resists, which is promising given that the latter is readily used in the treatment of low-grade ores for uranium extraction (Tuovinen and Kelly, 1974) but less than another thermophilic bacterium, *Thermoterrabacterium ferrireducens*, which is able to grow in uranium(VI) concentrations of up to 2.5 mM (Khijniak *et al.*, 2005) and much less than the

bacterium *Desulfovibrio desulfuricans* G20 which can grow in medium containing up to 3 mM of uranium(VI) (Payne *et al.*, 2002).

Table 3.8. Specific growth rate and doubling time values for growth curves of *T. scotoeductus* SA-01 in different concentrations of uranium.

Uranium(VI)	$\mu_{\text{Max}} (\text{h}^{-1})$	$t_d(\text{h})$
0.00 mM	0.32	2.19
0.25 mM	0.21	3.34
0.50 mM	0.11	6.81
0.75 mM	0.08	8.54
1.00 mM	0.02	32.49
1.25 mM	0.02	24.46
1.50 mM	5.0×10^{-4}	1386.30

3.3.4.1 Effect of uranium on the growth of *T. scotoeductus* SA-01 with pre-culturing

In an attempt to determine if *T. scotoeductus* SA-01 will be able to tolerate higher levels of uranium if pre-cultured before uranium addition, uranium was added after 3 and 6 hours of growth as described in section 3.2.5.2, thus in early and mid exponential growth phase. It was thought that younger cells might be more resilient to the uranium toxicity and thus better able to adapt. A final concentration of 1.5 mM, 2 mM, 3 mM and 5 mM uranium(VI) was used since the organism was previously unable to grow at these concentrations. Non pre-cultured growth at 1.5 and 2 mM of uranium(VI) was also observed as control. Figure 3.10 illustrates the growth curves of *T. scotoeductus*SA-01 in the different uranium concentrations.

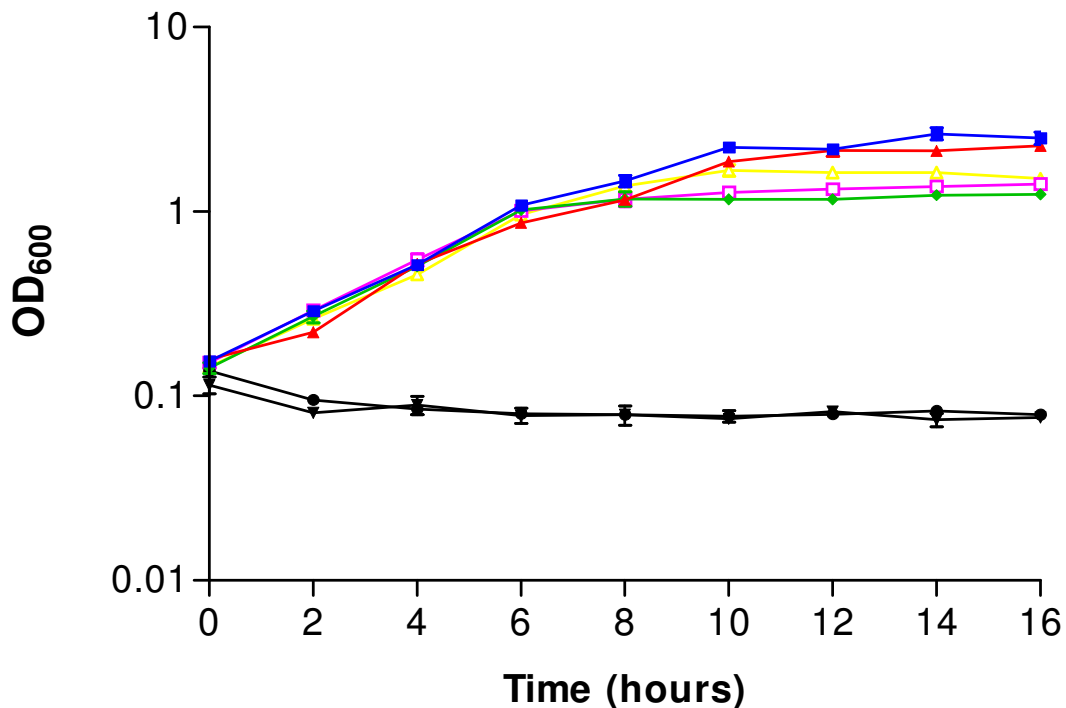


Figure 3.10: Growth curves for *T. scotoductus* SA-01 in TYG medium (■), amended with 1.5 mM (▲), 2.0 mM (◆), 3.0 mM (◻) and 5.0 mM (△) uranium(VI) after 6 hours of growth and 1.5 mM (▼) and 2.0 mM (●) uranium(VI) added during inoculation. Standard deviations are mostly smaller than symbols.

Only cells amended with 1.5 mM of uranium(VI) actually continued to grow, no actual increase in biomass was observed (Table 3.9) in the other experiments. In all the strains, with the exception of the growth spiked with 1.5 mM uranium(VI), growth was actually inhibited after the addition of the uranium(VI).

As for addition of uranium in early exponential growth phase, no growth was observed at higher uranium(VI) concentrations. It would seem that it is still too early in the cultures growth phase to effectively adapt to the uranium toxicity.

Table 3.9. Biomass before and after uranium(VI) addition.

Uranium(VI)	Biomass after 6 h (g.L ⁻¹)	Biomass after 16 h (g.L ⁻¹)
0.0 mM	0.403	1.006
1.5 mM	0.322	0.844
2.0 mM	0.373	0.407
3.0 mM	0.371	0.403
5.0 mM	0.333	0.350

3.3.5 Reduction of uranium(VI) by resting cells

A growing list of organisms capable of reducing uranium(VI) is being discovered (Wall and Krumholtz, 2006), but a complete understanding of the biochemistry of this process in any one of the bacteria is still far from complete. When *Thermus scotoducts* SA-01 was incubated anaerobically with uranium(VI) as described in section 3.2.7, a black precipitate forms in the cell pellet indicating the formation of uranium(IV) (Haas and Northop, 2004).

3.3.5.1 Uranium(VI) reduction by cells harvested in early as well as late exponential phase with lactate as electron donor

Uranium(VI) reduction was monitored as described in section 3.2.8.1. Figure 3.11(A) indicates that most of the uranium(VI) was reduced to uranium(IV) in under 20 hours which coincides with what was previously described in literature (Kieft *et al.*, 1999). Without an electron donor, and even after being autoclaved (Figure 3.12), *T. scotoductus* SA-01 was still able to reduce the uranium due to reducing conditions being present. Different growth phases were assayed to determine whether it would have any effect on reduction rate but it appears to have almost no impact on uranium reduction activity although cells harvested in late exponential phase seem to reduce the uranium(VI) at a slightly higher rate. No chemical reduction was observed in the cell-free controls indicating that the reduction must to be due to cellular activity. After completion of the experiment, the cells used were exposed to oxygen overnight which led to the disappearance of the black precipitate, Figure 3.11 (B) and (C).

(A)

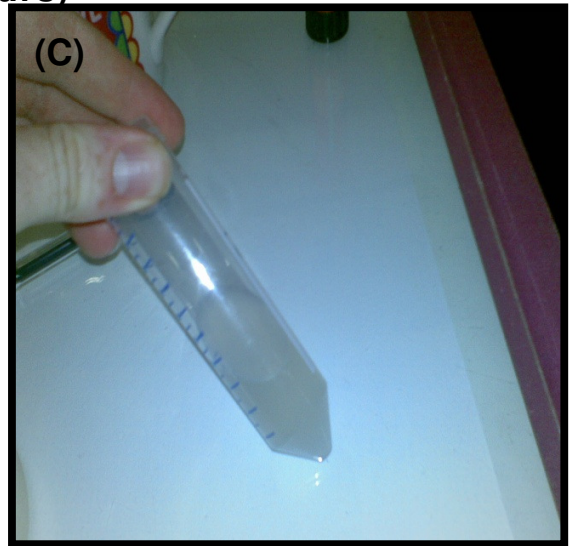
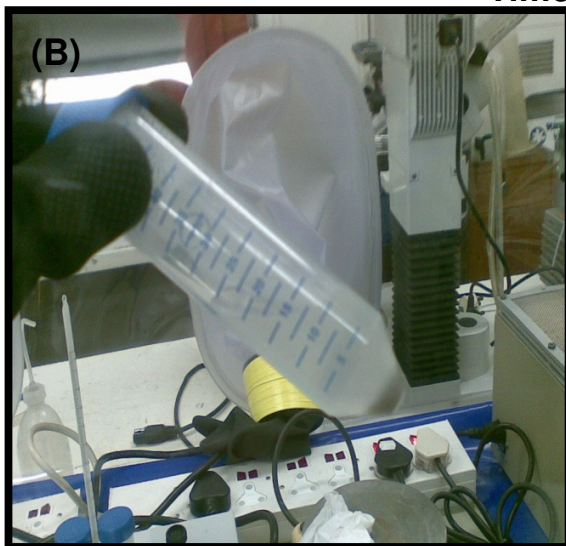
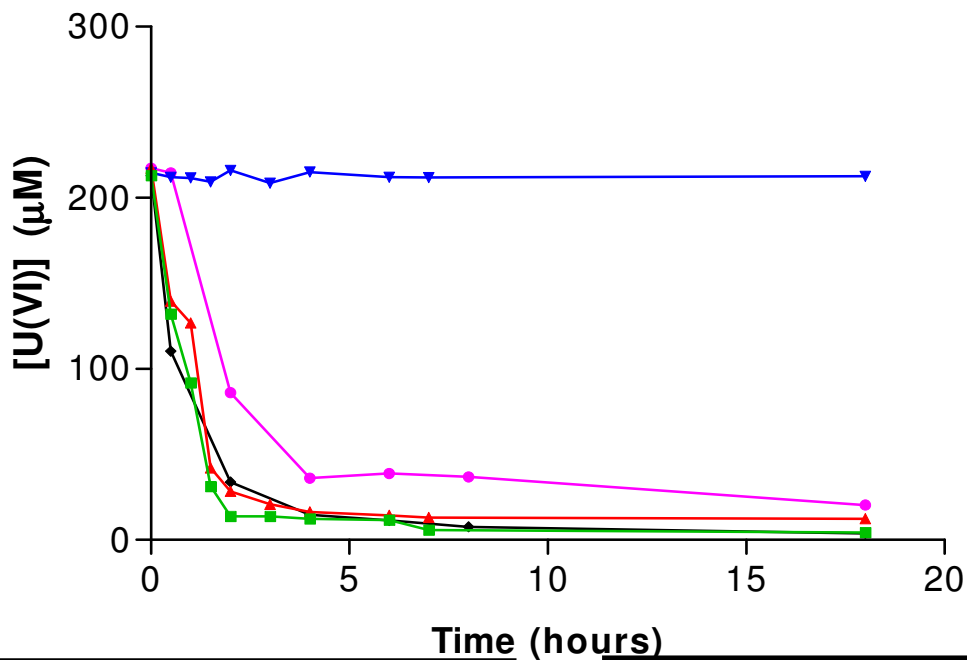


Figure 3.11:(A) Whole cell reduction of uranium(VI) by the thermophile *T. scoto ductus* SA-01 under anaerobic conditions. Cells harvested in late exponential phase with assay solution containing 0.25 mM uranium(VI) and 10 mM lactate as electron donor (■), control assay solution of cells harvested in late exponential phase containing 0.25 mM uranium(VI) and no electron donor (▲), cells harvested in early exponential phase with assay solution containing 0.25 mM uranium(VI) and 10 mM lactate as electron donor (◆), control assay solution of cells harvested in early exponential phase containing 0.25 mM uranium(VI) and no electron donor (◆), control assay solution lacking cells with 10 mM lactate (▼). Symbols represent an average of data in triplicate. (B) Whole cell reduction of uranium(VI) by the thermophile *T. scoto ductus* SA-01 under anaerobic conditions after 20 h, note the formed uranium(IV) black precipitate. (C) Cells from (B) after overnight exposure to oxygen, note the disappearance of the formed precipitate.

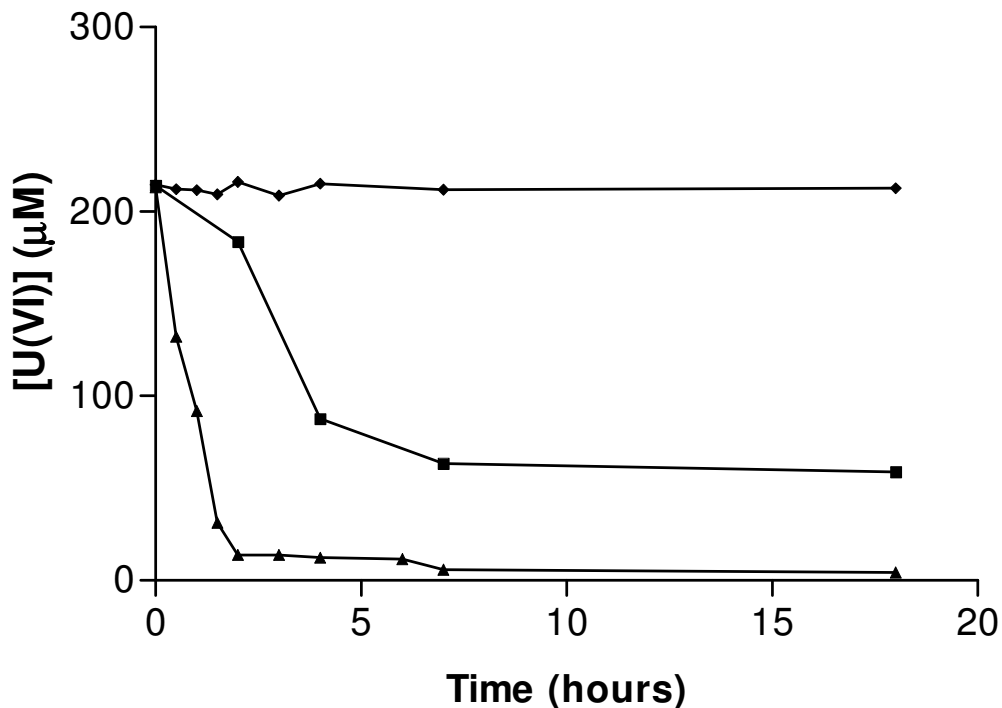


Figure 3.12: Whole cell reduction of uranium(VI) by the thermophile *T. scotoductus* SA-01 under anaerobic conditions. Autoclaved cells harvested in late exponential phase with assay solution containing 0.25 mM uranium(VI) and 10 mM lactate as electron donor (■), control assay solution of cells harvested in late exponential phase containing 0.25 mM uranium(VI) and 10 mM lactate as electron donor (▲), control assay solution lacking cells with 10 mM lactate (◆). Standard deviations are smaller than symbols. Symbols represent an average of data in triplicate

Uranium(VI) determination was performed after the exposure to air and it was found that most of the uranium(IV) in the sample was re-oxidized to uranium(VI). According to literature, this supports the belief that the reduction of uranium(VI) to uranium(IV) occurred since if complexes were formed by bioprecipitation or bioaccumulation, it would not have resulted in the reappearance of the uranium(VI) under aerobic conditions (Lovley *et al.*, 1991).

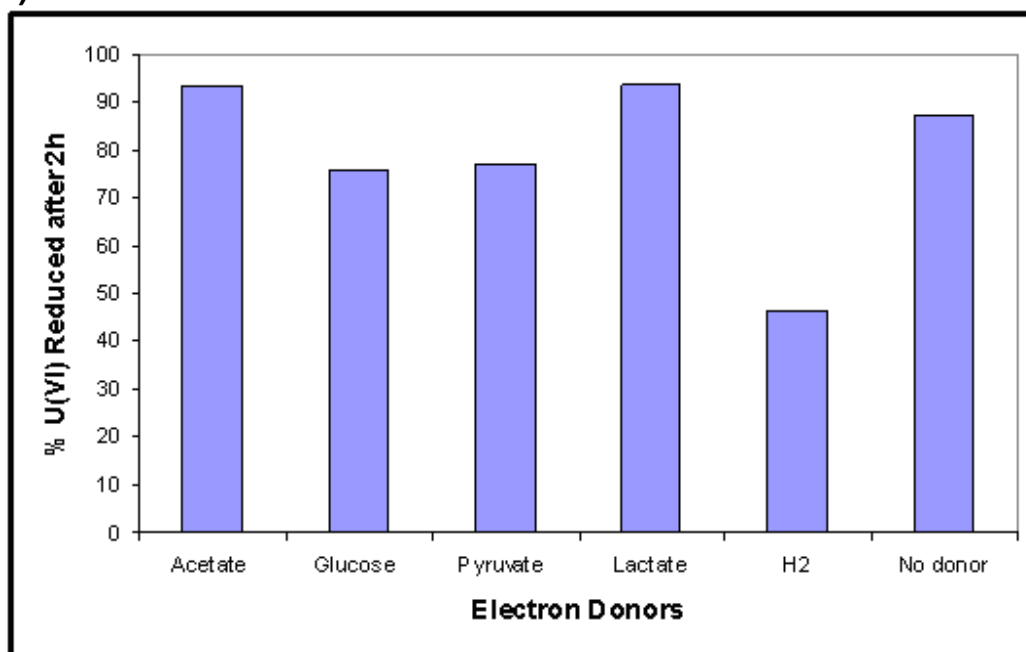
In literature, whole cell reduction of uranium(VI) has been mainly studied in cells containing a cytochrome *c3* protein which has been identified to be able to reduce uranium(VI) in conjunction with a periplasmic hydrogenase (Payne *et al.*, 2002; Shelobolina *et al.*, 2007). These cytochrome *c3* containing bacteria, such as *Geobacter metallireducens* and *Desulfovibrio desulfuricans*,

have both shown that reduction of uranium(VI) is dependant of the cells being alive as no uranium(VI) reduction was observed in heat killed cells and also that reduction of uranium(VI) is dependant on the presence of an electron donor (Lovley *et al.*, 1991; Lovley and Phillips, 1992). In contrast, from what we have established by searching through the draft genome (Gounder, 2009), *T. scotoductus* SA-01 does not contain a cytochrome *c3* and has also shown the ability to reduce uranium(VI) without any electron donor being present, therefore a possible novel interaction might infer this ability to *T. scotoductus* SA-01.

3.3.5.2 Uranium(VI) reduction with different electron donors

To determine the most effective electron donor for whole cell uranium(VI) reduction, various reduction assays were performed with electron donors determined to be most relevant as described in section 3.2.8.2. As can be seen depicted in Figure 3.13 (A) and (B), the specific electron donor did not have any real significant effect on uranium(VI) reduction. Uranium(VI) reduction is thus not directly coupled to the produced reducing equivalents. If, however, one is to observe reduction after 2 hours, as seen in Figure 3.13 (A), one would notice that the electron donors acetate and lactate are slightly more favored than the electron donors glucose, pyruvate and hydrogen. Here once again we see a contrast to what has been observed in literature pertaining to organisms containing cytochrome *c3* mediated reduction of uranium(VI). Lovley and Phillips (1992) found that when whole cell reduction of uranium(VI) by *D. desulfuricans* was monitored with both lactate and hydrogen as electron donors, there was no difference in the rate of reduction. Lovley and coworkers (1991) also found hydrogen to be the electron donor of choice when *G. metallireducens* was incorporated for uranium(VI) reduction. In the case of *T. scotoductus* SA-01 hydrogen delivered the lowest rate of reduction after 2 hours (Figure 3.13 A).

(A)



(B)

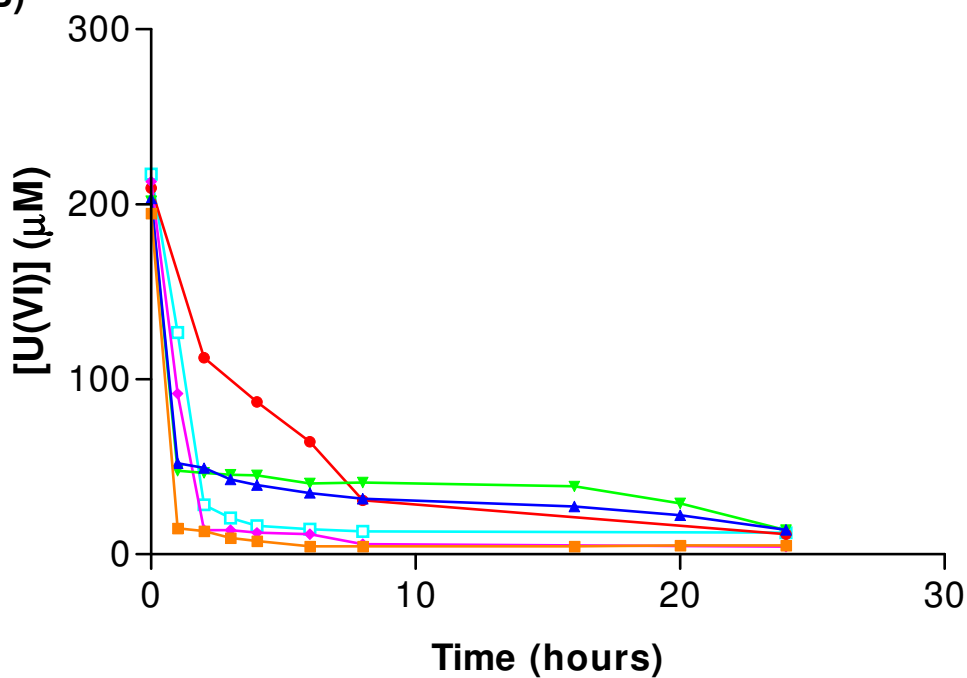


Figure 3.13: (A) Percentage uranium(VI) reduced by the thermophile *T. scotoeductus* SA-01 under anaerobic conditions with different electron donors after 2 hours. Symbols represent an average of data in triplicate. (B) Whole cell uranium(VI) reduction by the thermophile *T. scotoeductus* SA-01 under anaerobic conditions with different electron donors, Acetate (■), Glucose (▲), Pyruvate (▼), Lactate (◆), and H₂ (●). A control with no electron donor (□) can also be observed.

3.3.5.3 Uranium(VI) reduction at different pH and temperature values

Whole cell uranium(VI) reduction under non-growth conditions was performed as described in section 3.2.8.3, over a pH range of 5 to 9 as can be seen in Figure 3.14 (A). The pH that showed maximum activity was taken as 100%. The effect of the pH on the whole cell reduction is depicted in Figure 3.14 (B). The whole cell uranium(VI) reduction activity seemed to prefer a more neutral pH with maximum activity being observed at pH 7-8. Very low reaction rates were observed at pH values below 7, since all appropriate controls were evaluated this might be due to the fact that the assay does not function in this pH region.

The optimum temperature for whole cell uranium(VI) reduction was determined, as described in section 3.2.8.4, over a range of 35°C to 75°C, Figure 3.15. Temperature did not seem to have any significant effect on whole cell reduction.

Both *D. desulfuricans* and *G. metallireducens* have shown the ability to reduce uranium(VI) in acidic conditions. These experiments are usually conducted by determining the bacteria's capability to remove uranium(VI) from uranium contaminated mine water which has an acidic pH (Lovley *et al.*, 1991; Lovley and Phillips, 1992). What these experiments have also shown is that the reduction of uranium(VI) is dependant on the optimum growth temperature of the microorganism. In the case of *T. scotoductus* SA-01 a neutral pH is necessary for uranium(VI) reduction and temperature has almost no influence. The combination of what was seen here as well as in the previous sections give a strong indication that the reduction might be due to a non-specific low potential electron donor, a product of another, perhaps multitasking protein.

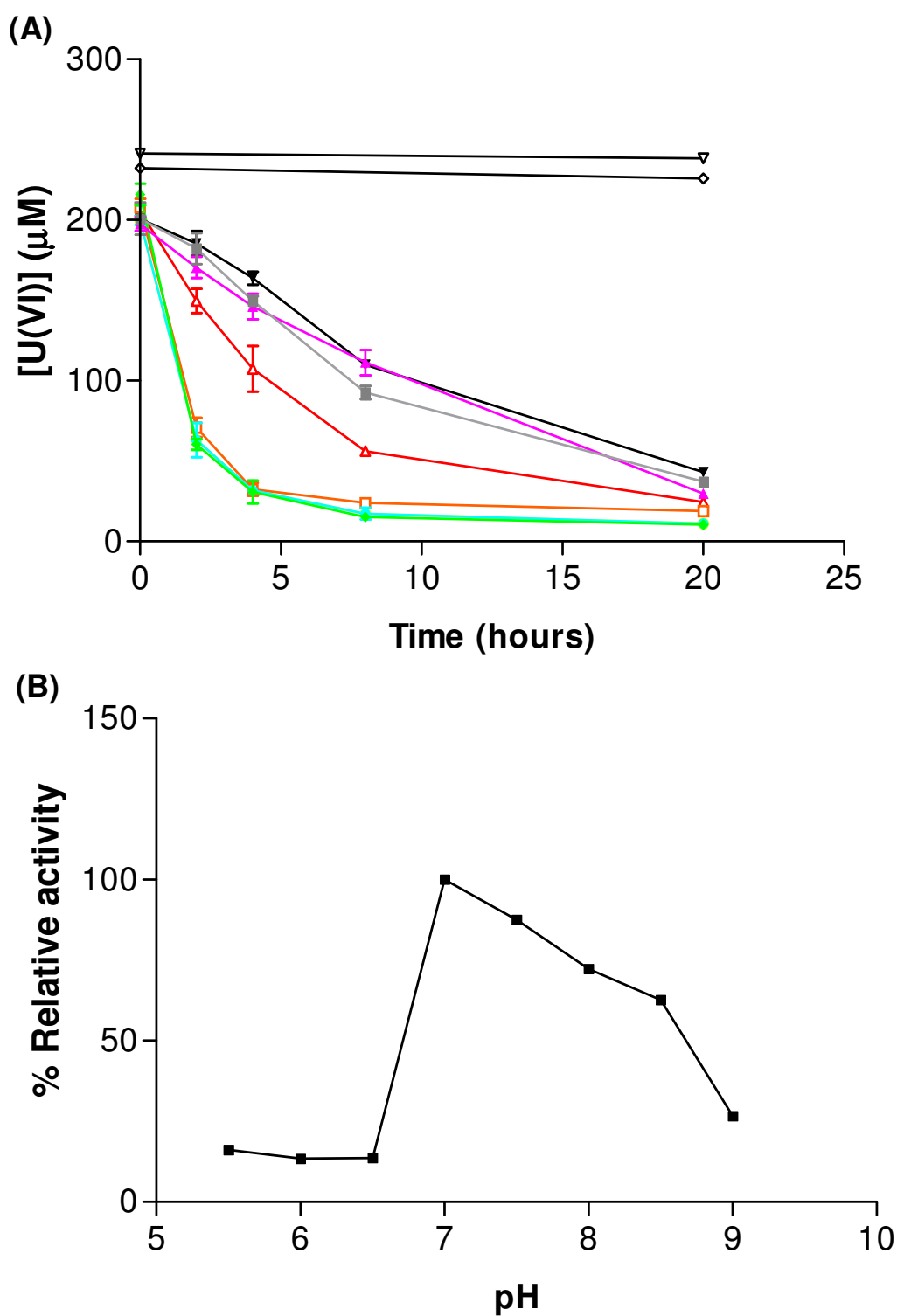


Figure 3.14: (A) Whole cell reduction of uranium(VI) by the thermophile *T. scotoductus* SA-01 under anaerobic conditions at different pH 5.5 (■), pH 6.0 (▲), pH 6.5 (▼), pH 7.0 (◆), pH 7.5 (●), pH 8.0 (◇), pH 8.5 (◻), pH 9.0 (△), pH 5.5 Blank (▽) and pH 9.0 Blank (○). Standard deviations are shown. (B) Optimum pH of whole cell uranium(VI) reduction.

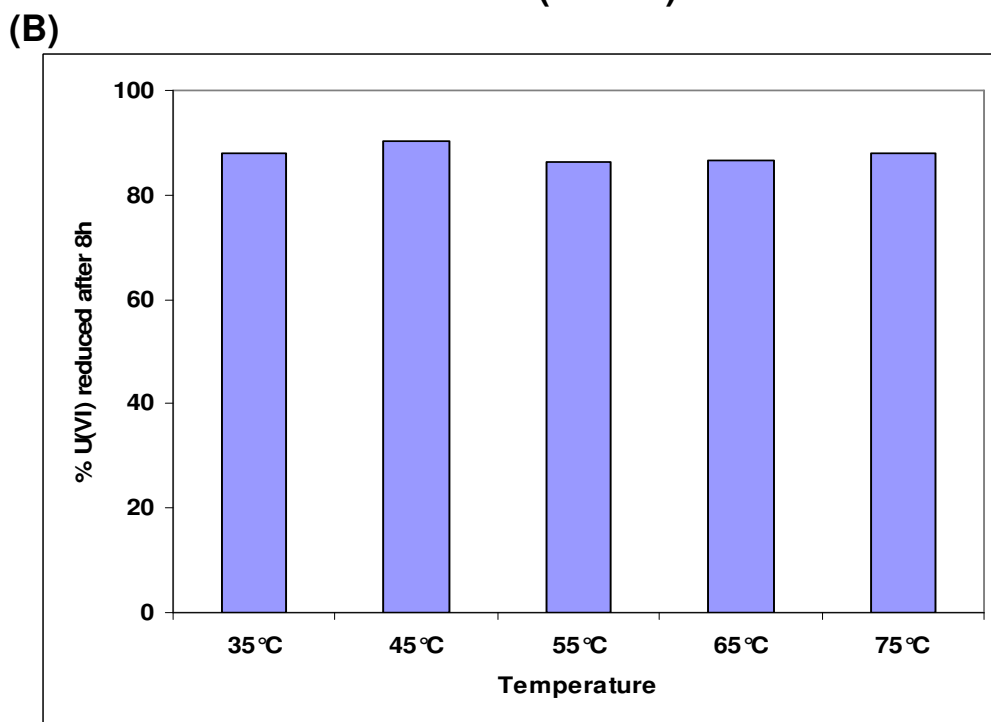
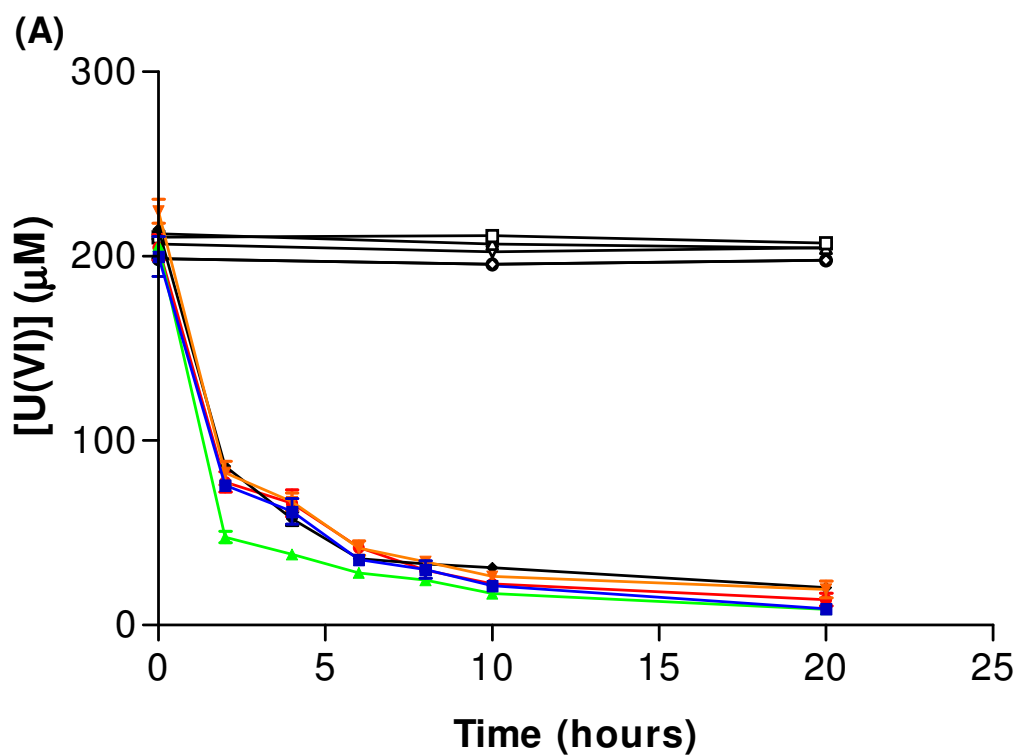


Figure 3.15: (A) Whole cell reduction of uranium(VI) by the thermophile *T. scotoductus* SA-01 under anaerobic conditions at temperature 35 °C (■), 45 °C (▲), 55 °C (▼), 65 (◆) and 75 (●) with the appropriate cell free controls at 35 °C (□), 45 °C (△), 55 °C (▽) 65 °C (○) and 75 °C (◇) Standard deviations are shown **(B)** Percentage uranium(VI) reduced after 8 hours.

3.3.6 Interactions of uranium with *T. scotoductus* SA-01

Electron microscopy was initially used to determine the association of *T. scotoductus* SA-01 with uranium, as described in section 3.2.9. Figure 3.16(B) shows an extracellular cluster that appears to be uranium crystals, note that these clusters were not observed in the uranium free control, Figure 3.16(A). In Figure 3.16(B) and 3.16(C) dark clusters can also be seen formed in and around the cell membrane, possibly indicating membrane related association of the reduced precipitated uranium(IV). The extracellular clusters were also described by Marshall and coworkers (2006), however to our knowledge, this is the first report of this activity from a microorganism isolated from the South African subsurface. In literature (Marshall *et al.*, 2006, Wall and Krumholtz, 2006), where these uranium clusters have also been found, uranium reductases in the form of membrane-bound cytochromes and periplasmic hydrogenases, along with other proteins in the cell membrane, have been identified. Comparison of micrographs with literature thus gives a clear indication that in the case of SA-01, the “uranium reductases” are also most likely to be membrane and periplasmic localized proteins.

Elemental analysis was done on the SEM-coupled EDS. The SEM was set so that heavy metals would appear lighter than organic material, thus as can be seen in Figure 3.17 (A), the cluster is definitely a heavy metal and since no other heavy metal other than uranium could be present in the sample, one would have to concur that the cluster is uranium. To verify this, mapping was done on the cluster site and the yellow dots seen in Figure 3.17 (B) indicate uranium in the cluster. Also pin-point analysis was done on an area in the cluster and the EDS spectra showed that at the given point 2.3% uranium was present.

Thus, it would seem that *T. scotoductus* does associate with the uranium particles in an extracellular manner, but as in the case of *T. scotoductus* SA-01,

the mechanism of how these bacteria are able to reduce uranium(VI) is not well understood.

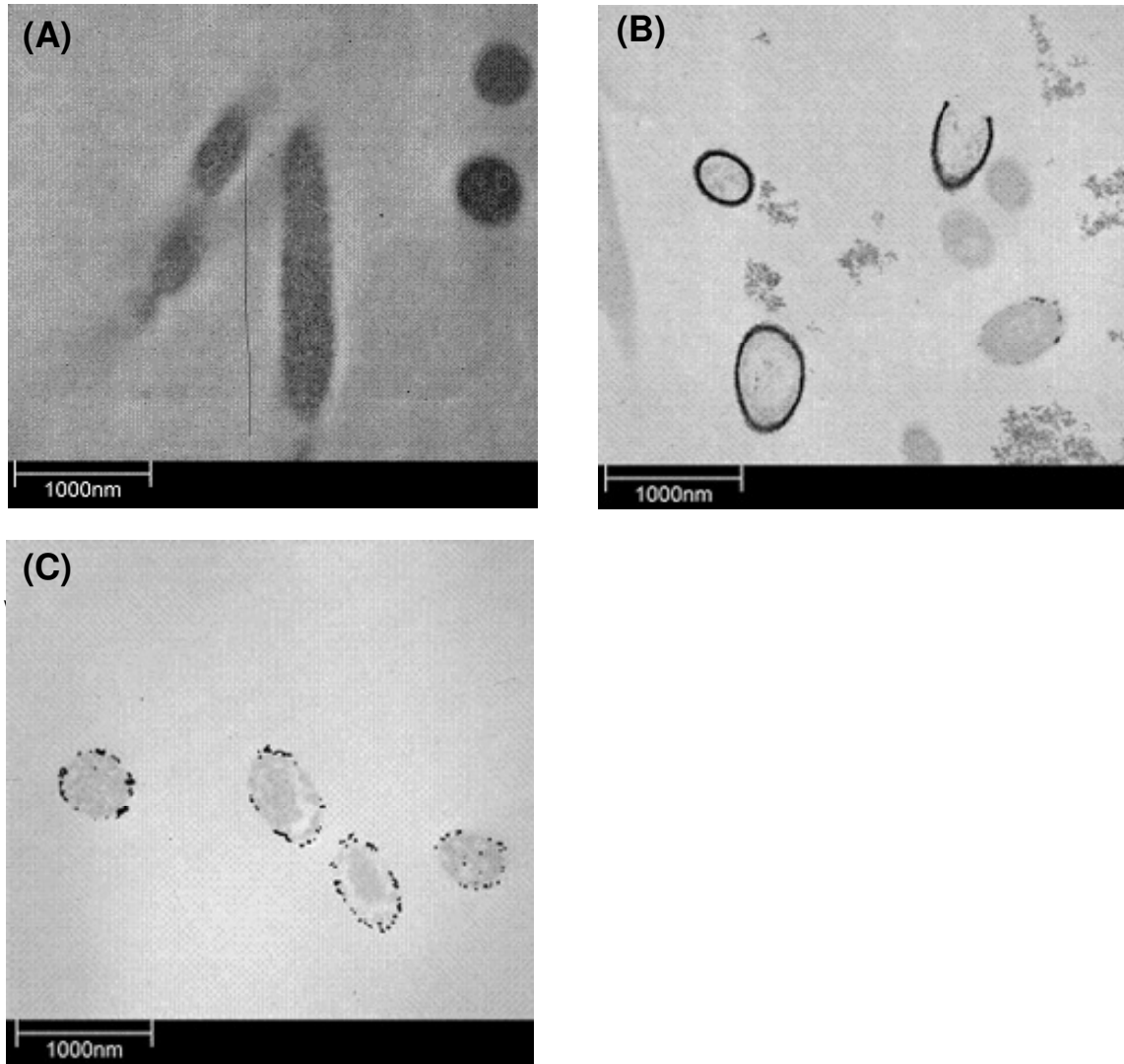


Figure 3.16:TEM electron micrographs of *T. scoto ductus* SA-01 cells in the absence of uranium (A) and in the presence of 1.25 mM of uranium (B, C).

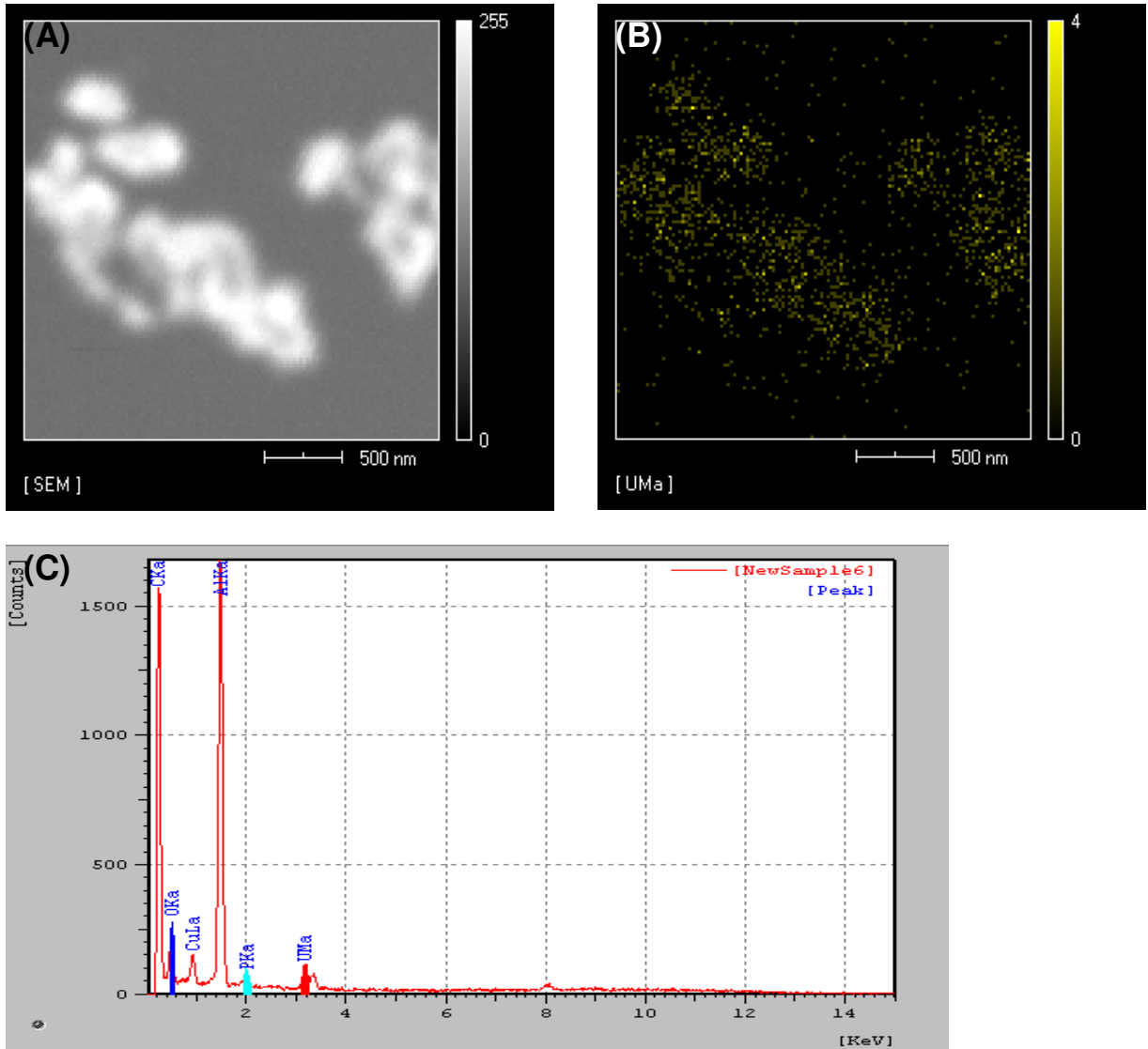


Figure 3.17: Elemental analysis with SEM-coupled EDS. (A) Heavy metal cluster. (B) Results from mapping showing uranium scattering. (C) Pin-point analysis performed by EDS.

3.4 Conclusions

An increase in interest in the microbial populations of extreme environments has led to the isolation and characterization of a great number of thermophilic bacteria, one of these being *Thermus scotoductus* SA-01. This extremophile is a thermophilic bacterium isolated from a deep gold mine in South Africa, and to our knowledge this is the first report pertaining to the effect of uranium(VI) on the growth of this organism. Uranium is quite abundant in the subsurface where gold is found in South Africa, thus making this organism a prime candidate for this type of study. *T. scotoductus* SA-01 has been described as a facultative anaerobe being able to grow anaerobically, coupling the oxidation of organic substrates to reduction of a wide range of electron acceptors (Kieft *et al.*, 1999). Aerobically, *T. scotoductus* SA-01 reached a late exponential growth phase after about 8 hours of growth in an organic rich medium such as TYG. When exposed to uranium during growth *T. scotoductus* SA-01 was able to grow in medium containing uranium up to concentrations of 1.25 mM, and even 1.5 mM after sufficient pre-culturing, indicating a high tolerance toward uranium. Optimum growth could only be maintained up to a uranium concentration of 0.5 mM, since a steady decrease in overall biomass was observed at higher concentrations.

Mobilization of uranium is mostly governed by its oxidation state, which is mainly either the hexavalent (uranium(VI)) or the tetravalent (uranium(IV)) states. In the hexavalent state, the uranium is very soluble, but in the tetravalent state, the solubility decreases leaving the uranium essentially immobile. Kieft and coworkers (1999) showed that *T. scotoductus* SA-01 can reduce low levels of uranium(VI) in under 20 hours with lactate as an electron donor. In this study, we extended on this very preliminary work to find that the favored electron donors are lactate and acetate, that the reaction has an optimum pH of between 7 and 8 and that whole cell reduction activity is still present over a wide range of temperatures with activity still being present as low as 35 °C and as high as 75 °C. The uranium was precipitated within the periplasm and outside the cell, as can

be seen in the TEM micrographs. However, the mechanism of reduction is not clear and also no uranium transport systems have been reported (Wall and Krumholtz, 2006). The localization of the uranium clusters implicates extracellular or membrane-bound proteins in the reduction activity but conclusive evidence as to which protein(s) are responsible for uranium reduction is still lacking but data from this aspect of the work hint that this too could be a ubiquitous protein moonlighting as a uranium reductase.

3.5 References

Balkwill, D. L., Kieft, T. L., Tsukuda, T., Kostandarithes, H. M., Onstott, T. C., Macnaughton, S., Bownas, J. and J. K. Fredrickson. (2004) Identification of iron-reducing *Thermus* strains as *Thermus scotoductus*. *Extremophiles*. **8**:37-44.

Brock T.D. 1984 The genus *Thermus*. In: Krieg NR, Holt JG (eds) Bergeys manual of systematic bacteriology. Williams & Wilkins, Baltimore. pp 333–337.

Fairbanks, G., Steck, T.L., Wallach, D.F., (1971) Electrophoretic analysis of the major polypeptides of human erythrocyte membrane. *Biochemistry* **10**:2606-2617.

Gounder, K. (2009) PhD thesis: Genome sequencing of the extremophile *Thermus scotoductus* SA-01 and expression of selected genes. University of the Free State, South Africa.

Haas, J.R. and Northup, A. (2004) Effects of aqueous complexation on reductive precipitation of uranium by *Shewanella putrefaciens*. *Geochemical Transactions*.**5**:41–48.

Johnson, D.A. and Florence, T.M. (1971) Spectrophotometric determination of uranium(VI) with 2-(5-bromo-2-pyridylazo)-5-diethylaminophenol. *Analitica Chimica Acta*.**53**:73-79.

Khijniak, T.V., Slobodkin, A.I., Coker, V., Renshaw, J.C., Livens, F.R., Bonch-Osmolovskaya, E.A., Birkeland, N.K., Medvedeva-Lyalikova, N.N. and Lloyd, J.R. (2005) Reduction of Uranium(VI) Phosphate during Growth of the Thermophilic Bacterium *Thermoterrabacterium ferrireducens*. *Applied and Environmental Microbiology*. **71**:6423-6426.

Kieft, T.L., Fredrickson, J.K., Onstott, T.C., Gorby, Y.A., Kostandarithes, H.M., Bailey, T.J., Kennedy, D.W., Li, S.W., Plymale, A.E., Spadoni, C.M. and Gray, M.S. (1999) Dissimilatory reduction of Fe(III) and other electron acceptors by a *Thermus* isolate. *Applied Environmental Microbiology*. **65**:1214-1221.

Labuschagne, M and Albertyn, J. (2007) Cloning of an epoxide hydrolase encoding gene from *Rhodotorula mucilaginosa* and functional expression in *Yarrowia lipolytica*. *Yeast*. **24**(2):69-78.

Lane, D. J. (1991) 16S / 23S Sequencing. In E. Stackebrandt & M. Goodfellow (ed.), *Nucleic Acid Techniques in Bacterial Systematics*. pp 115-175. John Wiley and Sons, New York.

Lovley, D.R., Phillips, E.J.P., Gorby, Y.A. and Landa, E.R. (1991) Microbial reduction of uranium. *Nature*. **350**:413-416.

Lovley, D.R. and Phillips, E.J.P. (1992) Bioremediation of uranium contamination with enzymatic uranium reduction. *Environmental Science*. **26**:2228-2234.

Madrid, R.E and Felice C.J. (2005) Microbial Biomass estimations. *Critical Reviews in Biotechnology*.**25**:97–112.

Marshall, M.J., Beliaev, A.S., Dohnalkova, A.C., Kennedy, D.W., Shi, L., Wang, Z., Boyanov, M.I., Lai, B., Kemner, K.M., McLean, J.S., Reed, S.B., Culley, D.E., Bailey, V.L., Simonson, C.J., Saffarini, D.A., Romine, M.F., Zachara, J.M. and Fredrickson, J.K. (2006) c-Type cytochrome-dependent formation of uranium(IV) nanoparticles by *Shewanella oneidensis*. *PLoS Biology*. **4**:e268.

Meyrath, J. and Suchanek G. (1972) Inoculation techniques. *Methods in Microbiology*. **7**:159–205. N.Y. Academic Press. (J.R. Norris, D.W. Ribbons, eds).

Opperman, D.J. and Van Heerden, E. (2007) Aerobic Cr(VI) reduction by *Thermus scotoductus* strain SA-01. *Journal of Applied Microbiology*. **103**:1907-1913.

Payne, R.B., Gentry, D.M., Rapp-Giles, B.J., Casalot, L. and Wall, J.D. (2002) Uranium Reduction by *Desulfovibrio desulfuricans* Strain G20 and a Cytochrome *c*₃ Mutant. *Applied and Environmental Microbiology*. **68**:3129-3132.

Ramirez-Arcos S., Fernandez-Herrero L.A., Berenguer J.(1998) A thermophilic nitrate reductase is responsible for the strain specific anaerobic growth of *Thermus thermophilus* HB8. *Biochimica et Biophysica Acta*. **1396**:215–227.

Shelobolina, E.S., Coppi, M.V., Korenevsky, A.A., DiDonato, L.N., Sullivan, S.A., Konishi, H., Xu, H., Leang, C., Butler, J.E., Kim, B., and Lovley, D.R. (2007) Importance of *c*-Type cytochromes for uranium(VI) reduction by *Geobacter sulfurreducens*. *BMC Microbiology*. **7**:16-25.

Tuovinen, O. H. and Kelly, D. P. (1974) Studies on the growth of *Thiobacillus ferrooxidans*. II. Toxicity of uranium to growing cultures and tolerance conferred by mutation, other metal cations and EDTA. *Archives of Microbiology*. **95**:153–164.

Wall, J.D. and Krumholz, L.R. (2006) Uranium reduction. *Annual Review of Microbiology*. **60**:149-66.

Chapter 4

Purification, identification, expression and characterization of the uranium(VI)-reductase

4.1 Introduction

Previous studies has shown that microorganisms can catalyze the reduction of uranium(VI) to uranium(IV) and has proven to be the dominant driving force in biogeochemical cycling of uranium (Ehrlich, 1990; Lovley *et al.*, 1991). Both sulphate- and iron-reducing bacteria have displayed the ability to reduce uranium(VI) (Lovley *et al.*, 1991; Lovley and Phillips, 1992) and in some of these organisms speculations pertaining to the mechanism of uranium(VI) reduction have been made. A purified hydrogenase and periplasmic cytochrome *c3* from *Desulfovibrio vulgaris* will reduce uranium(VI) to uranium(IV) with hydrogen as the electron donor (Lovley and Phillips, 1992), suggesting that cytochrome *c3* of *D. vulgaris* may be directly involved in uranium(VI) reduction. Cytochrome *c3* has also been found to be bound to precipitated uranium(IV) providing additional evidence that cytochrome *c3* may be involved in uranium(VI) reduction (Payne *et al.*, 2004). Electron microscopic images have shown that reduced uranium(IV) was not only present in the periplasm but also in the cytoplasm, indicating that the periplasmic cytochrome *c3* may be only partially responsible for the *in vivo* uranium(VI) reduction process, with an additional pathway in the cytoplasm (Sani *et al.*, 2006).

From the genome data obtained (Gounder, 2009), it was established that *Thermus scotoductus* SA-01 does not have a cytochrome *c3* type protein, but still it was able to reduce uranium(VI). In this chapter, a protein capable of uranium(VI) reduction from *T. scotoductus* SA-01 was identified as a ABC transporter, peptide-binding protein. ATP binding cassette (ABC) transporters are ubiquitous membrane proteins that facilitate unidirectional substrate translocation across the lipid bilayer by utilizing the energy obtained from the hydrolysis of ATP and have been found to be very diverse with respect to their physiological

function and substrate (Braibant *et al.*, 2000; Locher and Borths, 2004; Saurin *et al.*, 1999).

The aims of this chapter were:

- The purification and identification of the protein(s) involved in uranium(VI) reduction.
- The heterologous expression of the ABC transporter peptide-binding protein in the mesophile *Escherichia coli*.
- Characterization of the recombinant proteins under various parameters.

4.2 Materials and methods

4.2.1 Protein expression by *T. scotoductus* SA-01 in response to uranium exposure

Growth was initiated in 100 ml of TYG medium, supplemented with 1.25 mM of uranium(VI), from standardized stock inocula. Cells were grown to late exponential phase for maximum cell mass, cells were harvested by centrifuging (13 000 rpm, 5 min) cells and washing the pellet three times with 20 mM MOPS buffer, pH 7.4.

4.2.1.1 Protein extraction

Protein extraction was performed on the cells obtained in section 4.2.1 using the ReadyPrep™ Protein Extraction Kit (Total Protein) (Bio-Rad) according to the manufacturer's specifications.

4.2.1.2 Protein concentration determination

Protein concentrations were determined by the bicinchoninic acid (BCA) method using the BCA protein assay kit (Thermo Scientific) which is a highly sensitive spectrophotometric method for the determination of protein concentration. The procedure was conducted according to the manufacturer's instructions. Bovine serum albumin (BSA) (supplied with the kit) was used for preparations of standards. A set of protein standards was prepared with bovine serum albumin (BSA). Fifty microliters of each standard / unknown sample was pipetted into an eppendorf (50µl of diluent was used for a blank); 1ml of working reagent was added to each tube and vortexed. Tubes were incubated at 37°C for 30 minutes and the absorbance read at 562nm using a GENESYS 5 (Spectronic) spectrophotometer. Protein concentrations between 125 and 1000µg.ml⁻¹ could

be detected using incubation at 37°C. A reference curve (Figure 4.1) relating BSA concentration to Absorbance (562 nm) was constructed.

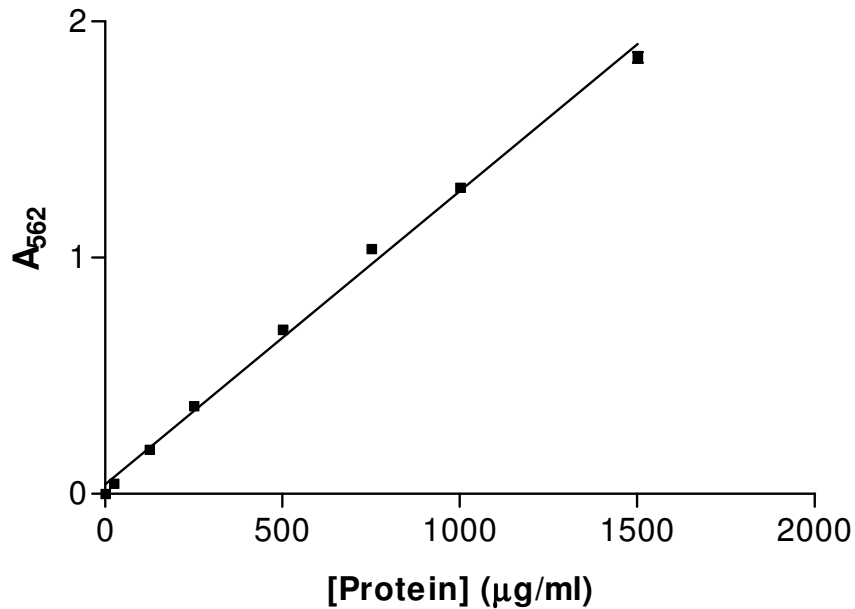


Figure 4.1: BCA protein assay kit standard curve ($R^2 = 0.9960$).

4.2.1.3 Two dimensional (2D) gel electrophoresis at pH gradients 3 to 10, 5 to 8 and 4 to 7

For the gradient of pH 3 to 10 the extracted samples from 4.2.1.2 were cleaned using the ReadyPrep™ 2-D Cleanup Kit (Bio-Rad) according to manufacturer's specifications. The solution was loaded by rehydration onto a 17-cm pH gradient IPG strip (Bio-Rad) overnight at room temperature. Isoelectric focusing was carried out with PROTEAN IEF (Bio-Rad) for 20 min at 250 V (linear), 2.5 h at 10 000 V (linear) and 4 h and 10 min at 10 000 V (rapid) (total about 50 000 Vh). After focusing, the strip was reduced for 20 min at room temperature in equilibration buffer 1 [50 mM Tris-HCl (pH 7.4), 6 M urea, 30% glycerol, 2% sodium dodecyl sulfate (SDS), and 10 mg/mL dithiothreitol] and finally alkylated for 20 min at room temperature in equilibration buffer 2 [50 mM Tris-HCl (pH 7.4), 6 M urea, 30% glycerol, 2% SDS, and 25 mg/mL iodoacetamide]. Gel strips were

then transferred onto a 10% Tris-glycine SDS-polyacrylamide gel, and the second-dimension separation carried out on the PROTEAN® II xi Cell system (Bio-Rad) at 16 mA/gel for 30 min and then at 24 mA/gel for 5 h. The gel was fixed (10% MetOH, 7% Acetic Acid) and stained with Coomassie® Brilliant Blue R-250 using the Fairbanks method (Fairbanks *et al.*, 1971).

For the gradient of pH 5 to 8 and pH 4 to 7 the separation by 2D gel electrophoresis was performed as described above with the exceptions that the protein solution was loaded by rehydration onto a 17-cm; immobilized pH gradient (IPG) strip and the final gel product was stained using the Flamigo® Fluorescent Gel Stain (Bio-Rad) according to manufacturers specifications.

4.2.2 Preparation of subcellular fractions

Subcellular fractions were prepared as described by Kaufmann and Lovley (2001). *T. scotoductus* SA-01 cells were harvested from growth standardized inocula at 8h and washed three times with 20 mM MOPS buffer, pH 7.0. Cells were then resuspended in 20 mM MOPS buffer, pH 7.0, containing 25% (w/v) sucrose. To accomplish cell wall lysis, lysozyme (20 mg) was added to cell suspension (approximately 1 g wet weight) and stirred for 20 min at 37°C. Na₂-EDTA was added to final concentrations of 5 mM and stirred for another 15 min at 37°C. Finally MgCl₂ was added to a final concentration of 13 mM and the suspension again stirred for 15 min at 37°C. Separation of the spheroplast and the periplasmic fractions was obtained by centrifugation (20 000 x g, 30 min) and the spheroplasts resuspended in 20 mM MOPS buffer, pH 7.0.

To obtain the membrane and cytoplasmic fraction, the protocol as described by Gaspard *et al.* (1998) was used. DNase and RNase was added to final concentrations of 5 µg/ml and 10 µg/ml respectively as well as protease inhibitors (Protease Inhibitor Cocktail Set V, Calbiochem) and the cells were broken by ultrasonic treatment (3 times, 75 W, 5 min) with a sonifier (Branson Sonic Power

Cell Disruptor B-30) in an ice-water bath. The suspension was then centrifuged (4000 x *g*, 10 min) at 4°C to remove cellular debris. To separate the membrane fraction from the cytoplasmic fraction the supernatant was centrifuged (100 000 x *g*, 90 min).

The extracted membrane fraction (supernatant from centrifugation step), periplasmic and cytoplasmic fractions were all dialysed against 20 mM MOPS buffer, pH 7.0, with Snakeskin® Pleated Dialysis Tubing (10 000 MWCO) at 4°C with 3 x 2L buffer changes.

4.2.3 SDS-PAGE

Sodium dodecyl sulphate polyacrylamide gel electrophoresis (SDS-PAGE) were performed to assess the presence of proteins as well as differences in the proteins of the membrane, periplasmic and cytoplasmic fractions. The relative molecular masses (*M_r*) of the proteins can also be estimated by comparing the electrophoretic mobility with the masses of known proteins, by using a 10% resolving gel and a 4% stacking gel (Laemmli, 1970). SDS-PAGE was performed using the “Mighty small” miniature slab gel electrophoresis unit, SE 200 from Hoefer Scientific Instruments according to the manufacturer's specifications.

The set of pre-stained protein standards (Bio-Rad) included recombinant protein standards with the following molecular masses: 250 000 Da, 150 000 Da, 100 000 Da, 75 000 Da, 50 000 Da, 37 000 Da, 25 000 Da, 15 000 Da and 10 000 Da.

The gel was stained with Coomassie® Brilliant Blue R-250 using the Fairbanks method (Fairbanks *et al.*, 1971).

4.2.4 Determination of uranium(VI) reduction activity in subcellar fractions

The periplasmic, cytoplasmic and membrane fractions obtained in 4.2.2 were subjected to uranium(VI) reduction experimentation as described in 3.2.7 under varying conditions described below. All uranium(VI) reduction experiments were performed in an anaerobic chamber to prevent reduced uranium(IV) from being oxidized to uranium(VI).

Uranium(VI) reduction was monitored in the presence and absence of hydrogen or reduced quinones as electron donors, and combination of both was also applied. To introduce hydrogen, fractions were flushed with 100% hydrogen prior to experimentation. Reduced quinones were introduced as 2 mM freshly prepared hydroquinones. To initiate the assay, uranyl acetate was added to a sample of the periplasmic, cytoplasmic and membrane fractions to a final concentration of 0.25 mM uranium(VI). To determine whether chemical reduction of uranium(VI) was being observed, the appropriate controls were prepared.

4.2.5 Optimization of protocol for isolation of uranium reductase(s) by chromatographic methods

4.2.5.1 Extraction of ionically-bound membrane proteins

The membrane pellet was resuspended in 20 mM MOPS buffer pH 7.0 by stirring overnight at 5°C. The volume of the membrane fraction was doubled with 1 M KCl in 20 mM MOPS buffer pH 7.0. The solution was then stirred for 2 h at room temperature to extract the peripheral membrane proteins and the resulting suspension ultra-centrifuged at 100 000 $\times g$ for 90 min at 4°C to pellet the membrane. The KCl extractable membrane fraction (supernatant from centrifugation step) was dialyzed against a 20 mM MOPS buffer pH 7.0 at 5°C with 3 \times 2L buffer changes (Ohlendieck, 2008).

4.2.5.2 Screening of optimum chromatographic media

Different strong and weak ion exchange resins were tested for the ability to separate the uranium(VI)-reducing proteins from the non-reducing proteins. CM-Toyopearl 650M (TosoHaas) and SP-Toyopearl 650M (TosoHaas) were chosen for cation exchange, while DEAE-Toyopearl 650M (TosoHaas) and Super Q-Toyopearl 650S (TosoHaas) were chosen for anion exchange. The dialyzed KCl extracted membrane fraction as well as the periplasmic fraction were applied to Super-Q, SP, DEAE and CM Toyopearl columns (5 cm x 1 cm) previously equilibrated with 20 mM MOPS buffer, pH 7.0. The columns were washed with 20 mM MOPS buffer, pH 7.0, until the $A_{280\text{ nm}}$ readings were less than 0.01, 20 mM MOPS buffer, pH 7.0, containing 0.5 M NaCl was used to elute bound proteins followed by MOPS buffer, pH 7.0, containing 1.0 M NaCl. The non-binding fractions, as well as the first and second bound fractions were subjected to protein determination using the BCA Protein Assay Kit (Thermo Scientific). Uranium(VI) reduction activity was also determined as described in 3.2.7.

4.2.5.3 Isolation of the membrane/periplasmic uranium reductase(s)

The dialyzed KCl extracted membrane fraction (4.2.5.1) as well as the periplasmic fraction were applied to Super-Q Toyopearl (8 cm x 2.8 cm) column previously equilibrated with 20 mM MOPS buffer, pH 7.0. A salt gradient of 0 – 1.0 M NaCl at a flow rate of 5 ml/min was used to elute bound proteins.

Uranium(VI) reduction activity (as described in 3.2.7) was determined in eluted fractions. Active fractions were pooled and dialysed against 20 mM MOPS buffer, pH 7.0, with Snakeskin® Pleated Dialysis Tubing (10 000 MWCO) at 4°C.

The dialysate was applied to SP Toyopearl (8 cm x 2.8 cm) column previously equilibrated with 20 mM MOPS buffer, pH 7.0. A salt gradient of 0 – 1.0 M NaCl

at a flow rate of 5 ml/min was used to elute bound proteins. Fractions were collected (10 ml) and analysed for uranium(VI) reduction activity (as described in 3.2.7).

SDS-PAGE electrophoresis was performed on selected fractions as described in 4.2.3.

4.2.6 Sequence determination of unknown protein

From the SDS-PAGE (obtained in section 4.2.5.3) a +/- 70 kDa protein band was possibly identified as the uranium(VI)-reductase. To determine the sequence of this unknown protein, both N-terminal sequencing as well as MS/MS sequencing was utilized.

4.2.6.1 N-terminal sequencing

The eluted fraction (obtained from 4.2.5.3) determined to contain the possible uranium reductase was loaded onto a 10% SDS-PAGE gel and run at 100V. The gel was blotted onto a PVDF membrane according to the manufacturer's specification. The blotted membrane was stained with Coomassie[®] Brilliant Blue and the protein band for a +/- 70 kDa protein was cut out and sent to the Protein Chemistry Facility of the Centro de Investigaciones Biológicas (CSIC; Madrid, Spain). N-terminal sequencing was performed by automated Edman degradation with an Applied Biosystems 477A gas-phase sequencer (Foster City, Calif).

4.2.6.2 MS/MS sequencing

The eluted fraction (obtained from 4.2.5.3), determined to contain the possible uranium reductase, was subjected to SDS PAGE analysis, and a +/- 70 kDa protein was cut out and lyophilized. The lyophilized sample was sent to the Centre for Proteomic and Genomic Research in Cape Town for MS/MS analysis

on a ESI/MALDI QToF, ToF/ToF (Agilent, Applied Biosystems). The protein was digested with trypsin before being analysed by mass spectrometry. A total of nine tryptic digested fragment spectra were obtained and analyzed using the Mascot Distiller software.

4.2.7 Protein expression and purification

4.2.7.1 Constructing plasmids containing the uranium(VI)-reductase gene

Primers were designed using the N-terminal and MS/MS sequencing results and the gene sequence obtained from the *T. scotoductus* SA-01 genome database. The genome sequence of *Thermus scotoductus* SA-01 was completed using a combination of GS20 and FLX-pyrosequencing (Gounder, 2009). The primers designed to amplify the coding region included restriction sites for the restriction enzymes *Nde*I and *Eco*R1. Using the forward primer for the mature protein (ABC_Fm_Nde), the reverse primer (ABC_R_Eco) and Excel® *Taq* polymerase (CoreBioSystem) the gene for the uranium(VI)-reductase was amplified by PCR. The PCR reaction was assembled as described in Table 4.1.

Thermal cycling was conducted with an initial denaturation step for 10 min at 94°C followed by 35 cycles of denaturation at 94°C for 45 sec, annealing at 55°C for 30 sec and elongation at 72°C for 30 sec. This was followed by 10 min elongation at 72°C. After amplification the PCR product was loaded onto a 0.8% agarose gel for fractionation by electrophoresis. The bands in question were excised from the gel using the Biospin Gel Extraction kit (Bioflux) according to the manufacturer's specifications.

Table 4.1. Master mix for the hot start PCR reactions using Excel® *Taq* polymerase (CoreBioSystem).

Component	Amount for 1 reaction (µl)
Primer ABC_Fm_Nde (10 µM)	1
Primer ABC_R_Eco (10 µM)	1
dNTPs (10 mM)	1
Buffer 10 X *	5
<i>Taq</i> polymerase (250 U/ µL)	0.2
Template (50 ng/µL)	2
Sterile water	39.80
Total	50

Primer ABC_Fm_Nde 5' – GGG CCC CAG GAC AAC AGC CTG G - 3'

Primer ABC_R_Eco 5' – GAA TTC TTA CTT GAC GGA AAG AGC GTA C - 3'

* The buffer contained adequate [Mg Cl₂]

A molar ratio of 3:1 of insert DNA to plasmid was utilized for the ligation. The reaction was incubated at 22 °C for 1 h followed by 4 °C for 8 h. The ligation reaction was assembled as shown in Table 4.2, T4 DNA ligase and ligation buffer from New England Biolabs was used.

Table 4.2. Ligation mixture composition for the pGEM®-T Easy vector system.

Component	Sample Volume (µl)	Control Volume (µl)
2X Rapid ligation buffer	5	5
pGEM®-T Easy vector (50 ng)	0.8	1
PCR product (75 ng)	0.8	-
pUC DNA	-	1
T4 DNA ligase (3 Weiss units/µl)	1	1
Sterilised MilliQ H ₂ O	1.2	1
Total	10	10

E. coli Top10 competent cells (50 µl), were thawed on ice and 5 µl of the ligation mixture added. This was incubated on ice for 30 min followed by a heat shock

step at 42°C for 40 sec and immediate cooling on ice for 2 min, after which 700 µl of SOC (prepared as described in section 3.2.2.2) medium was added. The culture was then incubated at 37°C for 1 h in a shaker rotating with 175 rpm. The transformation mix (50 µl) was plated out on AIX plates (prepared as described in section 3.2.2.2). The plates were incubated at 37°C for 16 h followed by selection of white colonies. Representative colonies (10 per plate) was inoculated into 5 ml LB medium supplemented with 30µg/mlkanamycin (finalconcentration) to provide the adequate antibiotic pressure and incubated at 37°C for 16 h while shaking at 175 rpm after which the cells were pelleted by centrifugation at 6000 x g and 4°C for 10 min. Plasmid DNA was isolated with the Biospin Plasmid DNA Extraction Kit (Bioflux)according to the manufacturer’s instructions. Plasmid DNA concentrations were determined on the NanoDrop Spectrophotometer ND-1000 (Thermo Scientific). Extracted plasmids were subjected to RFLP analysis as shown in Table 4.3 with data verification using standard gel electrophoresis techniques.

Table 4.3. Restriction digests reaction composition.

Component	Volume (µl)
Plasmid DNA	5
Buffer (10 X)	1
Sterile MilliQ H ₂ O	2
<i>Eco</i> RI (5 000 U/ml)	1
<i>Nde</i> I (5 000 U/ml)	1
Total volume	10

The vector, pET28b(+) (LabLife) Figure 4.2, was transformed into competent *E. coli* TOP 10 cells for propagation, as described in 3.2.2.2.

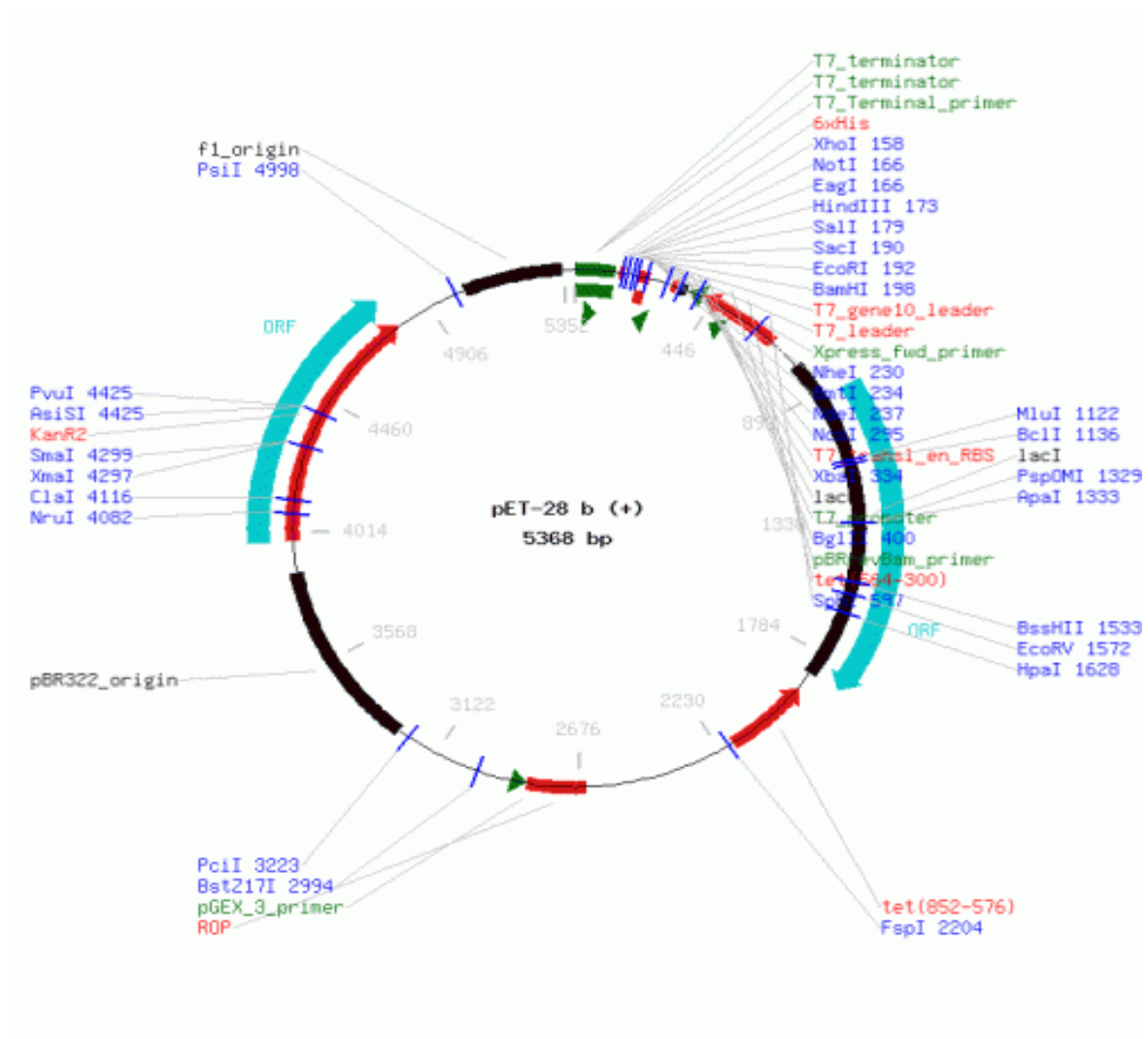


Figure 4.2: Vector map of pET28b(+).

Plasmid DNA was isolated with the Biospin Plasmid DNA Extraction Kit (Bioflux) according to the manufacturer's instructions. The concentration of the extracted plasmid was adjusted to 100 ng/ μ L and linearization performed with using *EcoRI* and *NdeI* endonuclease, to be compatible with the sticky end on the insert, as shown in Table 4.4.

Table 4.4. Restriction digest reaction composition.

Component	Volume (μl)
Plasmid DNA	80
Buffer (10 X)	10
<i>Eco</i> RI (5 000 U/ml)	5
<i>Nde</i> I (5 000 U/ml)	5
Total volume	100

The sample was incubated for 3 h at 37°C and digestion evaluated on a 0.8% agarose gel. The linearized plasmid was purified with the Biospin Gel Extraction Kit (Bioflux) according to the manufacturer's instructions.

The insert was ligated into the pET28b(+) (50 ng. μl^{-1}) vector as described above. The ligation reaction was assembled as shown in Table 4.5, T4 DNA ligase and ligation buffer from New England Biolabs was used.

Table 4.5. Ligation mixture composition for the pET28b(+) vector system.

Component	Sample Volume (μl)	Control Volume (μl)
2X Rapid ligation buffer	5	5
pET28b(+) (50 ng. μl^{-1})	0.8	1
Insert fragment	0.8	-
T4 DNA ligase (3 Weiss units. μl^{-1})	1	1
Sterilised MilliQ H ₂ O	1.2	1
Total	10	10

The ligated vector was transformed into *E. coli* Top 10 competent cells as described above with the exception that kanamycin (30 $\mu\text{g}.\text{ml}^{-1}$ final) was employed to provide the adequate antibiotic pressure. Plasmid DNA was isolated with the Biospin Plasmid DNA Extraction Kit (Bioflux) according to the manufacturer's instructions. To establish the presence of the insert in the obtained plasmids, 10 μl was double-digested with the restriction enzymes *Eco*RI

and *NdeI* as described above. Plasmid DNA concentrations were determined on the NanoDrop Spectrophotometer ND-1000 (Thermo Scientific). The plasmid selected for further work was sent to Inqaba Biotechnical Industries (PTY) LTD, South Africa for sequencing.

In order to confirm the nucleotide composition of the relevant gene, purified positive template was used in sequencing reactions along with the primers listed Table 4.6 below. The data were analyzed using Sequencing Analysis v. 3.3. Sequences were assembled using AutoAssembler v. 3.3. Reverse complementation and alignments were performed using DNAssist v. 2.0.

Table 4.6.Primer sequences utilized during sequencing.

Primer	Sequence
ABC_Fm_Nde	5' – GGG CCC CAG GAC AAC AGC CTG G - 3'
ABC_R_Eco	5' – GAA TTC TTA CTT GAC GGA AAG AGC GTA C - 3'
ABC_Int_F	5' - AGG ATG CGG AGA GGC TC - 3'
ABC_Int_R	5' - CGC TGG ATG TAG TCG TCG - 3'

4.2.7.2 Expression and purification of uranium(VI)-reductase

The expression vector, pET28b(+), containing the sequence for the possible uranium(VI)-reductase, was transformed into Rosetta-Gami 2(DE3)pLysS competent cells and inoculated into LB medium containing an antibiotic, kanamycin (30 µg/ml final) and incubated at 37°C while shaking at 175 rpm. Cells were grown to an optical density of between 0.8 – 1.0 after which protein expression was induced with the addition of 1mM (final concentration) IPTG. Four hours after induction the cells were harvested and washed three times with 20 mM MOPS buffer, pH 7.4. After the final wash the pellet from pET28b(+) was resuspended in 1X binding buffer (20 mM MOPS, 0.5 M NaCl, 20 mM imidazole, pH 7.4)(Khushiramani, 2006).

Cell disruption was performed using a French pressure cell. Unbroken cells were removed by centrifugation (6000 rpm, 15 min) and membranes removed by ultracentrifugation (100 000 x *g*, 90 min).

HisTrap™ columns, when charged with Ni²⁺ ions, will selectively bind proteins if complex-forming amino acid residues, in particular histidine, are exposed on the surface of the protein, e.g. poly-histidine tagged recombinant proteins. The protein expressed by the pET28b(+) has been engineered to have a poly(His) tail at both the carboxyl and amino terminus and can thus easily be purified using HisTrap™ purification kit.

The HisTrap™ column was prepared according to manufacturer's specifications. The supernatant, obtained above, was loaded onto the Superloop (GE) of the AKTA Prime Plus (Amersham Biosciences) system and subsequently applied to the HisTrap™ column. The poly-histidine tagged protein was then eluted with an imidazole gradient (20 mM to 500 mM) supplied by the combination of the 1X binding buffer (20 mM MOPS, 0.5 M NaCl, 20 mM imidazole, pH 7.4) and the elution buffer (20 mM MOPS, 0.5 M NaCl, 500 mM imidazole, pH 7.4).

The eluted peak was collected, dialysed against 20 mM MOPS buffer, pH 7, with 3X changes of buffer and loaded onto a 10% SDS-PAGE gel for analysis, as described in 4.2.3.

4.2.8 Modelling

A homology model of the ABC transporter peptide-binding protein of *T. scotoductus* SA-01 (Thsc-ABC) was compiled using Yasara Structure & Whatif. The template used was the oligopeptide-binding protein of *T. thermophilus* HB8 (2D5W-B) which has a 90% identity (95% similarity) with the ABC transporter, peptide-binding protein of *T. scotoductus* SA-01.

4.2.9 Uranium(VI) reduction by purified recombinant protein

Protein concentrations were determined by the bicinchoninic acid (BCA) method using the BCA protein assay kit (Thermo Scientific) as described in 4.2.1.2. Uranium(VI) reduction was monitored as previously described in 3.2.7. From section 4.2.8 it was evident that the uranium(VI)-reductase contains a surface exposed disulfide bond that could be involved in uranium(VI) reduction, 2 mM β -mercaptoethanol was utilized to reduce the disulfide bonds of the proteins before activity was determined.

Different pH and temperature conditions were used to characterize the recombinant protein in its ability to reduce uranium(VI). Variations in pH from 5.5 to 9.0 and temperatures from 35 – 75°C were evaluated with reactions where 800 $\mu\text{g}\cdot\text{ml}^{-1}$ protein for the pET28b(+) recombinant protein and 0.25 mM uranium(VI) was incubated for 20 hours. Usually pH characterization is conducted using a buffer cocktail containing equimolar concentrations of the components, but the cocktail caused uranium(VI) to precipitate out of solution forming a yellow precipitate. Individual buffers were thus used, 20 mM MES buffer was used for the range below pH 6, 20mM MOPS buffer for the neutral pH range and 20mM Tris-HCl buffer for the alkaline pH range. All pH values were adjusted at 65°C. Temperature characterization was performed in 20mM MOPS buffer, pH 7.0, with the buffers adjusted to pH 7.0 at the appropriate temperatures. The effect of protein concentration on the ability of the purified protein to reduce uranium(VI) was also evaluated. The reactions contained undiluted (800 $\mu\text{g}/\text{m}^1$), 2X and 4X diluted protein concentrations for 20 hours.

4.3 Results and discussion

4.3.1 Protein expression by *T. scotoductus* SA-01 in response to uranium exposure

Microorganisms have developed various defence mechanisms against the effect of heavy metals, such as uranium, which are usually highly toxic compounds. For example, Gupta and coworkers (1997) found thioredoxin-like genes in *E. coli* conferring to heavy metal tolerance. Sakamoto and coworkers (2007) found various proteins being formed in *Saccharomyces cerevisiae* due to a cellular response to the chemical effect of uranium but to date the proteins corresponding to exposure of uranium have not been characterized. Thus in certain microorganisms heavy metals will induce or suppress the expression of certain proteins.

2D SDS-PAGE electrophoresis is a very powerful technique since it resolves proteins on both pI values and size. This technique was applied in an attempt to observe a shift in protein expression pattern levels in *T. scotoductus* SA-01 due to the addition of uranium in the growth medium (as described in section 3.2.5.1). The extracted protein concentrations were determined with the BCA protein assay kit (described in section 4.2.1.2), and the standard curves utilized in protein concentration determination. 400 µg of protein was loaded onto the pH 3 to 10 IPG strip. In the case of the pH 7 to 4 and 5 to 8 IPG strips 80µg of protein was loaded.

In Figures 4.3, 4.4 and 4.5 respectively the effect of growth in uranium-containing medium on a protein level can be observed in the different pH ranges of the IPG strips along with the uranium free controls for each sample.

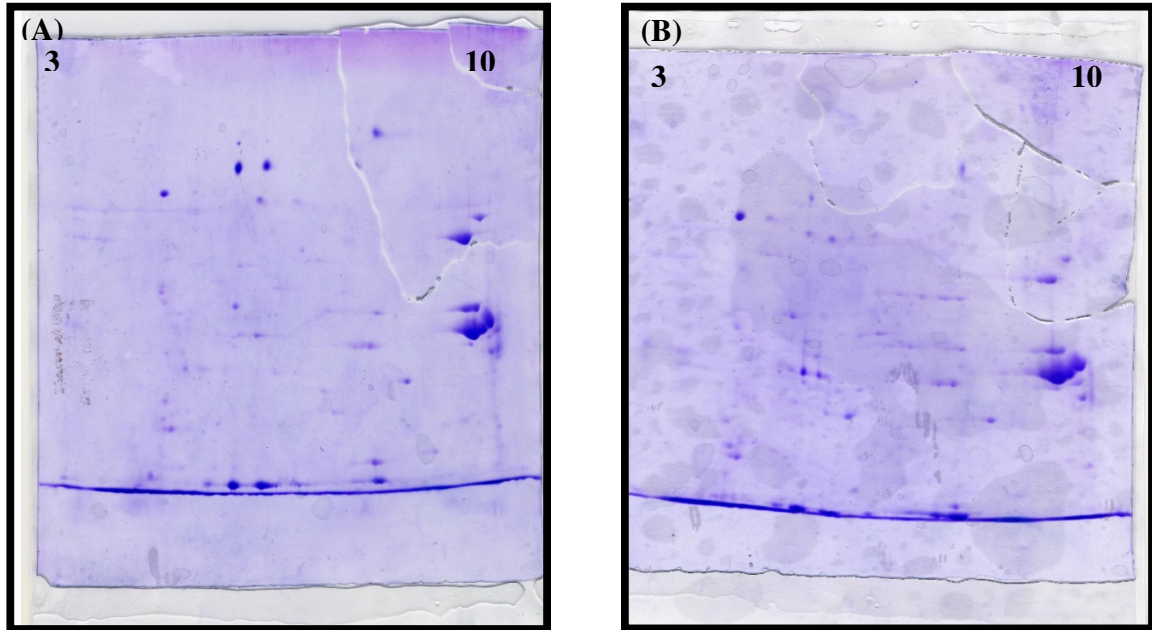


Figure 4.3: 2-D SDS-PAGE gels, stained with Coomassie® Brilliant Blue of IPG strips pH 3 to 10. (A) From cells grown in 1.25 mM uranium. (B) From cells grown in TYG medium with no uranium.

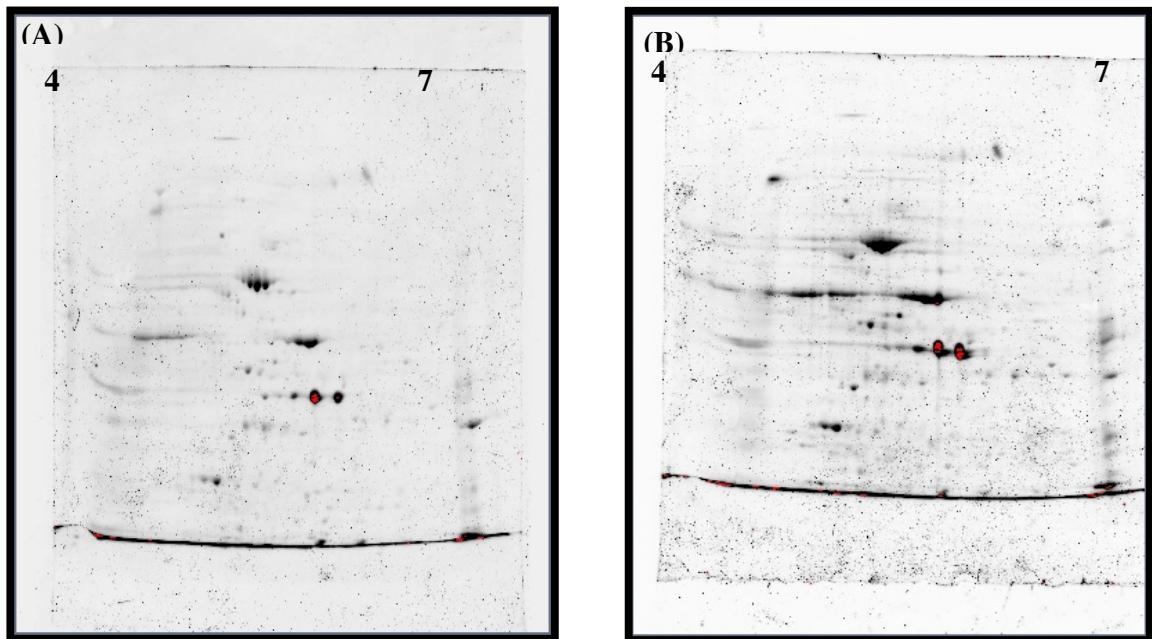


Figure 4.4: 2-D SDS-PAGE gels, stained with Bio-Rad Flamingo® Fluorescent Stain of IPG strips pH 4 to 7. A) From cells grown in 1.25 mM uranium. B) From cells grown in TYG medium with no uranium.

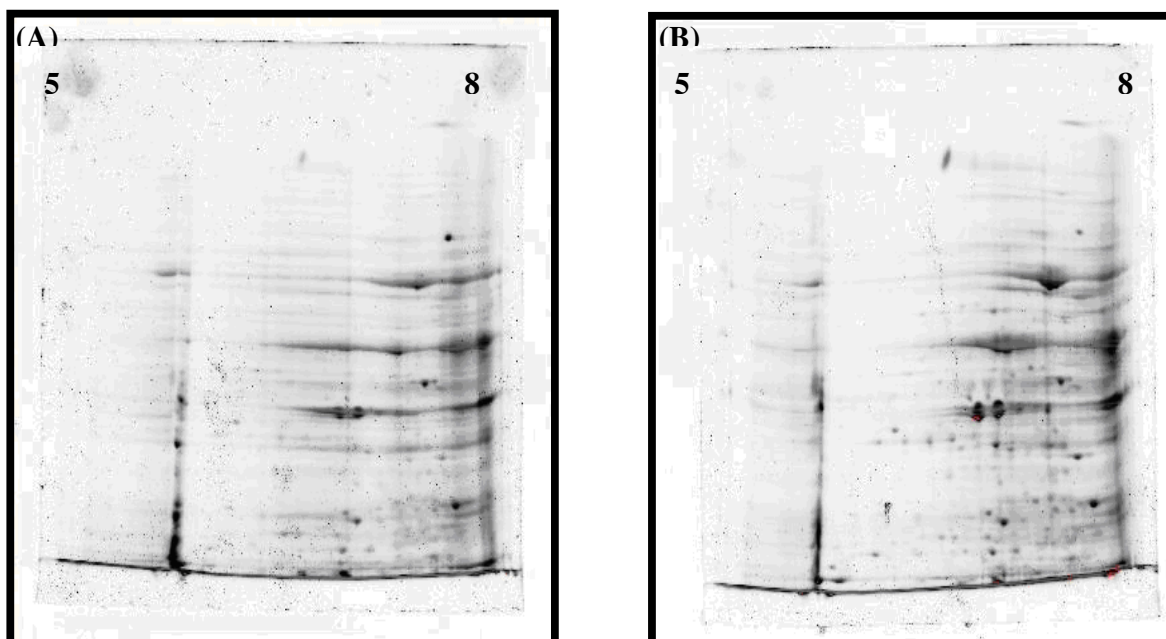


Figure 4.5: 2-D SDS-PAGE gels, stained with Bio-Rad Flamingo® Fluorescent Stain of IPG strips pH 5 to 8. A) From cells grown in 1.25 mM uranium. B) From cells grown in TYG medium with no uranium.

The Flamingo® Fluorescent Stain (Bio-Rad) was employed on the smaller pH range IPG strips since it has higher levels of sensitivity than the Coomassie® Brilliant Blue. Gels were compared using the PDQuest 2D Analysis Software (Bio-Rad) and with the exception of Figure 4.5, where proteins were subjected to isoelectric focusing between pH 5 to 8, visually no significant differences were observed between proteins expressed with or without uranium. In the pH range of 7 to 8, in Figure 4.5, some down regulation of proteins was observed as some of the protein spots were seen to disappear when the cells were exposed to uranium during growth but nothing as concrete as was observed by Sakamoto and coworkers (2007). However, further work is needed to validate this finding.

4.3.2 Determination of uranium(VI) reduction activity in subcellular fractions

Fractionation of the cells was conducted as described in section 4.2.2. After dialysis, all fractions namely, periplasm, cytoplasm and membrane as well as combinations of these fractions were subjected to uranium(VI) reduction assays.

Reduction of uranium(VI) was monitored as described in section 3.2.7. The disappearance of uranium(VI) in the periplasm fraction seemed to be the most prominent, but a yellow precipitate was formed (Figure 4.6) implicating uranium(VI) and not uranium(IV) which would have been a black precipitate (Haas and Northop, 2004), thus it was not reduction occurring in the sample but rather another reaction, such as bioprecipitation, causing the uranium(VI) to become inaccessible to the assay. In the samples where a black uranium(IV) precipitate was observed, reduction slowed down dramatically after about 60% of the uranium(VI) was reduced (Figure 4.7) and the samples appeared to be unable to reduce all of the uranium(VI). This initially fast level of reduction followed by cessation indicates that the protein involved is not a hydrogenase coupled to a cytochrome since an excess of electron donor would cause all of the uranium(VI) to be reduced. Also, an oxidoreductase is highly unlikely since the reducing equivalents would have been sufficient to reduce all of the uranium(VI). There seems to be some factor limiting the reduction of uranium(VI), but this will be discussed in more detail later.

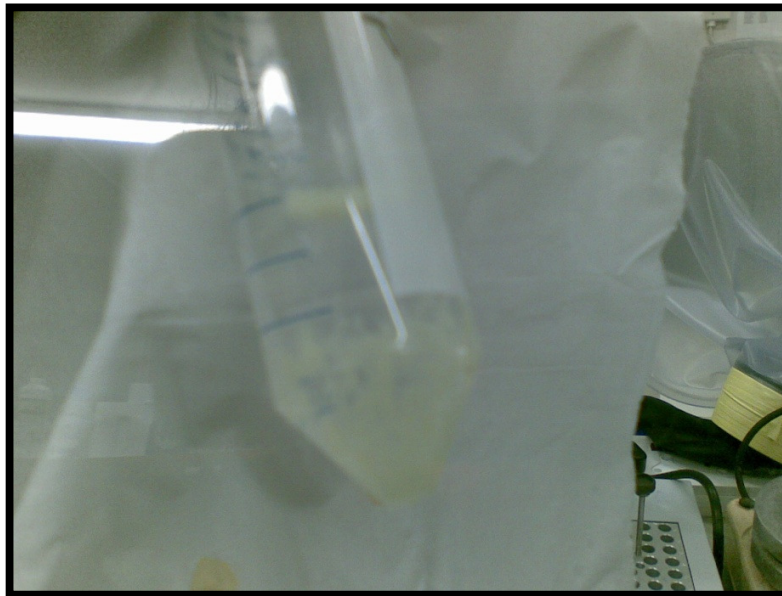


Figure 4.6: Uranium(VI) reduction activity of the periplasmic fractions of SA-01, after dialysis.

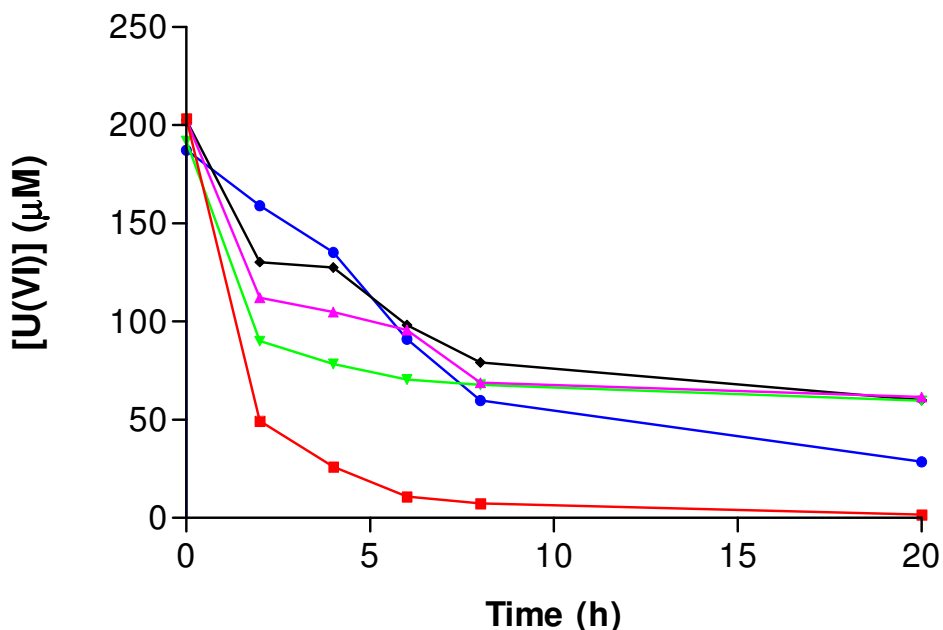


Figure 4.7. Uranium(VI) reduction activity of the different protein fractions from *T. scotoeductus* SA-01, after dialysis. (■) Periplasm; (▼) Cytoplasm; (◆) Membrane; (●) Combination of periplasmic and membrane fractions; (▲) Combination of the periplasmic, cytoplasmic and membrane fractions.

In an attempt to obtain a sample capable of reducing most of the uranium in the sample, combinations of fractions were assayed for uranium(VI) reduction capabilities and hydrogen was introduced as an electron donor. Hydrogen was introduced since Lovley and coworkers (1993) found hydrogen dependant uranium(VI) reduction in the soluble membrane-free fraction of *Desulfovibrio vulgaris*. Once again the periplasm fraction appeared to display the best level of reduction (Figure 4.8), but again only a yellow uranium(VI) precipitate could be observed. The periplasm in combination with the membrane fraction seemed to have the best reduction capabilities, with black uranium(IV) precipitate being present, which coincides with what has been indicated in literature (Marshall *et al.*, 2006) as well as observations made in previously done TEM (section 3.3.6) studies that the uranium seems to be precipitated outside of the cells and thus the proteins involved would also be associated with the membranes of the cells.

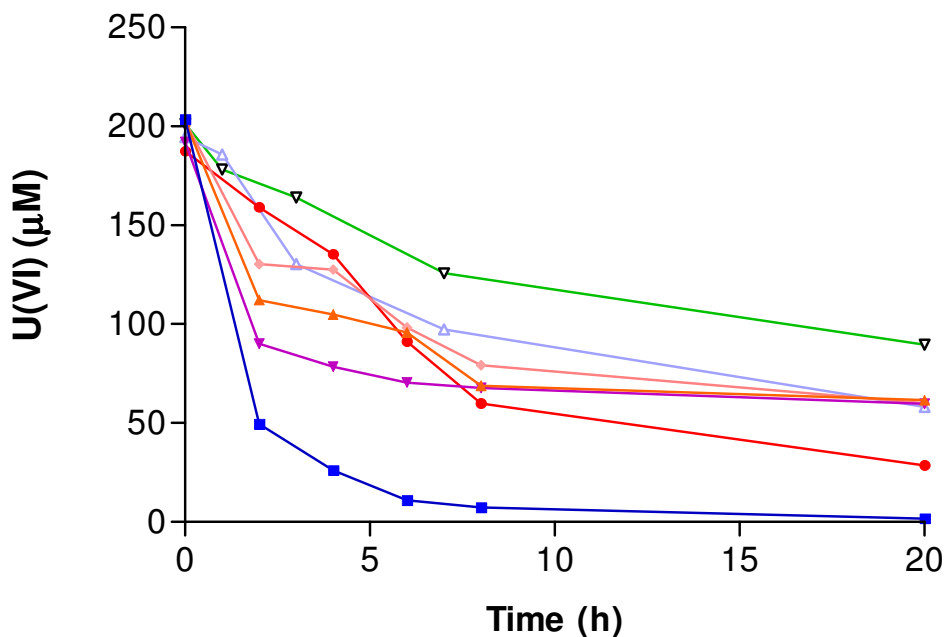


Figure 4.8: Uranium(VI) reduction activity of the different protein fractions from *T. scotoductus* SA-01, after dialysis and being purged with 10% H₂ mix gas. (■) Periplasm; (▼) Cytoplasm; (◆) Membrane; (▲) Combination of the periplasmic, cytoplasmic and membrane fractions; (●) Combination of the periplasmic and membrane fraction; (△) Combination of the periplasmic and cytoplasmic fractions; (▽) Combination of the membrane and cytoplasmic fractions.

Hydroquinone is another electron donor favoured for uranium reduction studies since cytochrome *c3* is able to utilize it as an electron donor for uranium reduction (Chamupathi and Tollin, 1989). The combination of the periplasm and membrane fractions were screened for uranium(VI) reduction activity, since this combination has shown the most promise pertaining to the presence of the uranium reductase and is also where the reductases have been found in literature (Lovley *et al.*, 1993). A combination of hydroquinone and H₂ was thus utilized as electron donors to increase reduction potential. Figure 4.9 indicates that there is no significant difference between a combination of the hydrogen and hydroquinone and only hydroquinone, Hydrogen produced the lowest level of reduction, contrary to what was expected if this was a cytochrome *c3* related protein, since cytochrome *c3* mediated reduction is hydrogen dependant (Lovley *et al.*, 1993; Payne, 2002). The best reduction activity was observed for samples containing hydroquinone. Figure 4.10 also showcases the blackish precipitate

being formed, thus for these sample we were not only observing the disappearance of uranium(VI) but also the appearance of uranium(IV) as indicated by Lovley and Phillips (1992).

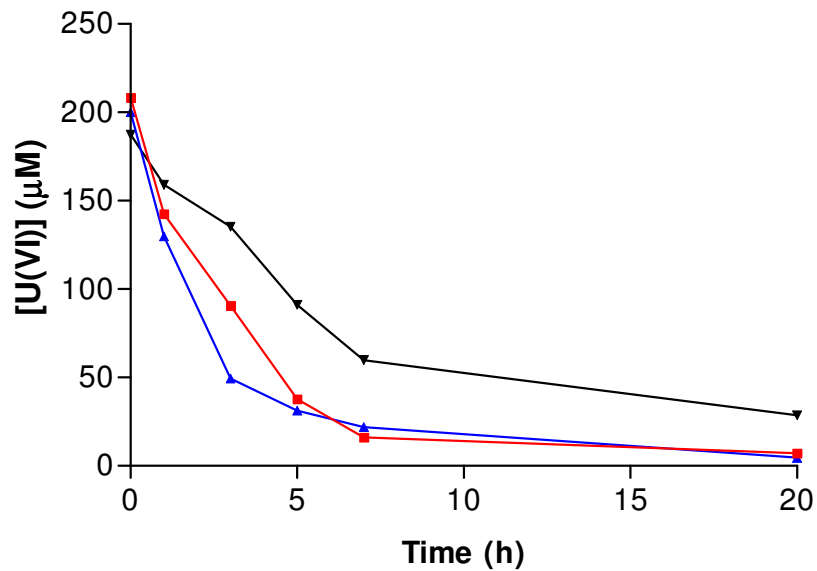


Figure 4.9: Uranium(VI) reduction activity of the combination of the membrane and periplasmic fractions from *T. scotoductus* SA-01, after dialysis and being purged with 10% H₂ gas, hydroquinone and a combination of both as electron donors. (■) H₂ and hydroquinone as electron donor; (▲) Hydroquinone as electron donor; (▼) H₂ as electron donor.

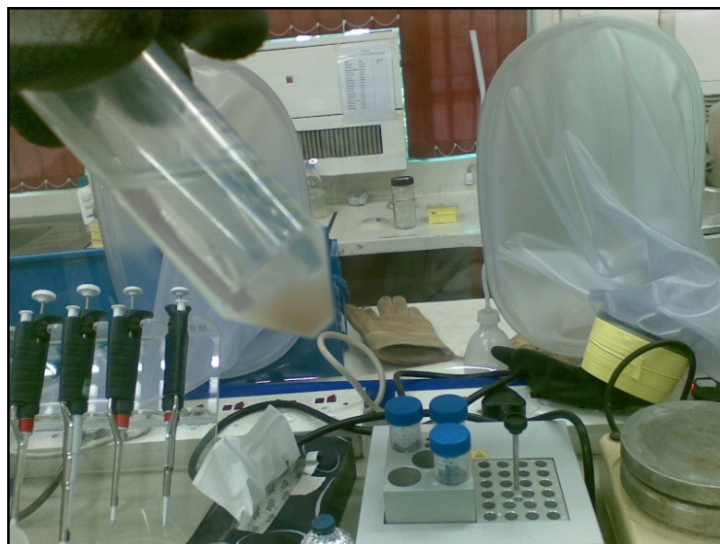


Figure 4.10: Formed precipitate from the reduction of uranium(VI) by the combination of the membrane and periplasmic fractions from *T. scotoductus* SA-01, after dialysis with 10% H₂ gas and hydroquinone as electron donors. Photo taken inside the anaerobic cabinet.

4.3.3 SDS-PAGE

SDS-PAGE electrophoresis was utilized to observe the presence of proteins in the membrane, periplasmic and cytoplasmic fractions. Protein analysis of these fractions (Figure 4.11) indicated a difference in protein composition between the soluble fraction and the membrane fraction and could explain the difference in the ability of these fractions to reduce uranium(VI) and that there might be more than one protein present with the ability to reduce uranium(VI).

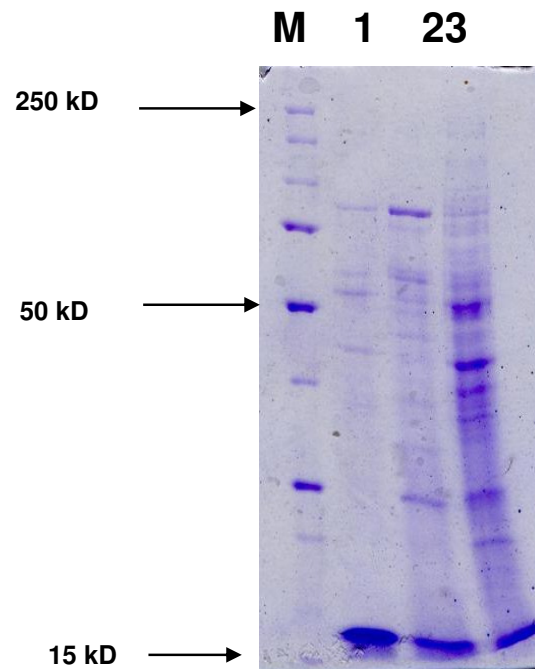


Figure 4.11: SDS-PAGE gel electrophoresis of subcellular fractions. Lane M, Precision Plus Protein™ Standards (Bio-Rad); Lane 1, Periplasmic fraction; Lane 2, Membrane fraction; Lane 3, Cytoplasmic fraction.

4.3.4 Isolation of uranium reductase(s) by chromatographic methods

4.3.4.1 Screening of optimum chromatographic media

From the respective data obtained in section 4.2.5.2 it was concluded that the SP and Super-Q Toyopearl would be the best chromatographic resins to utilize for

further isolation since they delivered the lowest protein concentration with the highest rate of activity in the first binding fraction.

4.3.4.2 Anion exchange (Super Q-Toyopearl)

First step in the isolation of the membrane/periplasmic associated uranium(VI)-reductase(s):

The combination of the periplasmic and membrane fractions was applied to the Super Q-Toyopearl resins described in section 4.2.5.3. After equilibration of the column with 20 mM MOPS buffer, pH 7.0, the sample loaded. The elution profile obtained showed several protein peaks (Figure 4.12), the A_{280} readings can be correlated to protein concentration. The peaks indicated on the elution profile were monitored for uranium(VI) reduction activity. The amount of protein not interacting with the resin (Figure 4.12 A-B) was quite low and did not show any uranium(VI) reduction activity. Of the proteins eluted with the salt gradient (Figure 4.12 C-D and E-F) only the smaller peak (Figure 4.12 C-D) displayed uranium(VI) reduction activity. Fraction C-D was dialyzed against 20 mM MOPS buffer, pH 7.0, concentrated and separated using the cation exchanger SP-Toyopearl.

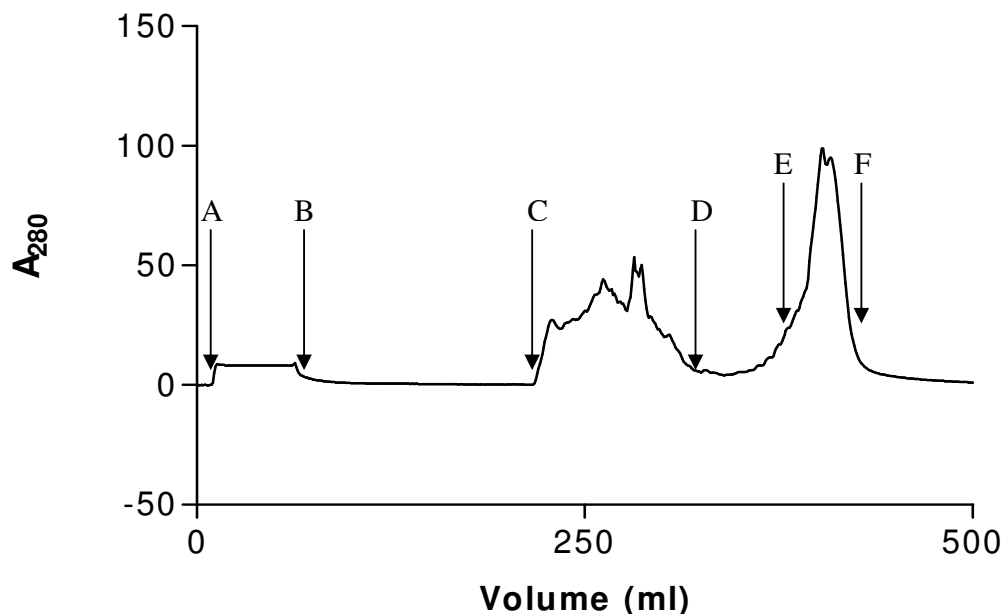


Figure 4.12: Elution profile obtained for the purification step on Super Q-Toyopearl anion exchange resin. The regions between the arrows (A-B), (C-D) and (E-F) were monitored for uranium(VI) reduction activity.

4.3.4.3 Cation exchange (SP-Toyopearl)

Second step in the isolation of the membrane/periplasmic associated uranium(VI)-reductase(s):

The proteins collected during the anion purification attempt (Figure 4.12 C-D) were applied to the SP-Toyopearl resins described in section 4.2.5.3. The elution profile obtained (Figure 4.13), showed only about five protein peaks eluting with the salt gradient. The amount of proteins not interacting with the resin (Figure 4.13 A-B) was quite low and no uranium(VI) reduction activity was observed. Of the proteins eluted with the salt gradient (Figure 4.13 C, D, E and F) a total of three (Figure 4.13 D, E and F) displayed uranium(VI) reduction activity.

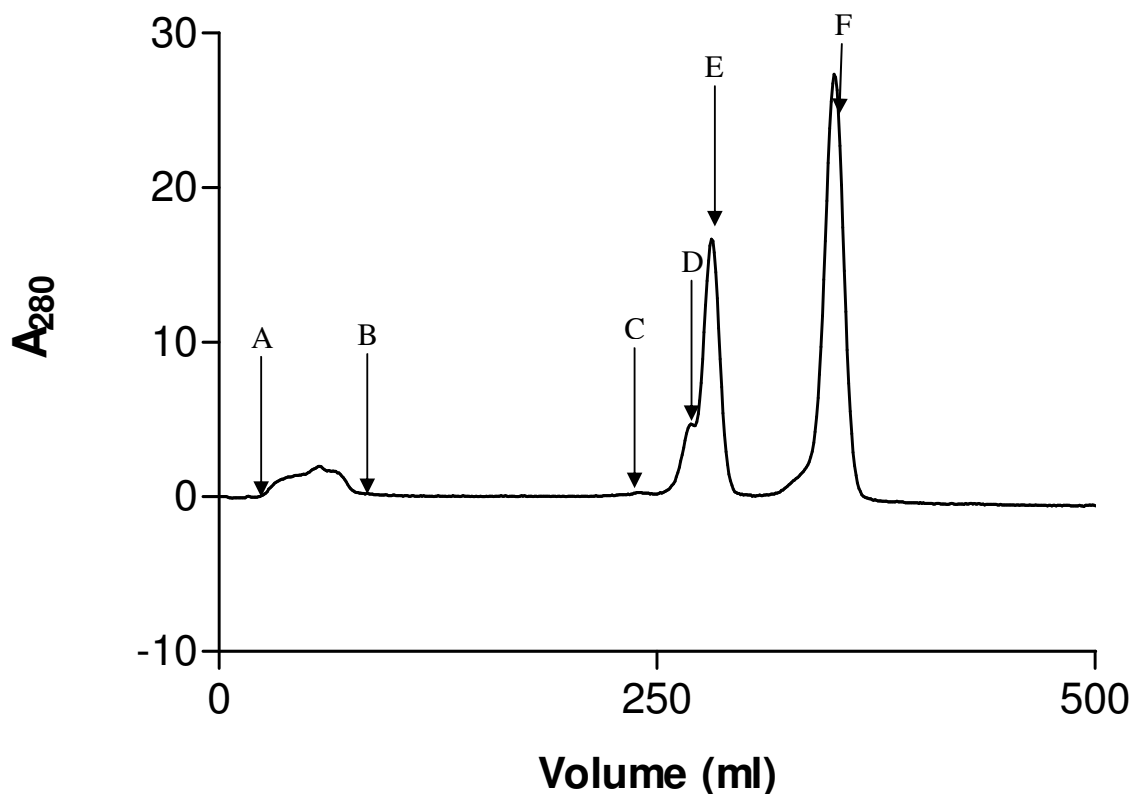


Figure 4.13: Elution profile for the SP Toyopearl, peaks D, E and F produced uranium(VI) reduction activity.

The resulting SDS-PAGE gel (Figure 4.14) indicated a +/- 70 kDa protein as the only protein present in all three these fractions where uranium(VI) reduction was present. Uranium(VI) reduction activity also coincides with the amount of said protein in the eluted fractions. If the observed activity in peak D is considered as 100%, the activity in both peak C and E was about 30%. The protein was thus identified as a possible “uranium reductase”.

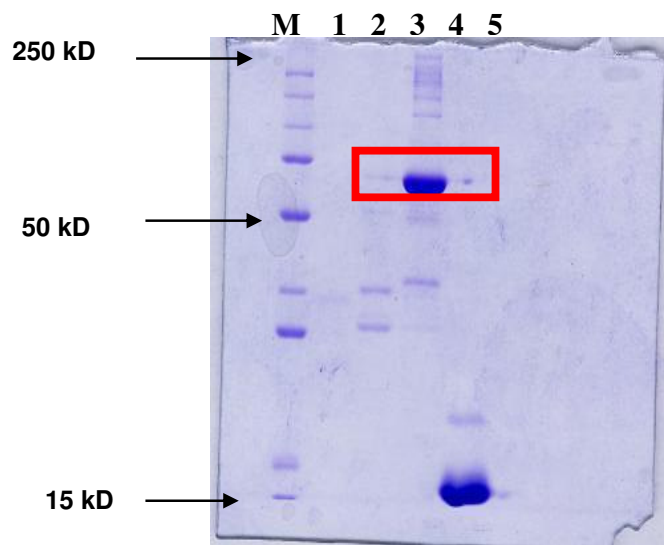


Figure 4.14: SDS-PAGE gel electrophoresis of selected fractions from chromatographic separation on the SP Toyopearl resin. Lane M, Precision Plus Protein™ Standards (Bio-Rad); Lane 1, Peak B; Lane 2, Peak C 16; Lane 3, Peak D; Lane 4, Peak E; Lane 5, Peak A-A.

4.3.5 Sequence determination of unknown protein

The N-terminal sequence of the soluble protein was determined using Edman degradation as described in section 4.2.6. The peak containing the largest concentration of protein (Figure 4.13 E) was run on a 10% SDS PAGE. The band of interest was excised and sent for sequencing. The result obtained was as follows:

N terminal sequence is: XPXDNSLVIG

BLASTP analysis in the NCBI web using "DNSLVIG" sequence resulted in 100% identity with various proteins, but the ones of interest are summarized in Table 4.7.

Table 4.7. Relevant proteins with a 100% sequence identity to the protein query DNSLVIG.

Solute-Binding Protein Family 5 From <i>Thermus aquaticus</i> Y51MC23 (GI:218296260)
Dipeptide-Binding Protein <i>T. thermophilus</i> HB27 (GI:46199573)
Peptide ABC Transporter, Peptide-Binding Protein <i>T. thermophilus</i> HB8 (GI:55981603)

When these proteins are aligned with the ClustalW program (Table 4.8) it becomes apparent that they share a high level of sequence similarity especially the peptide binding proteins from *T. thermophilus*. Therefore it is deduced that the first amino acid could be a G and the third residue could be a Q, resulting in the sequence GPQDNSLVIG for the N-terminal.

When a BLAST search is performed against the *T. scotoductus* SA-01 draft genome (Gounder, 2009) it results in 100% identity with a peptide ABC transporter, peptide-binding protein. Alignment of the proteins from *T. scotoductus* SA-01, *T. thermophilus* BG8 and HB27 indicates high levels of sequence similarities.

It confirmed with a high level of certainty that the N-terminal sequence obtained is that of the peptide ABC, peptide binding protein. This is very different from uranium reductases described in literature, but not completely unfounded since this same protein has shown was able to reduce gold(III) to elemental gold (Van Marwijk, 2010).

Table 4.8. ClustalW alignment of the proteins with 100% sequence identity to the protein query DNSLVIG.

HB8	MRNLGKLAVLGITALGLALAGPQDNSLVIGASQEPRVLAGDFLRSVSNQAIKSEIEQYLF	60
HB27	MRNLGKLAVLGITALGLALAGPQDNSLVIGASQEPRVLAGDFLSVISNQAISKSEIEQYLF	60
Y51MC23	MRKVGKLAVLGLTALGLALAGPQDNSLVIGASQEPRVLAGDFLSVISNQSIAKAEIENYLF	60
	** : ***** : ***** : ***** : ***** : ***** : ***** : ***** : ***** : *****	
HB8	APFIGFNADSQNFPVLATEVPTLENGRLRVTDIGGGKRRLEMDITIRPDAKWSGDRPITT	120
HB27	APFIGFNADSQNFPVLATEVPTLENGRLRVTDIGGGKRRLEMDITIRPDAKWSGDRPITT	120
Y51MC23	VPFITLNLDGQNTAVLATEVPTIQNGRVRFADIGQGRRLLEIDITIRPDARWSGDRPITT	120
	. *** : * . * . ***** : *** : * . : ***** : ***** : ***** : ***** : *****	
HB8	EDVAFYFEVKGAKGMPVLNPDFWERVNVRIKDARNFTLIFEPAYYYDITYGPINTYAPKHI	180
HB27	EDVAFYFEVKGAKGMPVLNPDFWERVNVRIKDARNFTLIFEPAYYYDITYGPINTYAPKHI	180
Y51MC23	EDVQFYFEVKGAKGMPVLDPDYWERVNLRVKDARNFTVIFEPAYATDLIGNPIGYAPKHI	180
	***** : * : ***** : * : ***** : ***** : *****	
HB8	MGPWEVRVKAARGLDPDKDAEKLNELYRNFFLKFATPQALNRGAMVYSGPFKLRWVPG	240
HB27	MGPWEVRVKAARGLDPDKDAEKLNELYRNFFLKFATPQALNRGAMVYSGPFMLRRWVPG	240
Y51MC23	MGAWEQVKRQTAGLDPTRDAARLAEIYRKFPTDFSTPAYLNQGMVYSGPFVLRWVPG	240
	* * . * : * : * * * : * : * : * * * : * : * * * : * : * * * : * : * * * : * : * * *	
HB8	NSIEMVRNPFPKPEGGESKYVQKVYRFIQNTNSLLVAVIGGSIDATSSVSLTFDQGR	300
HB27	NSIEMVRNPFPKPEGGESKYVQKVYRFIQNTNSLLVAVIGGSIDATSSVSLTFDQGR	300
Y51MC23	STVEMVRNPQFPITPPGGADKYVQKVYRFIQNTSSLQVAIMGGSIDALSRVGLTFDQAR	300
	. : : ***** : * * . * . * . * : ***** : * . * : : ***** : * . * . * . *	
HB8	SPQLVRRAPGRFDIWFVPGAWEHIDINKFENCQVVKDLGLNDKTRQAILHALNREGLV	360
HB27	SPQLVRRAPGRFDIWFVPGAWEHIDINKFENCQVVKDLGLNDKTRQAILHALNREGLV	360
Y51MC23	APQLVQRARGNFDIWFVPGAWEHIDVNQFANVPRVRELGLNDKTRQALLHAINREGFV	360
	: ***** : * * . ***** : * : * * : : ***** : * * : * * : *	
HB8	KAFFDGLQPVAHWTWIAPVNPVLPNPNVKKYEFDLKKAELLAEMGWRKGPDGILQRTVNGR	420
HB27	KAFFDGLQPVAHWTWIAPVNPVLPNPNVKKYGFDLKKAELLAEMGWRKGPDGILQRTVNGR	420
Y51MC23	RTVFQGLQPVSHWTWIAPVNPVLPNPNVKKYEFDLKKAELLAEMGWRKGPDGILQRTVDGR	420
	: . : * : * * * : * : * * * * . * * * : * : * * * * * : * : * * * * * : * * * * * : * * * * *	
HB8	TVRFEIEYVTTAGNVVRETRQFFAEDLKKIGIAVRINNAPSAVVFADDFIQRASECKWT	480
HB27	TVRFEIEYVTTAGNVVRETRQFFAEDLKKIGIAVRINNAPSAVVFADDFIQRASECKWT	480
Y51MC23	TVRFEIEWVTTAGNVVRETRQFFAEDFRKIGIAVRINNAPSAVVFADDFIQRASEGRWT	480
	***** : ***** : * * . : * : * * * : * : * * * * : * : * * * * : * * * * : *	
HB8	GMFMAVWSNLQEDGSLFYKLNLTGAIMVPTKENNYQGQNIIGWRNDEFDRLLTSQAVLE	540
HB27	GMFMAVWSNLQEDGSLFYKLNLTGAILVPTRENNYQGQNIIGWRNDEFDRLLTSQAVLE	540
Y51MC23	GMFMAVISNLKENGDLFSCR-----FRPTRENNYQGQNVGGWCNEEYDRLRDQAVVE	533
	***** : * . * : * * . : : * : * * * * * : * * * : * : * * * : * : *	
HB8	FDPERRQLFWRAQEIWAEEELPALPLYFRANPYVVRKGLVNYVASAYSGGYGYPGNNAWE	600
HB27	FDPERRQLFWRAQEIWAEEELPALPLYFRASPYVVRKGLVNYVASAYAGGFYGPGNNAWE	600
Y51MC23	FDFAKRKALFDRMQEIWAEEVAALPLYFRADPLIVRKGLVNYVASAYSGGFNYPNWEPWT	593
	* * : * : * * * * * * : * : * * * * * : * : * * * * * : * : * * * : * * : *	
HB8	IGWESRGAVKKWDQAKYALSTR	622
HB27	IGWESRGAVKKWDQAKYALSTR	622
Y51MC23	IGWTQRGAEKRWQAKYALTIR	615
	*** . *** : ***** : *	

amino acids. The obtained MS/MS fragment spectrum is the result of collision induced dissociation, (CID), occurring within a mass spectrometer and the fragmentation is produced in a collision cell in a tandem mass spectrometer. The fragment spectrum is then be used to determine the sequence of the fragment by either matching the peak list to a database or by subtracting the monoisotopic amino acid and immonium ion masses from the fragment size.

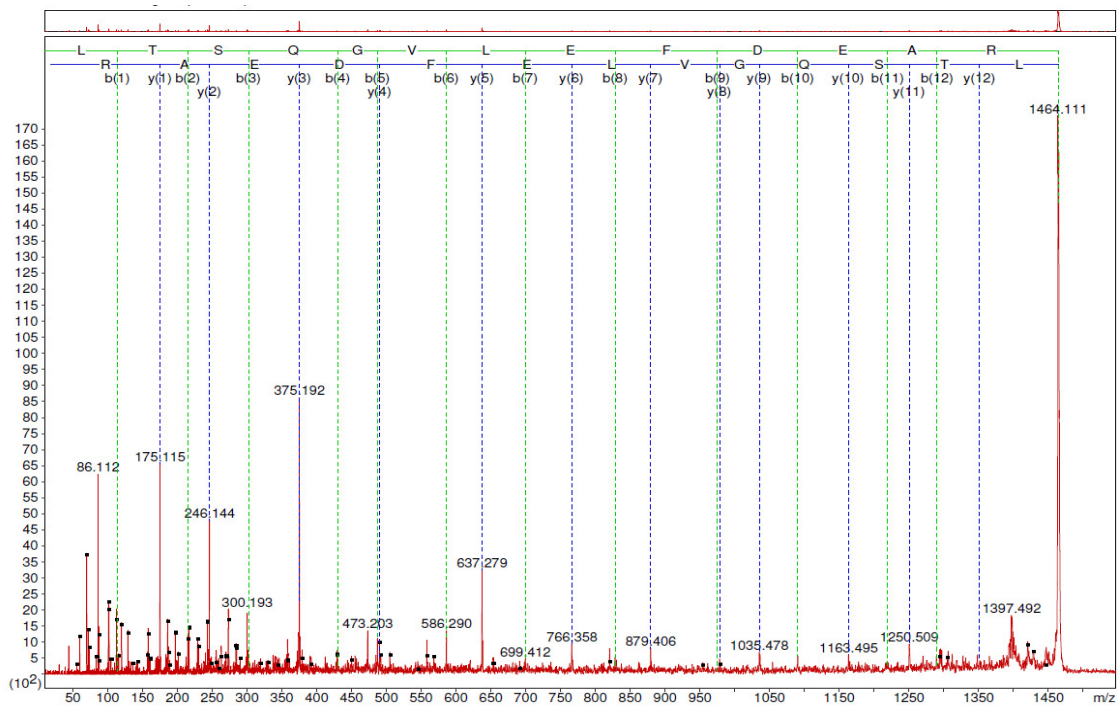
A total of nine tryptic digest fragment spectra was obtained from the Centre for Proteomic and Genomic Research in Cape Town, which was analyzed using the Mascot Distiller software by both matching the peak list to a database and by hand. Four of the spectra were annotated successfully (Figure 4.15) and the sequences obtained (Table 4.10) blasted against the *T. scotoductus* SA-01 draft genome (Gounder, 2009) resulted in 100% identity with the peptide ABC transporter, peptide-binding protein.

Table 4.10. Sequences obtained from fragmentation spectra.

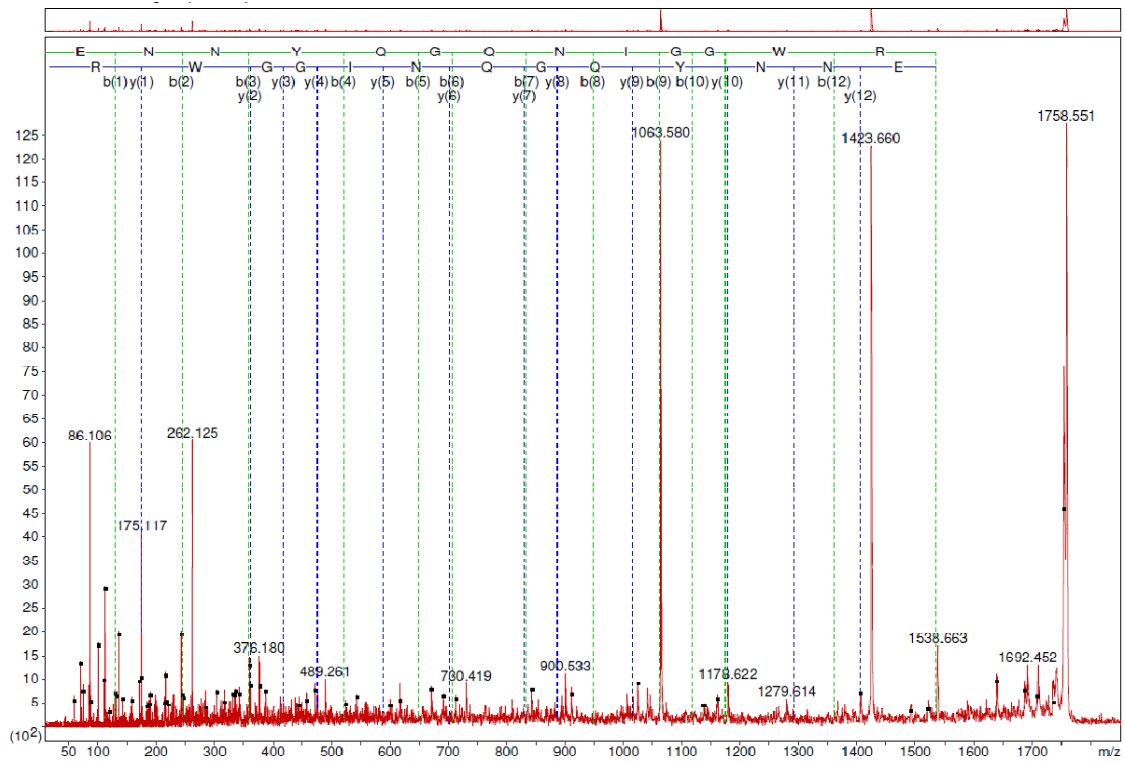
Fragment size (m/z)	Annotated amino acid sequence
1464.744	L T S Q G V L E F D E A R
1541	N P N F P I K P E G G E S R
1735.708	E N N Y Q G Q N I G G W R
1892	I N N A P S A V V F A D D Y I Q R

This result further validates the finding, that unlike in literature, where uranium(VI) reduction is largely mediated by cytochrome *c3* proteins (Lovley *et al.*, 1993), here we are presented with this highly unlikely candidate in the form of a peptide binding protein. An intense investigation was thus launched to confirm this reductive ability to this protein.

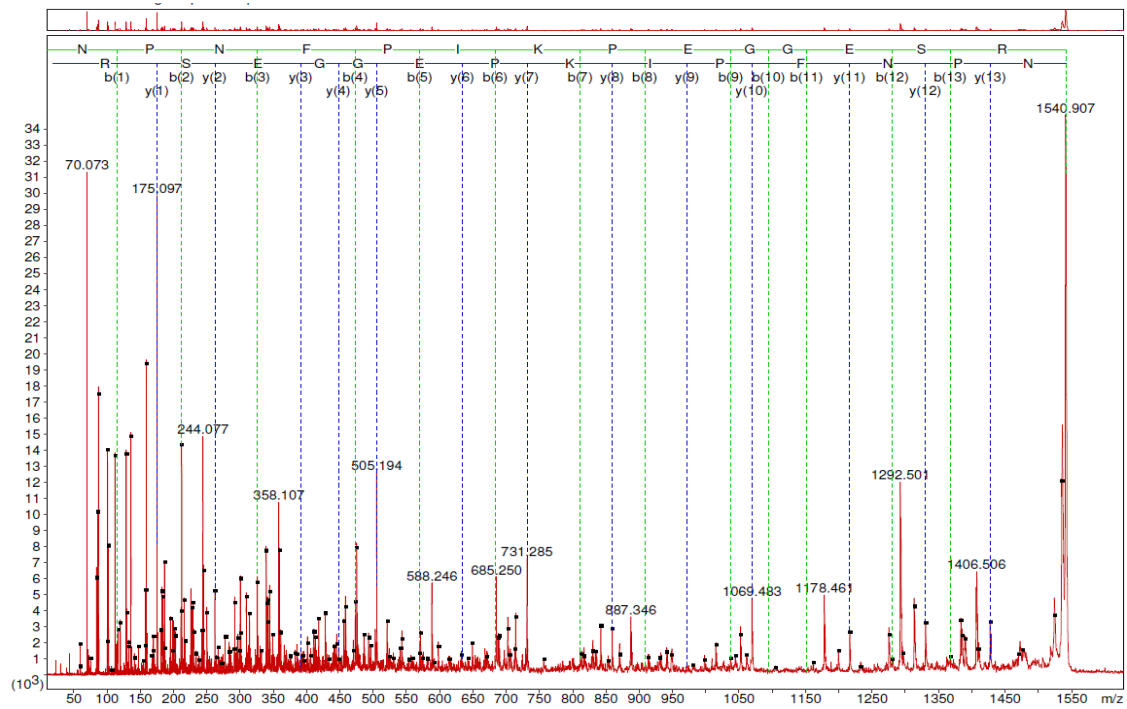
(A)



(B)



(C)



(D)

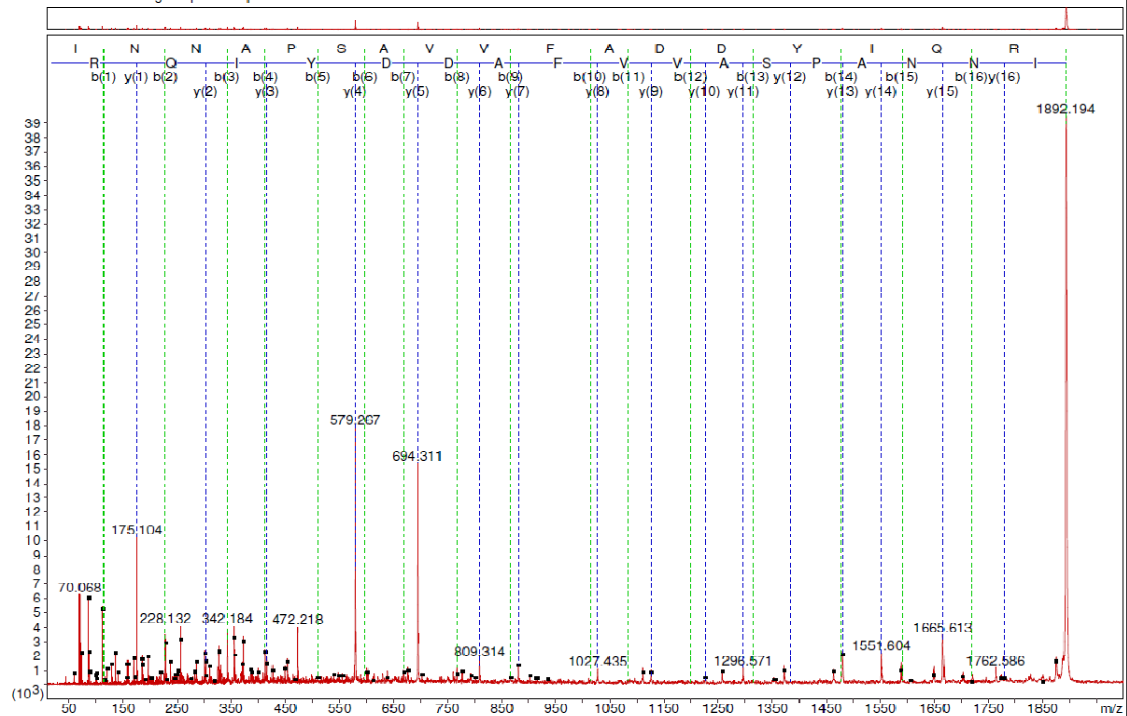


Figure 4.15: A-D show the annotated fragmentation spectra for the different sized spectra. All sizes are a value of mass divided by charge (m/z). (A) 1464.744; (B) 1753.86; (C) 1541; (D) 1892.

4.3.6 Protein expression and purification

4.3.6.1 Cloning and sequencing of the peptide ABC transporter, peptide-binding protein gene from *Thermus scotoductus* SA-01

The gene was amplified, cloned and expressed as described in section 4.2.7.1. A band approximately 1.9 kb was observed, which was the predicted size of for the amplification of the ABC protein (Figure 4.16) (Gounder, 2009). The band was purified from the gel and stored at -20°C until required for downstream experiments.

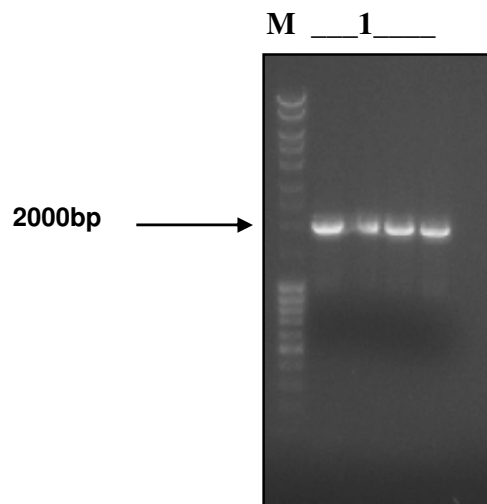


Figure 4.16: PCR product from amplification of the ABC transporter gene. Lane M, Molecular mass marker ; Lane 1, the amplified ABC transporter, peptide-binding protein.

The gel-purified PCR product was ligated into the pGEM[®]-T Easy vector system transformed into *E. coli* Top 10 competent cells and plated out on AIX plates from which colonies were selected for further inoculation and growth. Small-scale plasmid isolation and double-digestion were performed as described in section 4.2.7.1.

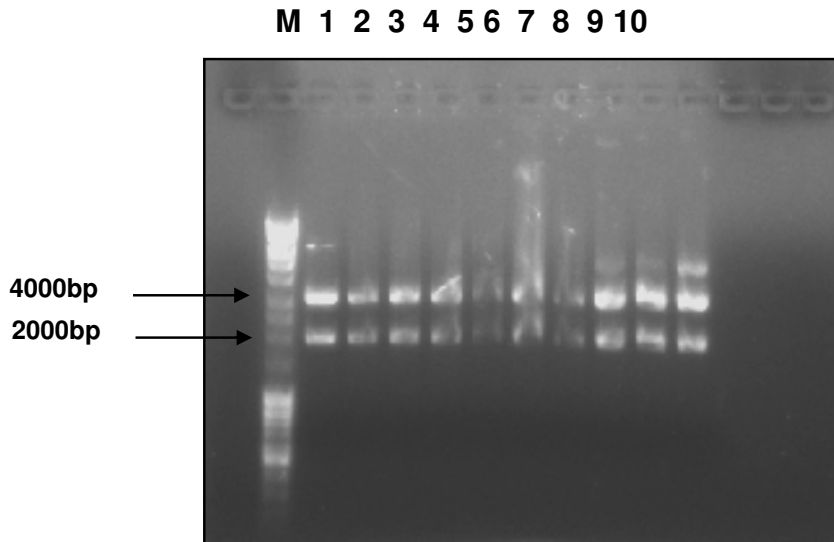


Figure 4.17: pGEM[®]-T Easy plasmid containing the ABC gene digested with *EcoRI* and *NdeI*. Lane M, Molecular mass marker; Lanes 1 to 10, the clones screened for inserts.

Double digestion confirmed the presence of the insert in all of the clones, the insert was purified from a gel and ligated into the double digested pET28b(+) vector system, obtained from section 4.2.7.1, and propagated using *E. coli* Top 10, as described in section 4.2.7.1, cells which was plated out on LB plates containing kanamycin. Single colonies were selected and inoculated into LB medium containing the same antibiotics and small-scale plasmid isolation was once again performed on the inoculated clones. The obtained plasmid DNA was screened for the insert by double digestion with the restriction enzymes *EcoRI* and *NdeI*, which was subsequently loaded onto a 1% agarose gel (Figure 4.18). All the clone digests confirmed the presence of an insert of the expected size and thus a single clone was selected for expression studies. The results from the sequencing of the selected clone confirmed that the sequence was correct (Table 4.11).

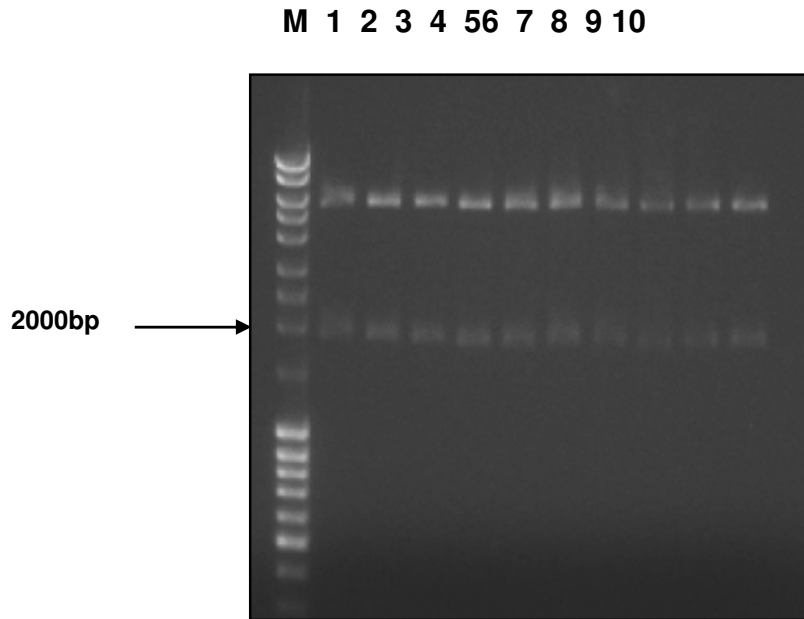


Figure 4.18: pET28b(+) plasmid containing the ABC gene digested with *EcoRI* and *NdeI*. Lane M, Molecular mass marker; Lanes 1 to 10 the clones screened for inserts.

Table 4.11. Sequence alignments of the reference ABC gene from the *T. scotoductus* SA-01 genome database and the cloned ABC gene from *T. scotoductus* SA-01.

SA-01	GGGCCCCAGGACAAAGCCTGGTCATAGGGGCTTCGCAGGAGCCCCGGGTCTGGCGGGG	60
Reference	GGGCCCCAGGACAAAGCCTGGTCATAGGGGCTTCGCAGGAGCCCCGGGTCTGGCGGGG	60

SA-01	GACTTCCTAAGCATCATCTCCAACCAAGTCCATCAAGTTGGAGATCGAGCAGTACCTCTTC	120
Reference	GACTTCCTAAGCATCATCTCCAACCAAGTCCATCAAGTTGGAGATCGAGCAGTACCTCTTC	120

SA-01	GCCCCCTCATCGGTTTCAACGCCAACAGCGAAAACCTTCCCGTGCTGGTACCGAGGTG	180
Reference	GCCCCCTCATCGGTTTCAACGCCAACAGCGAAAACCTTCCCGTGCTGGTACCGAGGTG	180

SA-01	CCCACCCGGCAAAACGGGCGTTTGCAGGATCGGCGGGGCAAGAAGCGCTTG	240
Reference	CCCACCCGGCAAAACGGGCGTTTGCAGGATCGGCGGGGCAAGAAGCGCTTG	240

SA-01	GAGATGGACCTCACCATCCGGCCGATGCCCGTGGTCCGACGGCAAGCCCATCACACC	300
Reference	GAGATGGACCTCACCATCCGGCCGATGCCCGTGGTCCGACGGCAAGCCCATCACACC	300

SA-01	GAGGATGTGGCCTTCTACTACGAGGTGGCAAGGCCAAGGGGATGCCGGTGCTCAACCCG	360
Reference	GAGGATGTGGCCTTCTACTACGAGGTGGCAAGGCCAAGGGGATGCCGGTGCTCAACCCG	360

SA-01	GACTACTGGGAGCGGGTGAACCTCCGGTCAAGGACGCCCCGCAACTTCCCGTATCTTT	420
Reference	GACTACTGGGAGCGGGTGAACCTCCGGTCAAGGACGCCCCGCAACTTCCCGTATCTTT	420

SA-01	GAGCCCGCTACTACTACGACACCTACGGCGGCACCTACGGCTCCCCATCGGCTACGCT	480
Reference	GAGCCCGCTACTACTACGACACCTACGGCGGCACCTACGGCTCCCCATCGGCTACGCT	480

SA-01	CCC AAGC A T C A T G G G C C C G A G T G G G A G A A G G T G A A A G C G G C C C G G A A C C T G G A T	540

```

Reference      CCCAAGCACATCATGGGCGCCAGTGGGAGAGGTGAAAGCGGCGGCCGGAACCTGGAT 540
*****

SA-01         CCCGATAAGGATGCGGAGAGGCTCAACGAGCTCTACCGCAACTTCTTCCTCAAGTTCGCC 600
Reference      CCCGATAAGGATGCGGAGAGGCTCAACGAGCTCTACCGCAACTTCTTCCTCAAGTTCGCC 600
*****

SA-01         ACTCCCCAGGCCCTAAACCGGGGAGCCATGGTCTACTCGGGGCTTCAAGCTGCGGCGC 660
Reference      ACTCCCCAGGCCCTAAACCGGGGAGCCATGGTCTACTCGGGGCTTCAAGCTGCGGCGC 660
*****

SA-01         TGGGTGCCGGGAACTCCATTGAGATGGAGCGGAACCCCAACTTCCCCATCAAGCCCGAG 720
Reference      TGGGTGCCGGGAACTCCATTGAGATGGAGCGGAACCCCAACTTCCCCATCAAGCCCGAG 720
*****

SA-01         GGTGGGAGAGCCGGTACGTGCAGAGGGTGGTCTACCGCTTCATCCAGAACCACCACTCC 780
Reference      GGTGGGAGAGCCGGTACGTGCAGAGGGTGGTCTACCGCTTCATCCAGAACCACCACTCC 780
*****

SA-01         CTCTGGTGGCCGCTCTGGGCGGGAGCATTGACGCCACCTCCAGCGTCTCCCTCACCTTT 840
Reference      CTCTGGTGGCCGCTCTGGGCGGGAGCATTGACGCCACCTCCAGCGTCTCCCTCACCTTT 840
*****

SA-01         GACCAAGGCCGTAGCCGCCAGCTCACCTCCGGGCCCTGGCCGCTTTGACATCTGGTTC 900
Reference      GACCAAGGCCGTAGCCGCCAGCTCACCTCCGGGCCCTGGCCGCTTTGACATCTGGTTC 900
*****

SA-01         GTGCCCGGGCCATCTGGGAGCACATTGACGTCAACAAGTTTGAGAACTGCCAGGCGGTC 960
Reference      GTGCCCGGGCCATCTGGGAGCACATTGACGTCAACAAGTTTGAGAACTGCCAGGCGGTC 960
*****

SA-01         CGCGACTTGGCCGTAAACGACGTCCGACCCGTCGGGCCCTCCTCCACGCTCTGAACCGC 1020
Reference      CGCGACTTGGCCGTAAACGACGTCCGACCCGTCGGGCCCTCCTCCACGCTCTGAACCGC 1020
*****

SA-01         GAGGGTTGGTCAAGGCCCTTCTTTGACGGCCTCCAGCCCGTGGCCACACCTGGATCGCC 1080
Reference      GAGGGTTGGTCAAGGCCCTTCTTTGACGGCCTCCAGCCCGTGGCCACACCTGGATCGCC 1080
*****

SA-01         CCCGTCAACCCCTCTTCAACCCCAATGTGCGGAAGTACGAGTTTGACCTGAAGAAGGCG 1140
Reference      CCCGTCAACCCCTCTTCAACCCCAATGTGCGGAAGTACGAGTTTGACCTGAAGAAGGCG 1140
*****

SA-01         GAGGCGCTCTTGGCGGAGATGGGCTGGAGGAGGGGCCGACGGCATCCTTCAGCGCAC 1200
Reference      GAGGCGCTCTTGGCGGAGATGGGCTGGAGGAGGGGCCGACGGCATCCTTCAGCGCAC 1200
*****

SA-01         GTGGGTGGCCGACCCGTGCGCTTTGAGATTGATTGTCACCAACCGGGCAACGCTATC 1260
Reference      GTGGGTGGCCGACCCGTGCGCTTTGAGATTGATTGTCACCAACCGGGCAACGCTATC 1260
*****

SA-01         CGGGAGCGCACCCAGCAGTTCTTCGCCGAGGACCTGAAGAAGATCGGCATCGCCGTAAG 1320
Reference      CGGGAGCGCACCCAGCAGTTCTTCGCCGAGGACCTGAAGAAGATCGGCATCGCCGTAAG 1320
*****

SA-01         ATCAATAACGCCCCAGCGCGTGGTCTTCGCCGACGACTACATCCAGCGGGCCAGCGAG 1380
Reference      ATCAATAACGCCCCAGCGCGTGGTCTTCGCCGACGACTACATCCAGCGGGCCAGCGAG 1380
*****

SA-01         TGAAGTGGACCGGCTGTTTGAAGTTCGTTGGGTTTCCAACTGGCCGAGGATGGCTCC 1440
Reference      TGAAGTGGACCGGCTGTTTGAAGTTCGTTGGGTTTCCAACTGGCCGAGGATGGCTCC 1440
*****

SA-01         CTCTCCAGTACAAGAACTGAACACCGGGCCATCATGGTGCCCAACAGGAGAACAAC 1500
Reference      CTCTCCAGTACAAGAACTGAACACCGGGCCATCATGGTGCCCAACAGGAGAACAAC 1500
*****

SA-01         TACCAGGGGAGAACATCGCGGCTGGCGCAACGACGAGTTGACCGTCTGACGAGCCAG 1560
Reference      TACCAGGGGAGAACATCGCGGCTGGCGCAACGACGAGTTGACCGTCTGACGAGCCAG 1560
*****

```

```

SA-01      GGTGTCCTGGAGTTGACGAGGCCAGGCGGAAGCAGCTCTTCTGGAGGGCCCAGGAGATC 1620
Reference   GGTGTCCTGGAGTTGACGAGGCCAGGCGGAAGCAGCTCTTCTGGAGGGCCCAGGAGATC 1620
*****

SA-01      TGGGCCGAGGAGCTGCCTGCCTTGCCCTCTACTTCCGCGCTAACCCCTACGTGGTGC GG 1680
Reference   TGGGCCGAGGAGCTGCCTGCCTTGCCCTCTACTTCCGCGCTAACCCCTACGTGGTGC GG 1680
*****

SA-01      AAGGGCCTGGTCAACTACGTGGCCAGCGCTTACGCGGGCGGCTACGGTTACCCCGGCTGG 1740
Reference   AAGGGCCTGGTCAACTACGTGGCCAGCGCTTACGCGGGCGGCTACGGTTACCCCGGCTGG 1740
*****

SA-01      AACGCTTGGGAGATCGGCTGGGAGAGCCGCGCGCCGTGAAGAAGTGGGACCCAGGCGAAG 1800
Reference   AACGCTTGGGAGATCGGCTGGGAGAGCCGCGCGCCGTGAAGAAGTGGGACCCAGGCGAAG 1800
*****

SA-01      TACGCTCTTTCCGTCAAGTAA 1821
Reference   TACGCTCTTTCCGTCAAGTAA 1821
*****

```

4.3.7 Expression and purification of the recombinant ABC protein

Expression and purification were performed as described in section 4.2.7.2. The gene sequence was obtained from the *T. scotoductus* SA-01 genome database constructed through pyrosequencing (Gounder, 2009). Reverse and forward primers were designed using the ORF and restriction sites were incorporated to facilitate cloning of the gene into pET28b(+) vector. The pET28b(+) plasmid containing the ABC transporter, peptide-binding protein was used to over-express the ABC transporter, peptide-binding protein. His-tag expression was done to aid the purification of the recombinant protein.

The purification of the pET28b(+) expressed protein was done using the nickel-affinity resin because the His-tag has an affinity for nickel and can be displaced by imidazole as they have basically the same functional group, but imidazole has a higher affinity for the nickel than the His-tag. Only one binding peak(Figure 4.19 A-B) was observed and it was dialyzed against 20 mM of MOPS buffer, pH 7.4 to rid the protein solution of the imidazole. The peak was analysed on SDS-PAGE (Figure 4.20) and showed the presence of the recombinant protein and also indicated that the recombinant protein was in excess to the other proteins in solution, thus further purification with a size-exclusion resin was excluded. The protein concentration was determined with the bicinchoninic acid (BCA) method,described in section 4.2.1.2,to be 779.6 µg/ml.

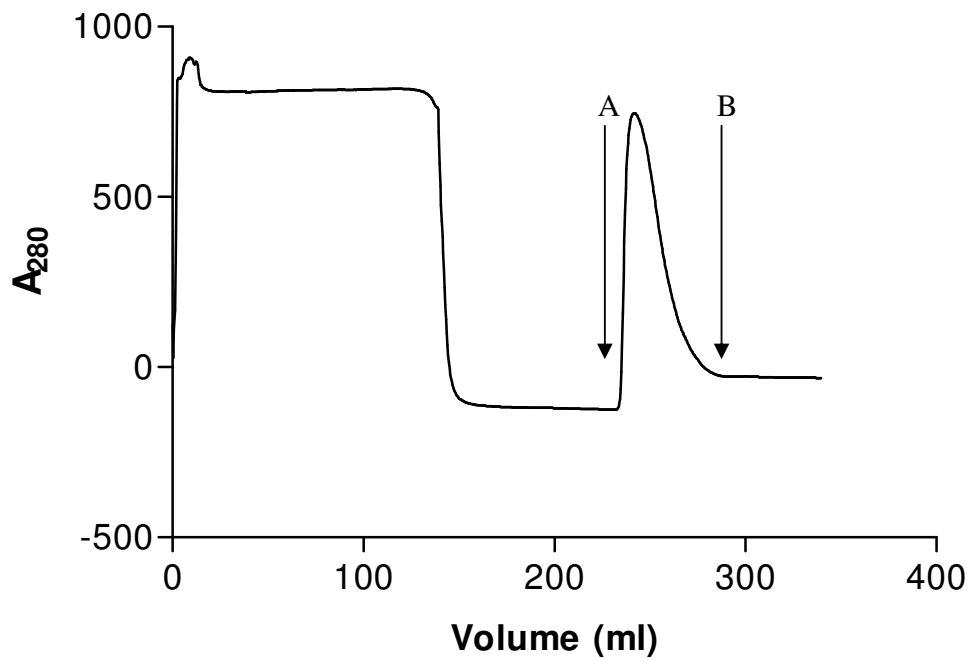
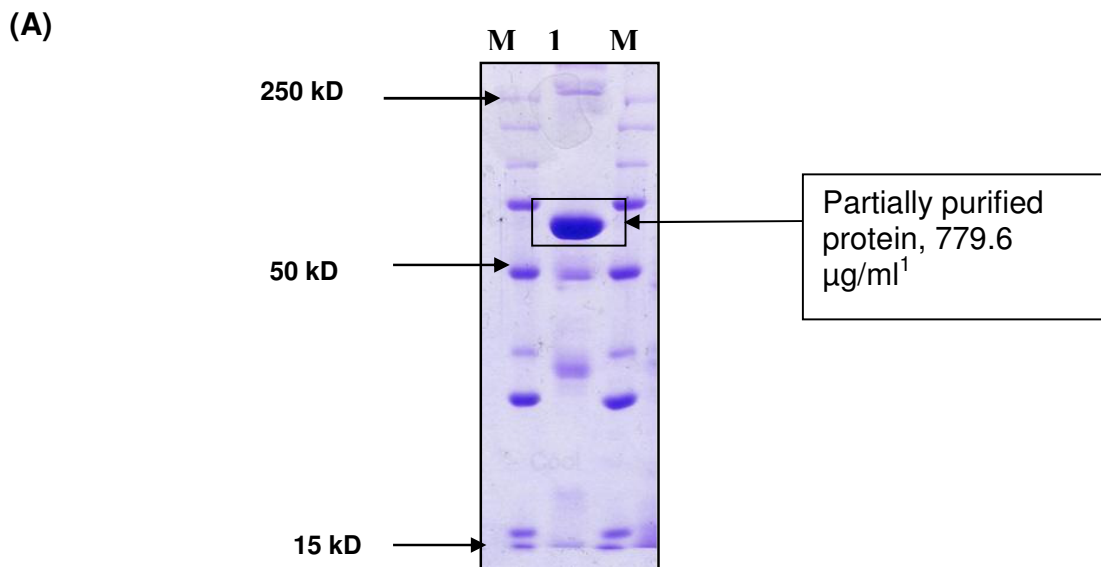


Figure 4.19: Elution profile for purification of the pET28b(+) expressed protein.



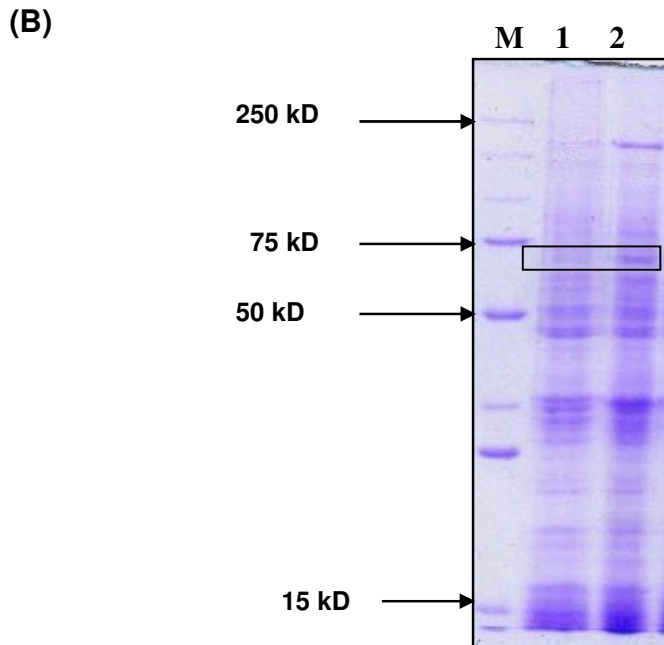
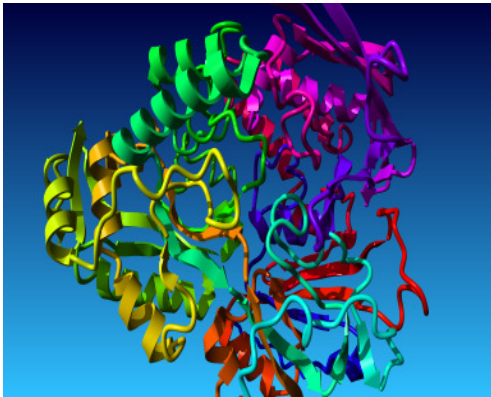


Figure 4.20: (A) SDS-PAGE analysis of the recombinant ABC protein when using the pET28b(+). Lane M, Precision Plus Protein™ Standards (Bio-Rad); Lane 1, Protein at 4h after induction. (B) SDS-PAGE analysis of all proteins after IPTG induction. Lane M, Precision Plus Protein™ Standards (Bio-Rad); Lane 1, 0h after induction; Lane 2, 2h after induction.

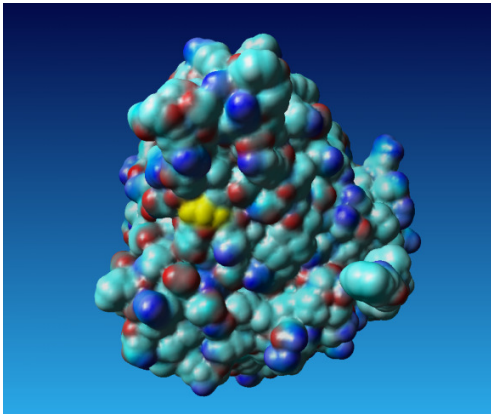
4.3.8 Modelling

As described previously in section 4.3.2 it was hypothesized that the protein involved in uranium(VI) reduction is not a hydrogenase or a oxidoreductase and was confirmed by the sequencing results obtained in 4.3.5, but a mechanism for uranium(VI) reduction still has to be determined. In an attempt to visualize potential catalytic options, a homology model of the protein was compiled. Modelling of the protein made it possible to find a disulphide bond (Figure 4.21) which is present on the exterior of the protein, thereby indicating that this could supply a possible nucleation site for uranium(VI) reduction once the bond has been broken by the addition of a reducing agent such as β -mercaptoethanol, sodium dithionite or dithiothreitol. Other proteins with cysteine thiol-disulfide bridges have shown the ability to reduce uranium(VI) such as a thioredoxin from *Desulfovibrio desulfuricans* strain G20 (Li and Krumholz, 2009).

(A)



(B)



(C)

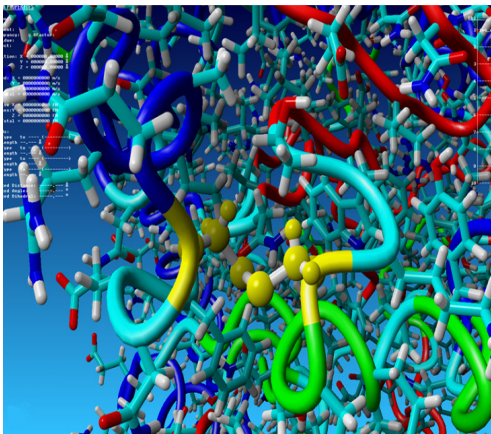


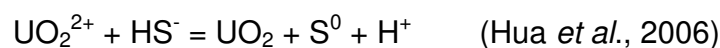
Figure4.21:(A) and (B) Homology model of ABC peptide binding protein from *T. scotoeductus* SA-01. The surface exposed disulphide bond which is hypothesized to be involved in the reduction of uranium is shown in yellow. (C) Detail of the environment of the disulphide bond.

4.3.9 Characterization of the recombinant ABC proteins

The recombinant protein was evaluated for the ability to reduce uranium(VI) as described in section 4.2.9. The recombinant protein was characterized using the same physico-chemical parameters as for characterizing the whole cells. In order for the disulphide bond observed during modelling (section 4.3.8) to be able to reduce uranium(VI), a reducing agent needed to be applied in order to reduce the thiol. Out of the possible reducing agents (dithiothreitol, sodium dithionite and β -mercaptoethanol) that were assayed with uranium(VI), β -mercaptoethanol produced the lowest level of chemical reduction of uranium(VI). An excess of β -mercaptoethanol was thus utilized to reduce the disulfide bonds of the proteins before experimentation.

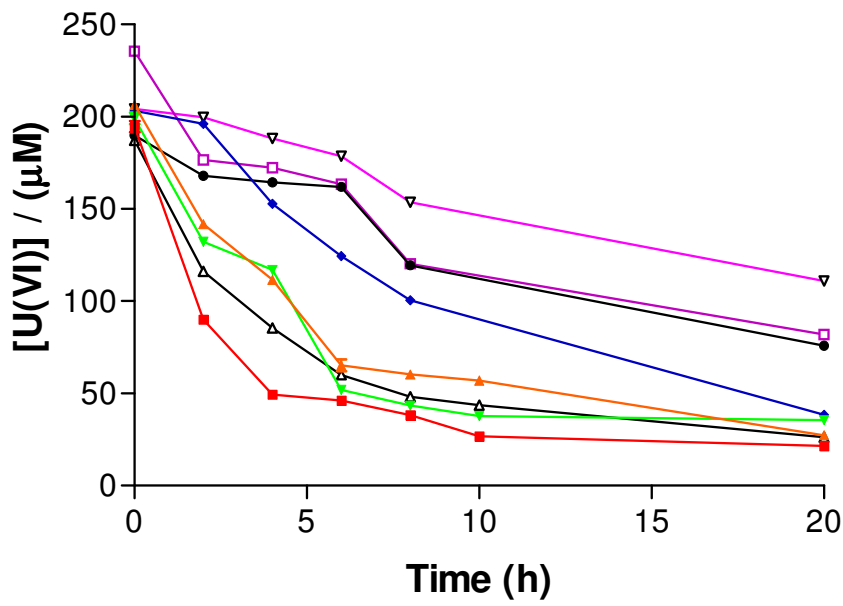
4.3.9.1 The effect of pH on uranium(VI) reduction

In essence, reduction performed with a reduced disulfide bond can be seen as reduction by hydrogen sulphide. Hua and coworkers (2006) observed that the reduction of uranium(VI) by hydrogen sulphide happened optimally at neutral pH values and could best be represented by:



The highest rate of reduction can be observed for pH values between 7 and 8, which coincides with what was observed in literature for sulphide reduction (Hua *et al.*, 2006). At pH values below 7 and above 8 the rate of chemical reduction of uranium(VI) by β -mercaptoethanol in the samples lacking protein are very high (Figure 4.22 (A) and (B)). This might be due to pH inhibition of the reduction of the disulphide bond, producing increasing amounts of β -mercaptoethanol free to reduce the uranium(VI).

(A)



(B)

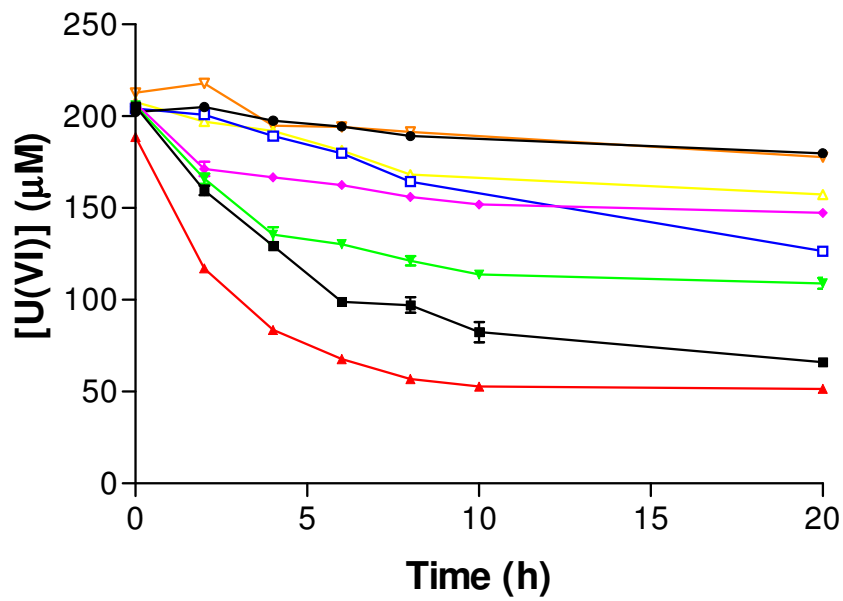


Figure 4.22: Reduction of uranium(VI) at different pH values. (A) pH values (■) 5.5, (▲) 6.0, (▼) 6.5, (△) pH 7.0, (◆) 5.5 protein free control, (●) pH 6.0 protein free control, (□) pH 6.5 protein free control, (▽) pH 7.0 protein free control. (B) pH values (▲) 7.5, (■) 8.0, (▼) 8.5, (◆) 9.0, (□) pH 7.5 protein free control, (●) pH 8.0 protein free control, (△) pH 8.5 protein free control, (▽) pH 9.0 protein free control.

4.3.9.2 The effect of temperature on uranium(VI) reduction

The highest rate of reduction can be observed for temperature values between 55°C and 65°C (Figure 4.23 C and D), coinciding with the optimal growth temperature for the organism (Kieft *et al.*, 1999). At temperatures below 45°C (Figure 4.23 A and B) almost no activity was observed and above 65°C (Figure 4.23 E) the rates of chemical reduction of uranium(VI) by β -mercaptoethanol in the samples lacking protein were very high.

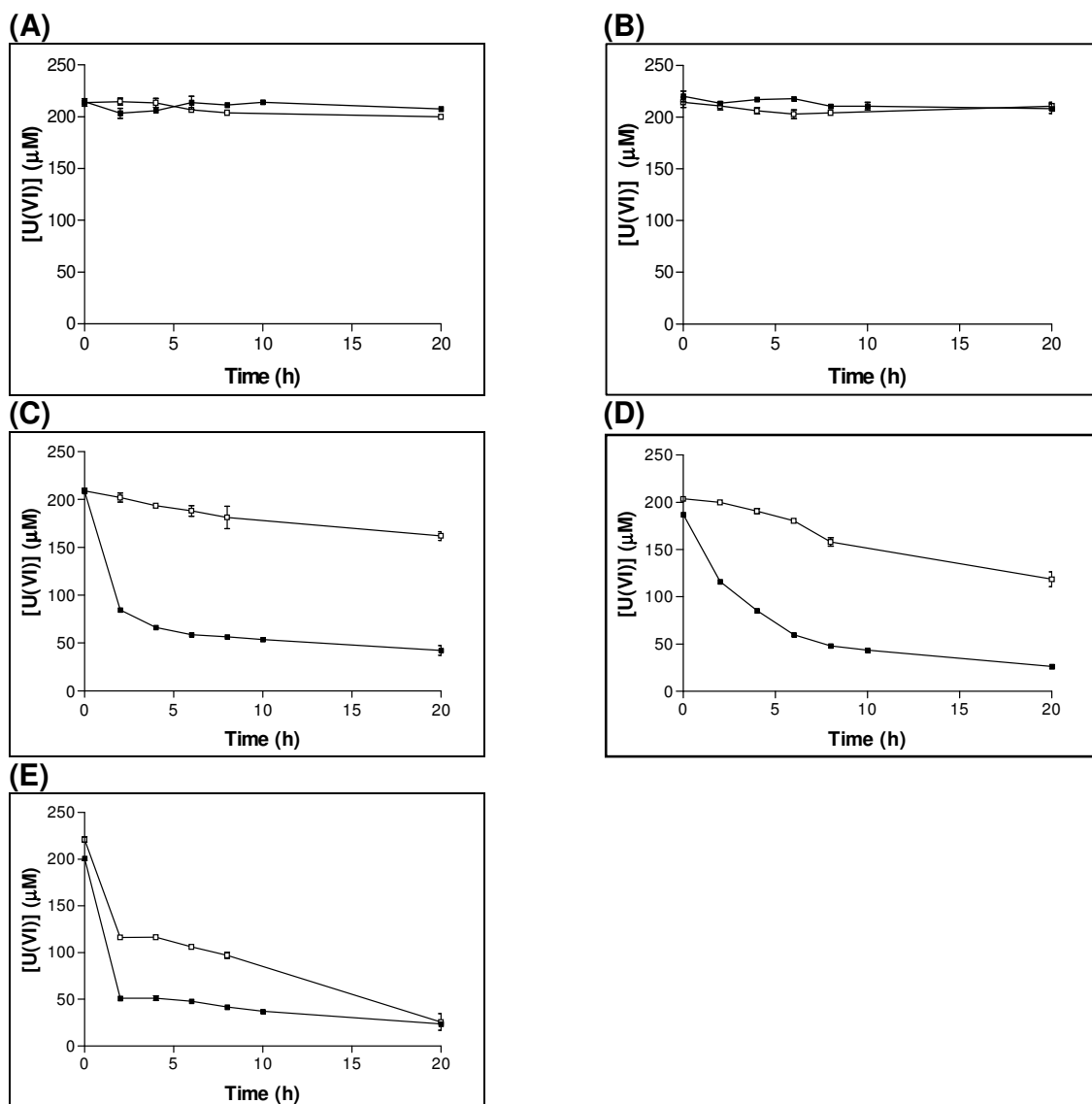


Figure 4.23: Reduction of uranium(VI) at different temperature values. (A) 35°C. (B) 45°C. (C) 55°C. (D) 65°C. (E) 75°C. (■) The indicated temperature, (□) protein free control.

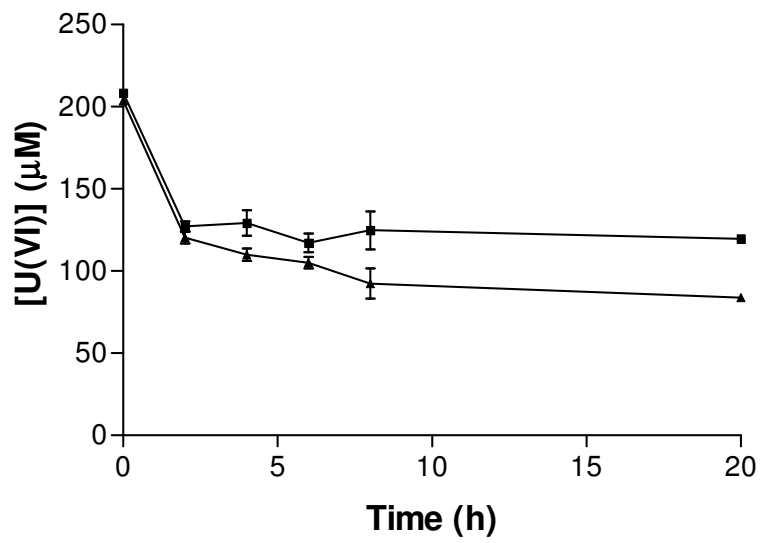


Figure 4.24: Reduction of uranium(VI) at 55°C (■) and 65°C (▲) with the blank rate subtracted.

4.4 Conclusions

In the past, literature has suggested a mechanism for periplasmic and membrane bound uranium(VI) reduction usually by hydrogenase such as a cytochrome *c3* type protein which utilizes hydrogen as an electron donor. More recently other low potential non-specific reductases have also been proven to reduce uranium(VI). Several oxidoreductases have shown the ability to reduce uranium(VI), where these proteins obtain electrons from NADH and are capable of two electron reduction of uranium(VI).

In this study it was investigated how an organism devoid of a cytochrome *c3* type protein is still able to reduce uranium(VI). To this end an uranium(VI)-reductase isolated from *T. scotoductus* strain SA-01 was described as a peptide ABC, peptide binding protein. This protein is not a known reductase but has the ability to reduce gold(III) to elemental gold (Van Marwijk, 2010). The reduction capabilities are believed to be due to the interaction of surface located disulphide bond. Recently, thioredoxin proteins have shown the ability to reduce uranium as well (Li and Krumholtz, 2009). Thioredoxin is similar to this ABC transporter protein since it also possesses a cysteine thiol-disulfide exchange mechanism which is utilised in the reduction of other proteins. However, the thioredoxin reduced uranium(VI) at a much faster rate at a very reduced protein level when compared to the peptide ABC, peptide binding protein.

Future studies might include purification of other proteins, that might be capable of uranium(VI) reduction as well as the production of uranium nanoparticles which can be utilized in industry. Future studies might also make use of site-directed mutagenesis to remove the cysteine residues of the disulphide bond thought to be responsible for the reduction of uranium(VI) to uranium(IV) within the ABC protein. This can be done to determine if uranium(VI) reduction by disulfide bond oxidation might truly be the mechanism involved as well as to assess the effect of the mutation *in vitro* and *in vivo*.

4.5 References

Braibant, M., Gilot, P. and Content, J. (2000) The ATP binding cassette (ABC) transport systems of *Mycobacterium tuberculosis*. *FEMS Microbiology Reviews* **24**: 449-467.

Chamupathi, V.G. and Tollin, G. (1989) Quionesas mediators of electron transfer from membrane-bound chlorophyll to cytochrome *c* in the aqueous phase in lipid bilayer vesicles: Synergistic enhancement of cytochrome *c* reduction by lipophilic/hydrophilic quinine pairs. *Photochemistry and Photobiology*. **51**:611-619.

Fairbanks, G., Steck, T.L., Wallach, D.F. (1971) Electrophoretic analysis of the major polypeptides of human erythrocyte membrane. *Biochemistry* **10**:2606-2617

Gaspard, S., Vasquez, F., and Holliger, C. (1998) Localization and solubilization of the Fe(III) reductase of *Geobacter sulfurreducens*. *Applied and Environmental Microbiology*. **64**: 3188-3194

Gounder, K. (2009) PhD thesis: Genome sequencing of the extremophile *Thermus scotoductus* SA-01 and expression of selected genes. University of the Free State, South Africa.

Gupta, S.D., Wu, H.C. and Rick, P.D. (1997) A *Salmonella typhimurium* genetic locus which confers copper tolerance on copper-sensitive mutants of *Escherichia coli*. *Journal of Bacteriology*. **179**:4977–4984.

Haas, J.R. and Northup, A. (2004) Effects of aqueous complexation on reductive precipitation of uranium by *Shewanella putrefaciens*. *Geochemical Transactions*. **5**:41–48.

Hua, B., Xu, H., Terry, J. and Deng, B. (2006) Kinetics of uranium(VI) reduction by hydrogen sulphide in anoxic aqueous systems. *Environmental Science and Technology*. **49**:4666-4671.

Kaufmann, F., and Lovley, D. (2001) Isolation and characterization of a soluble NADPH-dependant Fe(III) reductase from *Geobacter sulfurreducens*. *Journal of Biotechnology*. **183**: 4468-4467

Khushiramani, R., Girisha, S.K., Karunasagar, I. and Karunasagar, I. (2006) Cloning and expression of an outer membrane protein ompTS of *Aeromonas hydrophila* and study of immunogenicity in fish. *Protein Expression and Purification*. **51**:303-307.

Laemmli, U. K. (1970). Cleavage of structural proteins during the assembly of the head of bacteriophage T4. *Nature*.**227**:680-685.

Li, X and Krumholz X.R. (2009) Thioredoxin is Involved in U(VI) and Cr(VI) Reduction in *Desulfovibrio desulfuricans* G20. *Journal of bacteriology*.**191**:4924-4933.

Locher, K.P. and Broths, E. (2004) ABC transporter architecture and mechanism: implications from the crystal structures of BtuCD and BtuF. *FEBS Letters***564**: 264-268.

Lovley, D.R. and Phillips, E.J.P. (1992) Bioremediation of uranium contamination with enzymatic uranium reduction. *Environmental Science*. **26**:2228-2234.

Lovley, D.R., Widman, P.K., Woodward, J.C. and Phillips, E.J.P. (1993b). Reduction of uranium by cytochrome C3 of *Desulfovibrio vulgaris*. *Applied and Environmental Microbiology*. **59**: 3572-3576.

Ohlendieck, K. (2008) Extraction of membrane proteins. In: Cutler, P. (ed) *Methods in Molecular Biology, Protein Purification Protocols*, Second Edition. Humana Press, New York, pp. 283-293.

Payne, R.B., Gentry, D.M., Rapp-Giles, B.J., Casalot, L. and Wall, J.D. (2002) Uranium Reduction by *Desulfovibrio desulfuricans* Strain G20 and a Cytochrome *c3* Mutant. *Applied and Environmental Microbiology*. **68**:3129-3132.

Payne, R. B., Casalot, L., Rivere, T. Terry, J.H., Larsen, L., Giles, B.J. and Wall, J.D.(2004) Interaction between uranium and the cytochrome *c3* of *Desulfovibriodesulfuricans* strain G20. *Archives of Microbiology*. **181**:398-406.

Sambrook, J., Fritsch, E.F. and Maniatis, T.1989. *Molecular Cloning: A Laboratory Manual*, 2nd edn., Cold Spring Harbor Laboratory Press, Cold Spring Harbor, NY. pp.

Sakamoto, F., Nankawa, T., Kozai, N., Fujii, T., Iefuji, H., Francis, A.J. and Ohnuki, T. (2007) Protein expression of *Saccharomyces cerevisiae* in response to uranium exposure. *Journal of Nuclear and Radiochemical Sciences*. **8**:133-138.

Sani, R.K., Peyton, B.M. and Dohnalkova, A.(2006) Toxic effects of uranium on *Desulfovibrio desulfuricans* G20. *Environmental Toxicology and Chemistry*. **25**:1231-1238.

Saurin, W., Hofnung, M. and Dassa, E. (1999) Getting in or out: Early segregation between importers and exporters in the evolution of ATP-Binding cassette (ABC) transporters. *Journal of Molecular Evolution***48**: 22-41.

Van Marwijk, J. (2010) PhD thesis: **Biological synthesis of gold nanoparticles by *Thermus scotoductus* SA-01.** University of the Free State, South Africa.

Van Wyk, P.W.J. and Wingfield, M.J. (1991) Ascospore ultrastructure and development in *Ophiostoma cucullantum*. *Mycologia***83**: 698-707.

Summary

A thermophilic bacterium was isolated in 1999 by Kieft and co-workers from groundwater sampled at a depth of 3.2 kmbls in Mponeng, Republic of South Africa, which was later identified as *Thermus scotoducts* SA-01. *T. scotoductus* SA-01 has shown the ability to reduce certain metals under growth and non-growth conditions, including Mn(IV), Co(III)-EDTA, Cr(VI) and even uranium(VI). *T. scotoductus* SA-01 was grown in the presence of up to 1.25 mM uranium(VI), the specific growth rate decreased with the increasing uranium concentrations. A dramatic decline is seen at 0.5 mM, when compared to the control, where an apparent lag phase was observed. TEM and EDS analyses, subsequent to growth of *T. scotoductus* in uranium-containing medium, clearly show uranium metal clusters associated extracellularly with the cells.

Uranium reduction assays with the Br-PADAP complexing agent, showed that *T. scotoductus* SA-01 has the ability to reduce 0.25 mM of uranium in under 20 hours. The whole cell reduction under non-growth conditions exhibited an optimum temperature of 65-70 °C and an optimum pH of 7-8. Unfortunately 2D electrophoresis done on cultures grown in the absence and presence of uranium(VI) showed no dramatic shifts in protein expression. This, as well as the fact that uranium has no metabolic function, led us to believe that the protein involved in uranium reduction was more than likely a protein with another function but which can also reduce uranium and will not be expressed due to stressful conditions such as the presence of uranium.

Screening for uranium(VI) reduction activity in the subcellular fractions of cells, namely the periplasmic, cytoplasmic and membrane fractions, led to the discovery that activity is present in the periplasmic and membrane fractions. For further separation of these fractions chromatographic methods were applied and through a combination of anion and cation exchange columns a protein was identified which might be responsible for the uranium reduction activity. This

protein was sent for MS/MS and N-terminal sequence determination and both of these methods identified the protein in question as a peptide ABC transporter, peptide binding protein. This was quite an interesting find since all work done in literature has pointed to cytochromes c-type proteins as the “uranium reductases” but work done in our lab has previously shown this protein to be capable of reducing gold, thus we know it can function as a “reductase”.

The protein in question was expressed in *Escherichia coli* and purified using nickel affinity chromatography and uranium(VI) reduction activity was determined. Through structure modelling a disulphide bond believed to be responsible for uranium(VI) reduction was identified. Before uranium(VI) reduction was monitored over time, the disulfide moiety of the protein was reduced using β -mercaptoethanol. Just like the parameters observed for whole cell reduction, the protein reduced uranium(VI) at an optimum of 65-70 °C and an optimum pH of 7-8.

The aim of this study, namely to identify a protein involved in uranium(VI) reduction from *Thermus scotoductus* SA-01 was successfully completed.

Opsomming

'n Termofiliese bakterië was geïsoleer in 1999 deur Kieft en mede-werkers van grondwater op 'n diepte van 3,2 kmbls in Mponeng, Republiek van Suid-Afrika, die bakterië was later geïdentifiseer as *Thermus scotoductus* SA-01. *T. scotoductus* SA-01 het die vermoë getoon om sekere metale onder groei en nie-groei kondisies te reduceer. Die metale sluit in Mn (IV), Co (III)-EDTA, Cr (VI), en selfs uraan(VI). *T. scotoductus* SA-01 het gegroei in die teenwoordigheid van tot 1,25 mM uraan(VI), die spesifieke groeitempo het afgeneem met 'n toename in uraan konsentrasies. In vergelyking met die kontrole was daar 'n dramatiese afname in groei tempo te sien na 0.5 mM. TEM en EDS analise, na afloop van die groei van *T. scotoductus* in uraan-bevattende middel, toon duidelike uraan "clusters" geassosieer met die selle extraselluler.

Uraan reduksie was waargeneem met die Bromo-PADAP tegniek. Resultate het aangedui dat *T. scotoductus* SA-01 het die vermoë om 0.25 mM uraan te reduceer binne 20 uur. Die heel sel reduksie onder nie-groei kondisies blyk om optimaal by 'n temperatuur van 65-70 °C en 'n pH van 7-8 plaas te vind. Ongelukkig het 2D elektroforese, gedoen op kulture gekweek in die afwesigheid en teenwoordigheid van uraan(VI), geen dramatiese verskuiwings in proteïen uitdrukking in die teenwoordigheid van uraan getoon nie. Dit, asook die feit dat uraan geen metaboliese funksie het nie, impliseer dat die proteïen wat betrokke is by uraan reduksie meer as waarskynlik 'n proteïen met 'n ander funksie is, maar wat ook uraan kan reduceer. Dit sal dus ook nie vervaardig word indien stresvolle toestande soos die teenwoordigheid van uraan bestaan nie.

Ondersoek na uraan(VI) reduksie aktiwiteit in die subsellulere fraksies van die selle, naamlik in die periplasmiese, sitoplasmiese en membraan fraksies het gelei tot die ontdekking dat aktiwiteit teenwoordig is in die periplasmiese en membraan fraksies. Vir verdere skeiding van hierdie fraksies was chromatografiese metodes aangewend en deur 'n kombinasie van die anioon en

kation uitruilerkolomme was 'n proteïen geïdentifiseer wat dalk verantwoordelik kan wees vir die uraan reduksie aktiwiteit. Hierdie proteïene is gestuur vir MS/MS en N-terminale volgorde bepaling en beide van hierdie metodes het die proteïen geïdentifiseer as 'n peptied ABC vervoerder, wat 'n peptied bindende proteïen. Die bevinding is teenstreidig met die meeste literatuur verslae wat daarop dui dat sitochroom c-tipe proteïene uraan reduseer. Die vermoë van die geïsoleerde ABC peptide om goud te kan (Van Marwijk, 2010), impliseer dat die proteïen die vermoë het om as 'n "reduktase" te kan funksioneer.

Die proteïen van belang was bevestig in *Escherichia coli*, gesuiwer deur gebruik te maak van nikkel affiniteitschromatografie waarna uraan(VI) reduksie karakteristieke bepaal was. Deur ondersoek in te stel met betrekking tot die struktuur van die proteïen was 'n di-sulfide verbinding geïdentifiseer wat moontlik verantwoordelik kan wees vir die uraan(VI) reduksie aktiwiteit. Voordaturaan(VI) reduksie in aanvang geneem het, was die di-sulfide verbinding van die proteïen gereduseer met behulp van β -mercaptoethanol. Optimale eksperimentele parameters vir uraan(VI)reduksie met die betrokke proteïen was waargeneem tussen 65-70 °C en pH gebied tussen 7-8.

Die doel van hierdie studie, naamlik om 'n proteïen wat betrokke is by uraan(VI) reduksie in die termofiliese bakterië *T. scotoductus* SA-01 te identifiseer was suksesvol voltooi.